DISTRIBUTED ESTIMATION IN WIRELESS SENSOR NETWORKS UNDER A SEMI-ORTHOGONAL MULTIPLE ACCESS TECHNIQUE

A Thesis Submitted
to the College of Graduate Studies and Research
in Partial Fulfillment of the Requirements
for the Degree of Master of Science
in the Department of Electrical and Computer Engineering
University of Saskatchewan

by

Su Jian

Saskatoon, Saskatchewan, Canada

Permission to Use

In presenting this thesis in partial fulfillment of the requirements for a Postgraduate degree from the University of Saskatchewan, it is agreed that the Libraries of this University may make it freely available for inspection. Permission for copying of this thesis in any manner, in whole or in part, for scholarly purposes may be granted by the professors who supervised this thesis work or, in their absence, by the Head of the Department of Electrical and Computer Engineering or the Dean of the College of Graduate Studies and Research at the University of Saskatchewan. Any copying, publication, or use of this thesis, or parts thereof, for financial gain without the written permission of the author is strictly prohibited. Proper recognition shall be given to the author and to the University of Saskatchewan in any scholarly use which may be made of any material in this thesis.

Request for permission to copy or to make any other use of material in this thesis in whole or in part should be addressed to:

Head of the Department of Electrical and Computer Engineering
57 Campus Drive
University of Saskatchewan
Saskatoon, Saskatchewan, Canada
S7N 5A9

Acknowledgments

I would like to express my deepest appreciation and gratitude to my supervisor, Professor Ha Nguyen, for his great support during my study and research. He has been a great source of knowledge and has inspired me with many ideas which are very important for my research. The useful discussion and advice from him during our weekly meetings made my study and research flow easily and smoothly. The financial support from his research grant also made this thesis possible.

My special thanks goes to Professor Eric Salt who taught two wonderful courses. I admire his bright wisdom and precise attitude to teaching and research. He also provided many thoughtful suggestions to my future career and life.

I feel a deep sense of gratitude for my husband Hongzhong Yan. It is impossible to finish this thesis without his encouragement and help during my study and research in the last two years. To him and our baby on the way, I dedicate this thesis.

Especially, I would like to thank my parents for the endless love and support they provide through my entire life. They continuously inspire me to work harder in every stage of my life.

Finally, I wish to express my appreciation to all of those who gave me help when I studied at the University of Saskatchewan.

Abstract

This thesis is concerned with distributed estimation in a wireless sensor network (WSN) with analog transmission. For a scenario in which a large number of sensors are deployed under a limited bandwidth constraint, a semi-orthogonal multiple-access channelization (MAC) approach is proposed to provide transmission of observations from K sensors to a fusion center (FC) via N orthogonal channels, where $K \geq N$. The proposed semi-orthogonal MAC can be implemented with either fixed sensor grouping or adaptive sensor grouping.

The mean squared error (MSE) is adopted as the performance criterion and it is first studied under equal power allocation. The MSE can be expressed in terms of two indicators: the channel noise suppression capability and the observation noise suppression capability. The fixed version of the semi-orthogonal MAC is shown to have the same channel noise suppression capability and two times the observation noise suppression capability when compared to the orthogonal MAC under the same bandwidth resource. For the adaptive version, the performance improvement of the semi-orthogonal MAC over the orthogonal MAC is even more significant. In fact, the semi-orthogonal MAC with adaptive sensor grouping is shown to perform very close to that of the hybrid MAC, while requiring a much smaller amount of feedback.

Another contribution of this thesis is an analysis of the behavior of the average MSE in terms of the number of sensors, namely the scaling law, under equal power allocation. It is shown that the proposed semi-orthogonal MAC with adaptive sensor grouping can achieve the optimal scaling law of the analog WSN studied in this thesis.

Finally, improved power allocations for the proposed semi-orthogonal MAC are investigated. First, the improved power allocations in each sensor group for different scenarios are provided. Then an optimal solution of power allocation among sensor groups is obtained by the convex optimization theory, and shown to outperform equal power allocation. The issue of balancing between the performance improvement and extra feedback required by the improved power allocation is also thoroughly discussed.

Table of Contents

List of Tables

List of Figures

List of Abbreviations

WSN	Wireless Sensor Network
FC	Fusion Center
MAC	Multiple Access Channel
SNR	Signal-to-Noise Ratio
i.i.d.	independent and identically distributed
AWGN	Additive White Gaussian Noise
MSE	Mean Square Error
AMSE	Average Mean Square Error
LMMSE	Linear Minimum Mean Square Error
FSG	Fixed Sensor Grouping
ASG	Adaptive Sensor Grouping

List of Symbols

s	source signal
σ_s^2	variance of s
i	sensor index ($i = 1, 2, \ldots, K$)
v_i	observation noise at sensor i
σ_v^2	variance of v_i (identical for all sensors)
n	orthogonal channel index or sensor group index ($n = 1, 2, \ldots, N$)
γ_o	observation signal-to-noise ratio ($\gamma_o = \sigma_s^2/\sigma_v^2$)
P_{tot}	total transmit power of all sensors
h_i	response of wireless channel from the ith sensor to the fusion center
r_i	magnitude of h_i
φ_i	phase of h_i
ω	additive white Gaussian noise
σ_ω^2	variance of ω
γ_c	channel signal-to-noise ratio ($\gamma_c = P_{\text{tot}}/\sigma_\omega^2$)
$\check{s}$	estimator of s
ϵ	mean square error between s and $\check{s}$
a_i	power gain at sensor i
Ω_n	index set of sensors transmitting on the nth orthogonal channel
$\mathbf{g}^{(i)}$	channel allocation vector at sensor i
P_n	total transmitted power in the nth group
γ_{cn}	channel signal-to-noise ratio on the nth orthogonal channel ($\gamma_{cn} = P_n/\sigma_\omega^2$)

1. Introduction

A distributed wireless sensor network (WSN), which can be typically deployed for some special signal processing task (e.g. parameter estimation), is composed of a fusion center (FC) and a number of sensors (as shown in Figure 1.1) that operate under limited bandwidth and power resources. Each sensor in the network makes an observation of the quantity of interest, generates a local signal, and then sends it to the FC via a wireless fading channel. Based on the data collected from the sensors, the FC conducts certain data processing according to the tasks of the WSN. Such sensor network applications can be found in military surveillance, environmental monitoring, precision agriculture and intelligent transportation [2].

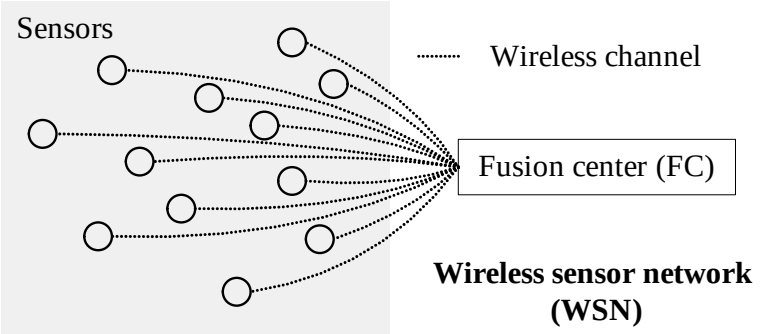

Figure 1.1 A wireless sensor network with a fusion center.

Distributed signal processing in WSNs can be classified into two main categories: distributed detection [3–11] and distributed estimation. In distributed estimation, there are two main options to transmit the observation from each sensor to the FC: digital [12–18] or analog [19–23]. In digital transmission, each sensor first converts its observation into a bit stream (quantization) and then communicates this bit stream reliably to the FC. In analog transmission, the sensors simply amplify their observations and then forward them to the FC. Compared to digital transmission, larger bandwidth is required to transmit analog signals.

However, the fidelity of the source signals can be better preserved with analog transmission since the transmitted signal is interfered by quantization noise in digital transmission.

This thesis is concerned with distributed estimation in a sensor network with analog transmission. Specially, a scalar Gaussian random variable is observed in a memoryless fashion by K sensors and each observation is subject to white Gaussian noise. The sensors amplify their observations and then transmit them to an FC via wireless channels. Using data collected from the sensors, the FC estimates the underlying source signal to within the smallest distortion possible.

There are many factors that affect the performance of distributed estimation in WSNs. These include the accuracy of sensors' observations (which is usually modelled as observation noise), the available bandwidth and power resources, the fading characteristics of the wireless channels between the sensors and the FC, the fusion rule used by the FC, etc. Regarding the wireless communications between the FC and the sensors, many different types of multiple access channelization (MAC)[1] can be used with analog transmission. For different types of MAC, the impacts of observation noise and channel noise on the estimation performance are different, and therefore the behaviour of the final estimation performance strongly depends on the type of MAC used by the sensor network.

In the coherent MAC studied in [21], signals from all sensors are coherently combined first and then transmitted on one wireless channel. It is bandwidth efficient. In addition, there is only one channel noise component at the FC and hence the impact of channel noise on the estimation performance is small. However, to obtain coherent combination, the channel phase information needs to be transmitted from the FC to the sensors, which requires a large amount of feedback. On the other hand, there is no need of any feedback in the orthogonal MAC [22]. This is because signal from each sensor is exclusively transmitted on one orthogonal channel in the orthogonal MAC. To accommodate multiple orthogonal channels, the orthogonal MAC requires a large transmission bandwidth. More importantly,

[1]It is pointed out that, in many research papers on the topic of distributed estimation in WSNs, the abbreviation MAC is used for "multiple access channel" but really refers to a multiple access technique. In keeping with the convention, the abbreviation MAC is also used in this thesis but it is clearly meant for "multiple access channelization" technique.

using K orthogonal channels means that there are K channel noise components at the FC, which makes the estimation performance suffer more from channel noise. The hybrid MAC [23] is a tradeoff between the coherent and orthogonal MACs, in which all sensors are divided into groups and the coherent MAC is used for sensors within each group, whereas the orthogonal MAC is used across different groups. Since the bandwidth requirement in this MAC is proportional to the number of sensor groups, it can be fixed to a small value to save bandwidth. In this MAC, although coherent combination is only required in each sensor group, the amount of channel phase information feedback is still the same as that of the coherent MAC.

Motivated from the above discussion, this thesis focuses on the design of a wireless sensor network in order to improve the estimation performance under both bandwidth and power constraints. Specially, considered is a scenario where there are N (a small number due to bandwidth constraint) orthogonal channels that are shared by K sensors, where $K \geq N$, for transmitting the sensors' observations to the FC. An obvious approach to the above design problem is sensor grouping, and the hybrid MAC discussed above is one solution. A flexible tradeoff between the coherent and orthogonal MACs can therefore be obtained by changing the number of groups and the number of sensors in each group. However, in the hybrid MAC, to obtain coherent combination in each group, the same amount of channel information feedback from the FC to the sensors as that of the coherent MAC is still required. In a sharp contrast to the hybrid MAC, the novel sensor grouping proposed in this thesis is such that sensors in one group transmit on one orthogonal channel without any channel phase compensation at the transmitter. This means that the signals from sensors within one group are directly superimposed instead of coherently combined as in the hybrid MAC. As a result, no channel phase information is required to be transmitted from the FC to the sensors. To distinguish from the other MACs discussed before, the proposed MAC shall be called a semi-orthogonal MAC.

Throughout this paper, the average mean squared error (MSE) between the source signal and its estimated version is adopted as the performance criterion for distributed estimation. Under a homogeneous assumption that the variances of observation noise and channel noise are identical for all sensors, two indicators of estimation performance are established based

on the MSE distortion: *the channel noise suppression capability* and *the observation noise suppression capability*. These two performance indicators are used extensively throughout this thesis to investigate and compare the distributed estimation performances of different MACs.

The proposed semi-orthogonal MAC can be implemented with either fixed or adaptive sensor grouping. In fixed sensor grouping, each sensor is assigned to transmit on the same orthogonal channel throughout the process of communication. Under the same bandwidth and power constraints, the semi-orthogonal MAC has the same channel noise suppression capability but nearly two times the observation noise suppression capability when compared to the orthogonal MAC. For adaptive sensor grouping, sensors are grouped according to the ranges (i.e., sub-regions) that their channel phases fall into. It is shown that, compared to fixed sensor grouping, the MSE performance of the semi-orthogonal MAC with adaptive grouping is improved by a large margin. In fact the performance of the semi-orthogonal MAC with adaptive grouping is very close to the performance of the hybrid MAC under the same bandwidth and power constraints and the same number of sensors. The only extra cost for implementing the proposed semi-orthogonal MAC is a few bits of feedback information from the FC to the sensors to indicate orthogonal channel allocation. However, this amount of feedback overhead is significantly smaller than what required for channel phase information in the coherent and hybrid MACs.

Although it is very complicated to derive the exact expression of the average MSE of the proposed semi-orthogonal MAC, some of its properties can still be studied and analyzed. For example, one important property of the average MSE, namely the achieved scaling law which describes the decaying trend achieved by the average MSE as a function of the number of sensors K, is investigated in this thesis. The scaling laws of different cases of the semi-orthogonal MAC are established. It is shown that only the semi-orthogonal MAC with adaptive sensor grouping can achieve the optimal scaling law of $1/K$ of the estimation system using wireless sensor networks as defined in this thesis. As a reference, the coherent MAC can also achieve the optimal scaling law, but it requires a large amount of feedback.

In all previous studies, the estimation is conducted under equal power allocation. In the last part of this thesis, the issues of improved power allocation in which the total transmitted

power is divided and allocated to the sensors according to factors such as observation noise, channel response, and channel noise are addressed. The task is divided into two steps: power allocation in each sensor group and power allocation among sensor groups. In each sensor group, two improved strategies are provided for scenarios with especially large observation signal-to-noise ratio (SNR) and especially large channel SNR, respectively. In addition, equal power allocation is recommended for the scenario in which the observation SNR is comparable to the channel SNR. Among the sensor groups, an optimal power allocation solution is obtained based on the convex optimization theory and shown to outperform equal power allocation. Note that to implement the improved power allocation, extra feedback from the FC to the sensors is required. As a result, it is important to balance the performance improvement brought by the improved power allocation and the required extra feedback overhead.

The remainder of this thesis is organized as follows.

Chapter 2 first introduces the basic concepts of WSNs including structure, applications, design criteria, and protocol stack. Two main classes of distributed data processing in WSNs, namely detection and estimation, are discussed later. Finally, a general system model of a sensor network with analog transmission is established for the studies in the following chapters.

Chapter 3 presents three popular MACs used in WSNs, the coherent, orthogonal and hybrid MACs. These three MACs are compared in terms of estimation performance and bandwidth and feedback requirements. Specially, two performance indicators are established based on the MSE distortion to assess the observation noise and channel noise suppression capabilities of these MACs.

Chapter 4 proposes a novel semi-orthogonal MAC. Two versions of this semi-orthogonal MAC, fixed sensor grouping and adaptive sensor grouping, are developed and analyzed in detail based on the two performance indicators established in Chapter 3. The proposed semi-orthogonal MAC is also compared with the three MACs studied in Chapter 3.

Chapter 5 includes two main parts. The first part investigates the scaling law achieved by the proposed semi-orthogonal MAC. Specially, the scaling laws of different cases of the semi-orthogonal MAC are established. The second part addresses issues of improved power

allocation in the semi-orthogonal MAC, including power allocations in each sensor group and among sensor groups.

Chapter 6 draws conclusions of this thesis and gives suggestions for future research.

2. Background

2.1 Wireless Sensor Networks

Recent advances in wireless communications and electronics have enabled the development of low-cost, low-power, multi-functional sensor nodes that are small in size and can communicate in short distance. These tiny sensor nodes, which consist of sensing, data processing, and communicating components, leverage the idea of sensor networks. A sensor network is composed of a large number of sensor nodes that are densely deployed for certain tasks, such as military surveillance, environmental monitoring, precision agriculture and intelligent transportation [2]. An example of sensor network applications of environmental monitoring is described in the following [1].

Redwood trees are so large that entire ecosystems exist within their physical envelope. Climatic factors determine the rate of photosynthesis, water and nutrient transport, and growth patterns. Substantial variations are known to exist over the volume of an individual specimen, and researchers believe that the micro-climate structure varies over regions of the forest. In addition, water transport rates and the scale of respiration may influence the micro-climate around a tree, effectively creating its own weather. All these factors influence the habitat dynamics of species existing in and on the tree.

Researchers use multiple sensor nodes to monitor the micro-climate around a redwood tree. As shown in Figure 2.1, an entire weather station fits in a tube about the size of a film canister. On top, two incident-light sensors measure total solar radiation, specifically light and photosynthetically active radiation, the bands at which chlorophyll is sensitive. In addition, on the bottom, there are environmental sensors to monitor relative humidity, barometric pressure, and temperature. The center of the tube contains a small central processing unit, a data storage, a battery, and a low-power radio to collect data, process

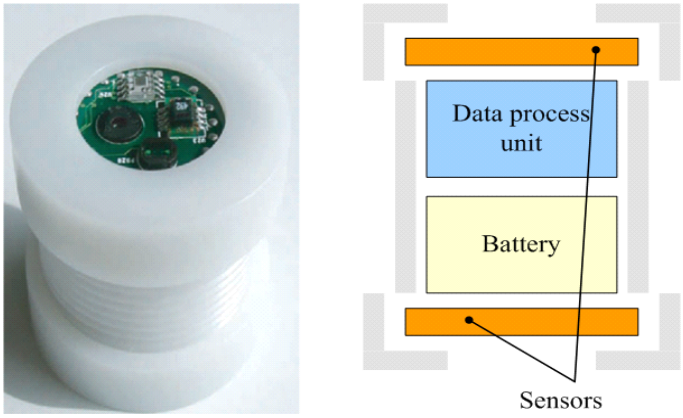

Figure 2.1 Models of a sensor node for environmental monitoring fitting in a tube about the size of a film canister [1].

it, and route information among the nodes and to the outside world. This provides a cost-effective means of obtaining simultaneous measurements at many points in the tree, spanning elevation and radial direction over a prolonged period. For example, in a 36-meter study tree, 16 nodes are deployed at four elevations to sample climate data every five minutes.

Figure 2.2 shows humidity and temperature profiles over three days, collected from 16 sensor nodes. The WSN samples climate data every five minutes and computes average humidity and temperature at each elevation.

The design of such sensor networks is influenced by many factors [24–29], including fault tolerance, scalability, sensor network topology, production costs, hardware constraints, operating environment, transmission media, and power consumption. Some sensor nodes may fail or be blocked due to lack of power, or have physical damage or environmental interference. The failure of sensor nodes should not affect the overall task of the sensor network. This is the reliability or fault tolerance issue. Depending on the applications, the number of sensor nodes deployed in studying a phenomenon may range from several to an order of hundreds or thousands. The sensor network must be able to work with this number of nodes and utilize the high density of the sensor nodes. When deploying a high number of nodes densely, it requires careful handling of topology maintenance. In addition, the cost of each sensor node has to be kept low. Usually, a sensor node is made up of four basic components: a sensing unit, a processing unit, a transceiver unit, and a power unit. All of these subunits may need to fit into a match box-sized module. Apart from size, there are

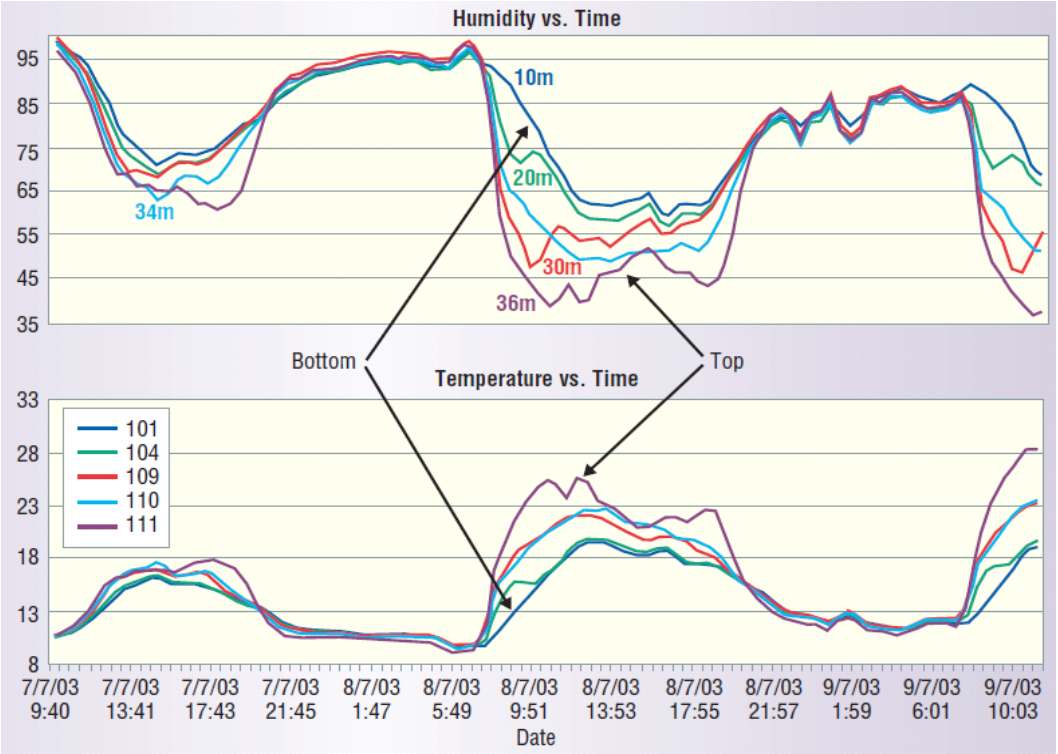

Figure 2.2 WSN climate data [1].

some other stringent constraints for sensor nodes. For example, these nodes must be light enough and adaptive to various operating environments. In most operating environments, the sensor nodes are linked to the network and each other by a wireless medium. These links can be formed by radio, infrared, or optical media. However, much of the current hardware for sensor nodes is based on radio-frequency circuit design. For a wireless sensor node, it usually can be equipped with a limited power source and it might be impossible to recharge the batteries. As a result, sensor node lifetime shows a strong dependence on battery lifetime. Hence, power conservation and power management are very important in wireless sensor network design.

Regarding the topology of WSNs, there are two popular deployments characterized by the presence or absence of a fusion center (FC). When an FC is present, there is no inter-sensor communication. All sensors are connected to the FC via wireless channels and communication is only between the sensors and the FC. Using data collected from the sensors, the FC conducts certain processing according to the tasks of the WSNs. In ad hoc WSNs, there is no FC. The network itself is responsible for processing the collected information, and to

this end, the sensors communicate with each other through the shared wireless medium. In addition, hybrid topologies are also possible in which the WSN is partitioned into clusters with a hierarchical structure. Each cluster has a local FC generating intermediate data, which in turn are combined to obtain a final result for the tasks of the WSN. This thesis focuses on the data processing in WSNs with a FC.

The protocol stack used by the wireless sensor network consists of five layers: physical layer, data link layer, network layer, transport layer, and application layer [24]. The physical layer addresses the needs of simple but robust modulation, transmission and receiving techniques. In the data link layer, the medium access control protocol is used to minimize collision with neighbours' broadcasts. The network layer takes care of routing the data supplied by the transport layer. The transport layer helps to maintain the flow of data if the sensor network's application requires it. Depending on the sensing tasks, different types of application software can be built and used on the application layer. The research in this thesis focuses on the multiple access channelization in the physical layer of WSNs.

2.2 Distributed Detection and Estimation in WSNs

In distributed signal processing in WSNs, instead of sending all the raw data to the FC, the sensors use their processing abilities to locally carry out simple computations (e.g., simple compression) and transmit only the required and partially processed data [4]. Some of the advantages of distributed signal processing are reduced bandwidth requirement, increased reliability, and reduced cost. There may be performance loss in distributed systems since the FC has only partial information as communicated by the sensors. However, the performance loss can be made small by optimizing signal processing at the sensors. There has been rich research in distributed signal processing [3–23], including detection and estimation, in WSNs. The next two subsections review relevant research and results on distributed detection and distributed estimation.

2.2.1 Distributed Detection

The canonical detection problem is to fabricate a reasonable decision between a pair of hypotheses, the presence of a signal (hypothesis H_1) and the absence of a signal (hypothesis H_0), based on a series of observations [3]. Furthermore, it can be extended to making a

decision among multiple hypotheses. The detection problem becomes "distributed" when the observations are quantized prior to their insertion to a decision rule. The existing literature on distributed detection is abundant [3–11]. However, since distributed detection is outside the scope of this thesis, only two examples are briefly discussed in the following.

In [4], a binary hypothesis testing problem in which the observations at all sensors either correspond to the presence of a signal (hypothesis H_1) or to the absence of a signal (hypothesis H_0) was studied. Each sensor employs a mapping rule and passes the quantized observation to the fusion center or other sensors. Based on the received signals, the FC or certain sensors arrive at a global (for the FC) or local (for the certain sensors) decision which favours either H_1 or H_0. Two formulations were considered in [4]. With the Neyman-Pearson formulation, the task of the distributed detection problem can be stated as follows: for a prescribed bound on the global probability of false alarm, find optimal global or local decision rule that minimizes the global probability of miss. With the Bayesian formulation, the objective is to minimize the Bayesian risk, which is a sum of weighted risks of possible courses of action. Assignment of costs to different courses of action and knowledge of prior probabilities are required for the solution of this problem. In addition, some advanced topics that involve locally optimal detection, sequential detection, non-parametric methods, and robust procudures are presented in [5].

In [6], an universal distributed detection algorithm, which consists of the local quantization at the sensors and the final fusion strategy at the FC, was designed for the hypothesis problem mentioned above when the distribution of observation noise is unknown. This detector is especially bandwidth efficient because each sensor only needs to send a 1-bit message to the FC. In addition, the error probability of this detector decays exponentially as the number of sensors increases.

2.2.2 Distributed Estimation

In distributed estimation, the source signal is in analog form. Data is collected from the sensors and then transmitted to the FC to obtain an estimate of the exact value of the source signal. For analog source signals, there are two approaches to transmit observations from the sensors to the FC: *digital* or *analog*.

In digital transmission, the sensors first convert its observations into a bit stream and

then communicate this bit stream reliably to the FC. One of the most important topics in sensor networks with digital transmission is the CEO problem. The CEO problem can be summarized as follows. A firm's Chief Executive Officer (CEO) is interested in a data sequence $\mathbf{X}$ which cannot be observed directly, perhaps because it represents tactical decisions by a competing firm. The CEO deploys a team of K agents who observe independently corrupted version of $\mathbf{X}$. Since $\mathbf{X}$ is only one among many pressing matters to which the CEO must attend, the combined data rate at which the agents may communicate information about their observations to the CEO is limited to R bits per second. The agents could use their R bits per second to provide the CEO with a representation of $\mathbf{X}$ with a fidelity D. The target of the CEO problem is to characterize the rate-distortion function $R(D)$. The CEO problem was first introduced in [12, 13] and the quadratic Gaussian version was solved in [14].

The $R(D)$ function obtained from the CEO problem serves as a performance benchmark for distributed estimation under bandwidth constraints. In [15–18], effective local quantization schemes and estimators were designed for different source and observation noise signal models. The corresponding mean square error (MSE) performances were compared with the performance benchmark obtained from the CEO problem. For example, in the Gaussian quadratic CEO problem, [14] derived an asymptotic total rate distortion function of the form $D = \sigma^2/(2R)$ when both K and R are large, where R is the total rate and σ^2 is the observation noise variance. For the special case of $R_k = 1$ bit per sensor sample, the total communication rate $R = K$, and thus the best achievable MSE performance dictated by rate distortion theory is no less than $\sigma^2/(2K)$. In [15], the source signal is a deterministic scalar and the observation noise is known to be a random variable of Gaussian distribution. In that paper, a simple distributed estimator which compares the sensor observations with a certain threshold to obtain the 1-bit transmit signals was designed and it achieves an asymptotic MSE performance of $\pi\sigma^2/(2K)$ when the threshold can be taken close to the value of the source signal. The MSE only increases by a factor of π with respect to the performance benchmark. In [16–18], the simple design of local quantizers and estimators which requires only one to several bits per sensor were extended to more pragmatic signal models, for example, the probability density function (pdf) of the observation noise is known

with a finite number of unknown parameters or the pdf is totally unknown. It was shown that the resulting estimators turned out to exhibit MSEs that can come surprisingly close to the performance benchmark.

In analog transmission, the sensors simply amplify their observations and then forward them to the FC. Compared to digital transmission, larger bandwidth is required to transmit analog signals. However, the fidelity of the source signals can be better preserved with analog transmission since the transmitted signal is interfered by quantization noise in digital transmission. As proved in [20], with certain multiple access channelization from the sensors to the FC, analog transmission is exactly optimal for a simple sensor network with multiple Gaussian statistical assumptions. In this thesis, several issues of distributed estimation in such a Gaussian sensor network with analog transmission will be studied.

2.3 Distributed Estimation in a WSN with Analog Transmission: System Model

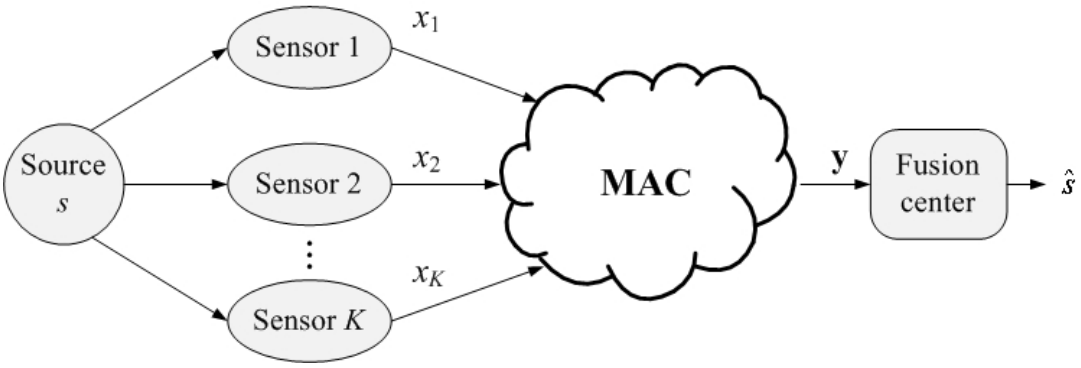

Figure 2.3 System model for distributed estimation in a WSN.

In this thesis, a sensor network with Gaussian statistical assumptions is considered. Specifically, as shown in Figure 2.3, a scalar Gaussian random variable s is observed in a memoryless fashion by K sensors and each observation is subject to white Gaussian noise. The observation of the ith sensor can be expressed as

$$x_i = s + v_i, \quad 1 \leq i \leq K, \tag{2.1}$$

where the source signal s and observation noise v_i are treated as random variables with zero mean and variances σ_s^2 and σ_v^2, respectively. Here, an assumption of identical observation

noise variance for all sensors is used to facilitate the performance analysis. The observation signal-to-noise ratio (SNR) is defined as $\gamma_o = \frac{\sigma_s^2}{\sigma_v^2}$. In practice, the observation noise is affected by various factors and its variance might be different from sensor to sensor. A more complicated system model with different observation noise variances can be considered in the future to better fit the reality.

With analog modulation, the ith sensor simply amplifies x_i with a gain a_i and transmits the result to the FC. The total transmit power in this WSN is P_{tot}.

Signals from the sensors will be transmitted to the FC via wireless fading channels. Let h_i, $i = 1, \ldots, K$, represent the channel response from sensor i to the FC. These channel responses are modeled as independent and identically distributed (i.i.d.) complex Gaussian random variables with zero mean and unit variance. Let $h_i = r_i e^{j\varphi_i}$. Then the magnitude r_i and phase φ_i of a Gaussian wireless channel can be modeled as independent random variables with Rayleigh and uniform distributions, respectively.

On each wireless fading channel, the transmitted signal will be disturbed by additive white Gaussian noise (AWGN). The AWGN sample, denoted as ω, is modeled as a complex Gaussian random variable with zero mean and variance σ_ω^2. The channel SNR is defined as $\gamma_c = \frac{P_{\text{tot}}}{\sigma_\omega^2}$.

The received signal at the FC is denoted by $\mathbf{y} = [y_1, y_2, \ldots, y_N]$, where $\mathbf{y}$ can be a scalar or a vector. The dimension N and expression of $\mathbf{y}$ in terms of a_i, x_i, h_i and ω depend on the type of multiple access channelization (MAC) used from the sensors to the FC. Research on MAC is the main focus of this thesis and will be elaborated in the next three chapters. Based on $\mathbf{y}$, the FC estimates the underlying source signal to within the smallest distortion possible. The Bayesian mean square error (MSE) between the source signal and the estimator $\check{s}$ is adopted as the performance criterion, which is

$$\epsilon = \text{Bmse}\left(\check{s}\right) = \mathcal{E}\left\{\left(s - \check{s}\right)^2\right\}, \tag{2.2}$$

where the expectation is with respect to the pdf $p\left(\mathbf{y}, s\right)$. The linear minimum mean square error (LMMSE) estimator is considered in this thesis [30], in which the estimator is of the form

$$\check{s} = \sum_{n=1}^{N} b_n y_n + b_{N+1}, \tag{2.3}$$

and the weighting coefficients b_n's are chosen to minimize the MSE. The final LMMSE estimator is

$$\check{s} = \mathcal{E}\{s\} + \mathbf{C}_{s\mathbf{y}}\mathbf{C}_{\mathbf{yy}}^{-1}\mathbf{y} = \mathbf{C}_{s\mathbf{y}}\mathbf{C}_{\mathbf{yy}}^{-1}\mathbf{y}, \tag{2.4}$$

where $\mathbf{C}$ means a covariance matrix. The second equal sign is because that the mean of the source signal s is assumed to be zero in this case. The corresponding MSE is

$$\epsilon = C_{ss} - \mathbf{C}_{s\mathbf{y}}\mathbf{C}_{\mathbf{yy}}^{-1}\mathbf{C}_{\mathbf{y}s}. \tag{2.5}$$

Note that the MSE obtained above is for certain realizations of channel responses h_i's. To evaluate the long-term performance of a WSN, the average MSE (AMSE) is defined as follows

$$\text{AMSE} = \mathcal{E}\{\epsilon\}, \tag{2.6}$$

where the expectation is taken over channel response realizations.

When calculating $\check{s}$, it is assumed that the FC knows the first-order and second-order statistics of the source signal, observation noise and AWGN related to all sensors. It is also assumed that the FC can obtain the channel responses of all links between the sensors and the FC. These assumptions are reasonable when the network condition and the signal being estimated change slowly.

2.4 Summary

This chapter discussed the problems of distributed detection and distributed estimation in WSNs. A system model for distributed estimation in a sensor network with analog transmission was then described in detail. In the following chapters, the effect of the MAC used in the system on the final estimation performance will be investigated under different aspects. For a scenario in which a large number of sensors are deployed under limited bandwidth constraint, a novel semi-orthogonal MAC will be proposed and its performance will be analyzed.

3. Multiple Access Channelizations in WSNs

3.1 Introduction

In wireless sensor networks (WSN), one or several wireless channels may be used for transmission from the sensors to the FC, depending on the available bandwidth. A multiple access channelization (MAC) can be considered as a way to decide how the sensors share those wireless channels. The type of MAC has a strong influence on the performance of distributed estimation in WSNs based on analog transmission. This is because observation noise and channel noise are the two main factors that affect the estimation performance. For different types of MAC, the impacts of observation noise and channel noise on the estimation performance are different, and therefore the behaviour of the final estimation performance strongly depends on the type of MAC used by the network.

In this chapter, three different MACs are studied and compared in terms of estimation performance, bandwidth and feedback requirements. In the coherent MAC [21], signals from all sensors are coherently combined first and then transmitted on one wireless channel. It is bandwidth efficient. However, to obtain coherent combination, the channel phase information needs to be transmitted from the FC to the sensors, which requires a large amount of feedback. On the other hand, there is no need of any feedback in the orthogonal MAC [22]. This is because signal from each sensor is exclusively transmitted on one orthogonal channel in the orthogonal MAC. To accommodate multiple orthogonal channels, the orthogonal MAC requires a large transmission bandwidth. The hybrid MAC [23] is a tradeoff between the coherent and orthogonal MACs, in which all sensors are divided into groups and the coherent MAC is used for sensors within each group, whereas the orthogonal MAC is used across different groups. Since the bandwidth requirement in this MAC is proportional to the number of sensor groups, it can be fixed to a small value to save bandwidth. In this MAC, although

coherent combination is only required in each sensor group, the amount of channel phase information feedback is still the same as that of the coherent MAC.

In terms of estimation performance, two aspects are considered in this chapter: accuracy and reliability. The average MSE is adopted as the performance criterion of estimation accuracy. Two performance indicators, namely the channel noise suppression capability indicator and the observation noise suppression capability indicator, are developed to quantify the impacts of channel noise and observation noise on the average MSE performance, respectively. In addition, a performance criterion of estimation reliability, namely the outage probability, is also studied in this chapter.

3.2 Coherent MAC

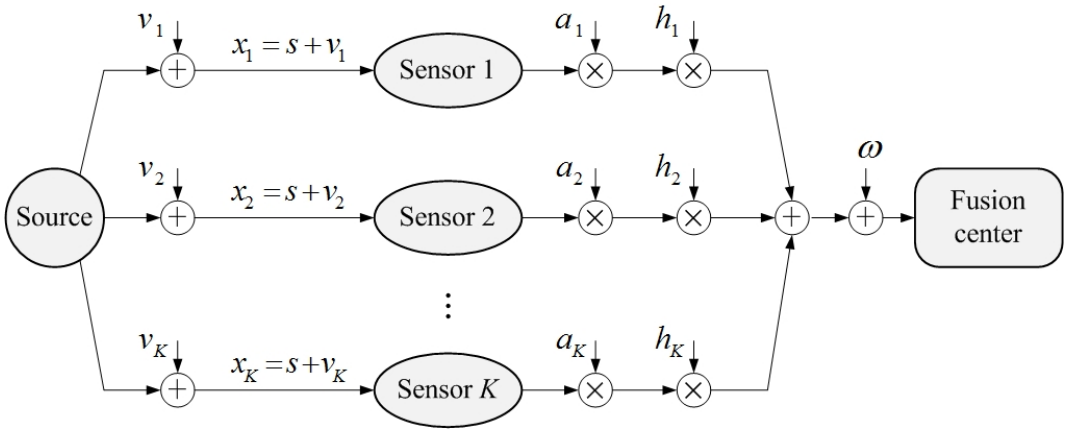

Figure 3.1 System model of a wireless sensor network using the coherent MAC.

Figure 3.1 shows a wireless sensor network with the coherent MAC [21]. Signals from all sensors are transmitted on one wireless channel. This means that there is only one channel noise component at the FC and hence the impact of channel noise on the estimation performance is small. To obtain coherent combination at the FC, phases of channel responses are compensated at the sensors. To realize phase compensation at the transmitters, knowledge of wireless channel responses needs to be transmitted from the FC to all sensors, which represents a large amount of feedback. This requirement presents a serious challenge in implementing the coherent MAC.

After phase compensation, the transmitted signal at the ith sensor is $x_i = a_i (s + v_i) e^{-j\varphi_i}$. At the FC, all the useful information resides in the real part of the received signal, which can be expressed as

$$y = \sum_{i=1}^{K} a_i (s + v_i) r_i + \mathcal{R}\{\omega\}. \tag{3.1}$$

Based on y, the LMMSE estimator and the corresponding MSE are

$$\check{s} = \left[\frac{\left(\sum_{i=1}^{K} a_i r_i\right) \sigma_s^2}{\left(\sum_{i=1}^{K} a_i r_i\right)^2 \sigma_s^2 + \left(\sum_{i=1}^{K} a_i^2 r_i^2\right) \sigma_v^2 + \frac{\sigma_\omega^2}{2}} \right] y \tag{3.2}$$

and

$$\epsilon = \left[\sigma_s^{-2} + \frac{\left(\sum_{i=1}^{K} a_i r_i\right)^2}{\left(\sum_{i=1}^{K} a_i^2 r_i^2\right) \sigma_v^2 + \frac{\sigma_\omega^2}{2}} \right]^{-1}. \tag{3.3}$$

With equal power allocation, $a_i = \sqrt{P_{\text{tot}}/K\,(\sigma_s^2 + \sigma_v^2)}$ and equation (3.3) turns to

$$\epsilon = \sigma_s^2 \left[1 + \frac{\left(\sum_{i=1}^{K} \frac{r_i}{\sqrt{K}}\right)^2}{\left(\sum_{i=1}^{K} \frac{r_i^2}{K}\right) \frac{1}{\gamma_o} + \frac{1}{2\gamma_c}\left(1 + \frac{1}{\gamma_o}\right)} \right]^{-1}. \tag{3.4}$$

3.3 Orthogonal MAC

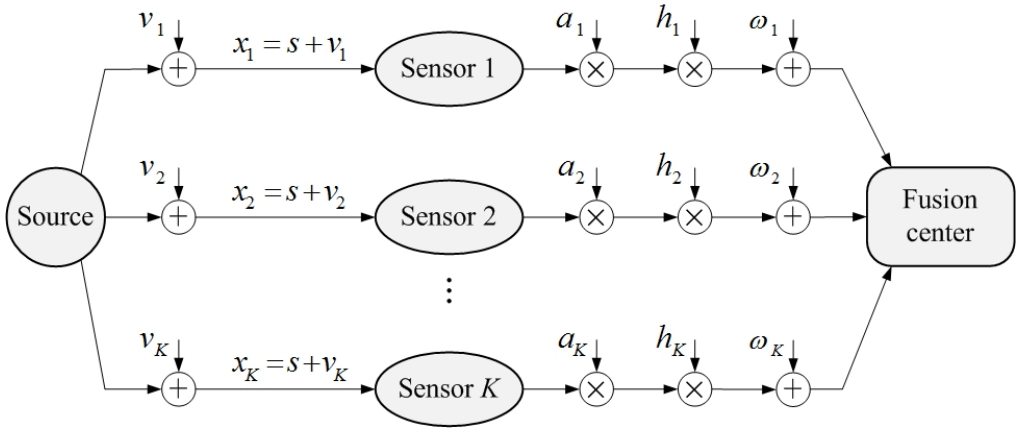

Figure 3.2 System model of a wireless sensor network using the orthogonal MAC.

Figure 3.2 shows a wireless sensor network with the orthogonal MAC [22]. In this MAC, K sensors transmit their observations to the FC via K orthogonal channels, which can be

realized with orthogonal frequency-division multiplexing. The orthogonal MAC removes the requirement of feedback of channel responses form the FC to the sensors, and hence is more favourable for implementation. However, the key disadvantage of the orthogonal MAC is that it requires larger transmission bandwidth to realize multiple orthogonal channels. More importantly, using K orthogonal channels means that there are K channel noise components at the FC, which makes the estimation performance suffer more from channel noise.

At the FC, the channel phase on each wireless channel is compensated first. After such phase compensation, all the useful information is found in the real parts of the processed signals. On the ith wireless channel, by taking the real part, one has[1]

$$y_i = a_i \left(s + v_i\right) r_i + \mathcal{R}\left\{\omega e^{-j\varphi_i}\right\} = a_i r_i s + a_i v_i r_i + \mathcal{R}\left\{\omega e^{-j\varphi_i}\right\} = \bar{r}_i s + \bar{v}_i + \bar{\omega}_i, \tag{3.5}$$

where $\bar{r}_i = a_i r_i$, $\bar{v}_i = a_i v_i r_i$ and $\bar{\omega}_i = \mathcal{R}\left\{\omega e^{-j\varphi_i}\right\}$. Let $\mathbf{y} = \left[y_1, y_2, \ldots, y_K\right]^\top$, $\bar{\mathbf{r}} = \left[\bar{r}_1, \bar{r}_2, \ldots, \bar{r}_K\right]^\top$, $\bar{\mathbf{v}} = \left[\bar{v}_1, \bar{v}_2, \ldots, \bar{v}_K\right]^\top$ and $\bar{\boldsymbol{\omega}} = \left[\bar{\omega}_1, \bar{\omega}_2, \ldots, \bar{\omega}_K\right]^\top$. Then equation (3.5) turns to

$$\mathbf{y} = \bar{\mathbf{r}} s + \bar{\mathbf{v}} + \bar{\boldsymbol{\omega}}. \tag{3.6}$$

The LMMSE estimator of s based on $\mathbf{y}$ is

$$\check{s} = \sigma_s^2 \bar{\mathbf{r}}^\top \left(\sigma_s^2 \bar{\mathbf{r}} \bar{\mathbf{r}}^\top + \boldsymbol{\Sigma}_{\bar{\mathbf{v}}} + \boldsymbol{\Sigma}_{\bar{\omega}}\right)^{-1} \mathbf{y}, \tag{3.7}$$

where

$$\boldsymbol{\Sigma}_{\bar{\mathbf{v}}} = \mathcal{E}\left\{\bar{\mathbf{v}} \bar{\mathbf{v}}^\top\right\} = \operatorname{diag}\left(a_1^2 r_1^2 \sigma_v^2,\, a_2^2 r_2^2 \sigma_v^2,\, \ldots,\, a_K^2 r_K^2 \sigma_v^2\right) \tag{3.8}$$

and

$$\boldsymbol{\Sigma}_{\bar{\omega}} = \mathcal{E}\left\{\bar{\boldsymbol{\omega}} \bar{\boldsymbol{\omega}}^\top\right\} = \operatorname{diag}\left(\frac{\sigma_\omega^2}{2}, \frac{\sigma_\omega^2}{2}, \ldots, \frac{\sigma_\omega^2}{2}\right). \tag{3.9}$$

The corresponding MSE distortion is

$$\epsilon = \left[\sigma_s^{-2} + \bar{\mathbf{r}}^\top \left(\boldsymbol{\Sigma}_{\bar{\mathbf{v}}} + \boldsymbol{\Sigma}_{\bar{\omega}}\right)^{-1} \bar{\mathbf{r}}\right]^{-1} = \left(\sigma_s^{-2} + \sum_{i=1}^{K} \frac{a_i^2 r_i^2}{a_i^2 r_i^2 \sigma_v^2 + \frac{\sigma_\omega^2}{2}}\right)^{-1}. \tag{3.10}$$

With equal power allocation, $a_i = \sqrt{P_{\text{tot}} / K\left(\sigma_s^2 + \sigma_v^2\right)}$ and equation (3.10) turns to

$$\epsilon = \sigma_s^2 \left[1 + \sum_{i=1}^{K} \frac{\frac{r_i^2}{K}}{\frac{r_i^2}{K}\frac{1}{\gamma_{\text{o}}} + \frac{1}{2\gamma_{\text{c}}}\left(1 + \frac{1}{\gamma_{\text{o}}}\right)}\right]^{-1}. \tag{3.11}$$

[1]For complex scalars, vectors and matrices, $\mathcal{R}\{\cdot\}$ denotes the real part and $\mathcal{I}\{\cdot\}$ denotes the imaginary part.

3.4 Hybrid MAC

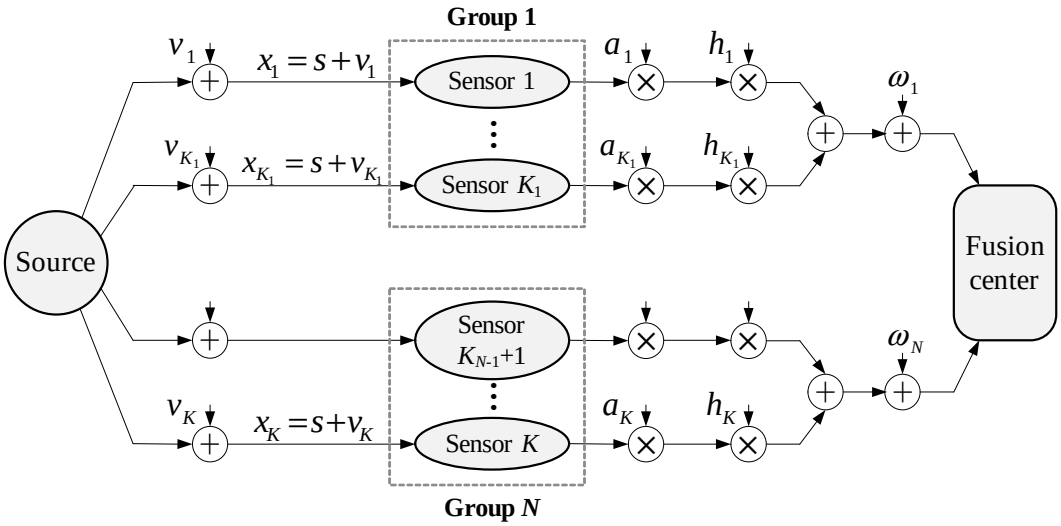

Figure 3.3 System model of a wireless sensor network using the hybrid MAC.

Figure 3.3 shows a wireless sensor network with the hybrid MAC [23]. In this MAC, all sensors are divided into groups and the coherent MAC is used for sensors within each group, whereas the orthogonal MAC is used across different groups. This MAC provides a solution for scenarios where are N (a small number due to bandwidth constraint) orthogonal channels that are shared by K sensors, where $K \geq N$. In addition, a flexible tradeoff between the coherent and orthogonal MACs can be obtained by changing the number of groups and the number of sensors within each group. As indicated in [23], in such a MAC, the MSE performance is dominated by intra-group coherent MACs using less sensors and can be minimized by assigning K sensors to N groups as uniformly as possible.

In this hybrid MAC, to obtain coherent combination in each group, channel phase information feedback from the FC to the sensors is still required and the amount of feedback is the same as that of the coherent MAC. In addition, the required transmission bandwidth in this MAC depends on the number of sensor groups.

After phase compensation, the transmitted signal at the ith sensor is $x_i = a_i\,(s + v_i)\,e^{-j\varphi_i}$. At the FC, on the nth wireless channel, all the useful information is in the real part of the

received signal, which can be expressed as

$$\begin{aligned} y_n &= \sum\nolimits_{i\in\Omega_n} a_i\left(s+v_i\right) r_i + \mathcal{R}\left\{\omega_n\right\}, \quad n=1,2,\ldots,N, \\ &= \left(\sum\nolimits_{i\in\Omega_n} a_i r_i\right) s + \left(\sum\nolimits_{i\in\Omega_n} a_i v_i r_i\right) + \mathcal{R}\left\{\omega_n\right\} = \bar{r}_n s + \bar{v}_n + \bar{\omega}_n, \end{aligned} \tag{3.12}$$

where Ω_n is the index set of sensors in the nth group, $\bar{r}_n = \sum_{i\in\Omega_n} a_i r_i$, $\bar{v}_n = \sum_{i\in\Omega_n} a_i v_i r_i$ and $\bar{\omega}_n = \mathcal{R}\left\{\omega_n\right\}$. Let $\mathbf{y} = \left[y_1, y_2, \ldots, y_N\right]^\top$, $\bar{\mathbf{r}} = \left[\bar{r}_1, \bar{r}_2, \ldots, \bar{r}_N\right]^\top$, $\bar{\mathbf{v}} = \left[\bar{v}_1, \bar{v}_2, \ldots, \bar{v}_N\right]^\top$ and $\bar{\boldsymbol{\omega}} = \left[\bar{\omega}_1, \bar{\omega}_2, \ldots, \bar{\omega}_N\right]^\top$, then similar to the orthogonal MAC, the LMMSE estimator of s based on $\mathbf{y}$ is

$$\check{s} = \sigma_s^2 \bar{\mathbf{r}}^\top \left(\sigma_s^2 \bar{\mathbf{r}}\bar{\mathbf{r}}^\top + \boldsymbol{\Sigma}_{\bar{\mathbf{v}}} + \boldsymbol{\Sigma}_{\bar{\omega}}\right)^{-1} \mathbf{y}, \tag{3.13}$$

where

$$\boldsymbol{\Sigma}_{\bar{\mathbf{v}}} = \mathcal{E}\left\{\bar{\mathbf{v}}\bar{\mathbf{v}}^\top\right\} = \operatorname{diag}\left(\sum\nolimits_{i\in\Omega_1} a_i^2 r_i^2 \sigma_v^2, \sum\nolimits_{i\in\Omega_2} a_i^2 r_i^2 \sigma_v^2, \ldots, \sum\nolimits_{i\in\Omega_N} a_i^2 r_i^2 \sigma_v^2\right) \tag{3.14}$$

and

$$\boldsymbol{\Sigma}_{\bar{\omega}} = \mathcal{E}\left\{\bar{\boldsymbol{\omega}}\bar{\boldsymbol{\omega}}^\top\right\} = \operatorname{diag}\left(\frac{\sigma_\omega^2}{2}, \frac{\sigma_\omega^2}{2}, \ldots, \frac{\sigma_\omega^2}{2}\right). \tag{3.15}$$

The corresponding MSE distortion is

$$\epsilon = \left[\sigma_s^{-2} + \bar{\mathbf{r}}^\top \left(\boldsymbol{\Sigma}_{\bar{\mathbf{v}}} + \boldsymbol{\Sigma}_{\bar{\omega}}\right)^{-1} \bar{\mathbf{r}}\right]^{-1} = \left[\sigma_s^{-2} + \sum_{n=1}^{N} \frac{\left(\sum_{i\in\Omega_n} a_i r_i\right)^2}{\left(\sum_{i\in\Omega_n} a_i^2 r_i^2\right)\sigma_v^2 + \frac{\sigma_\omega^2}{2}}\right]^{-1}. \tag{3.16}$$

With equal power allocation, $a_i = \sqrt{P_{\text{tot}}/K\left(\sigma_s^2 + \sigma_v^2\right)}$ and equation (3.16) turns to

$$\epsilon = \sigma_s^2 \left[1 + \sum_{n=1}^{N} \frac{\left(\sum_{i\in\Omega_n} \frac{r_i}{\sqrt{K}}\right)^2}{\left(\sum_{i\in\Omega_n} \frac{r_i^2}{K}\right)\frac{1}{\gamma_{\text{o}}} + \frac{1}{2\gamma_{\text{c}}}\left(1 + \frac{1}{\gamma_{\text{o}}}\right)}\right]^{-1}. \tag{3.17}$$

3.5 Performance and Overhead Comparison

In previous subsections, three important MACs have been introduced. In the following, the performance and overhead of these MACs will be studied and compared.

3.5.1 Average MSE Performance

Figure 3.4 shows the average MSE distortion achieved by the coherent, orthogonal and the hybrid MACs. Each point in the figure is obtained by averaging over 10,000 independent channel realizations. According to the simulation results, one has the following observations:

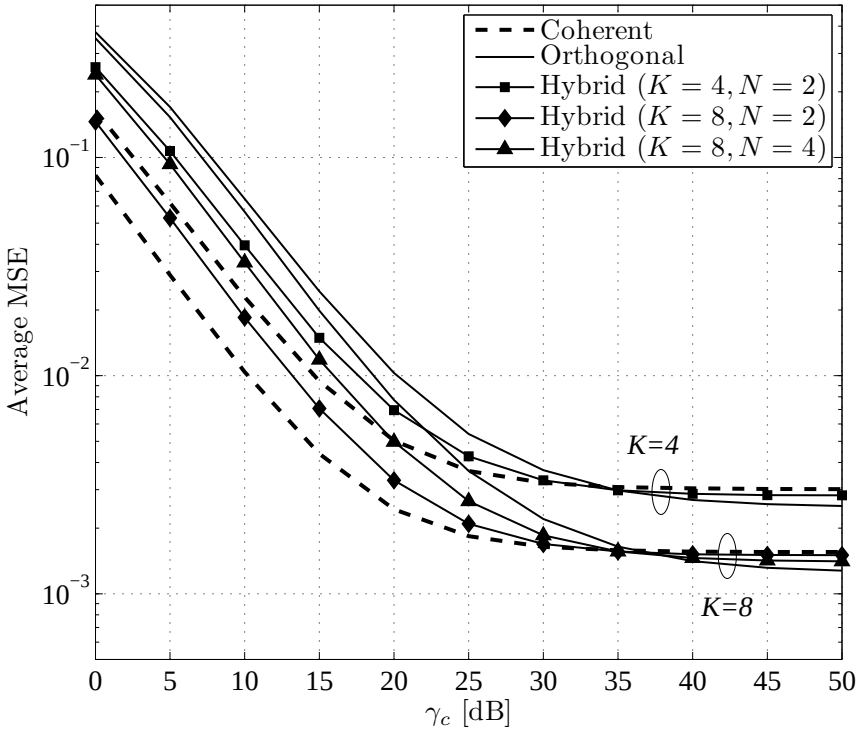

Figure 3.4 Average MSE performance of the coherent, orthogonal and hybrid MACs: $\gamma_o = 20$ dB.

- For all three MACs, the final average MSE decreases as the total transmitted power P_{tot} increases. However, the effect of increasing P_{tot} on the average MSE fades away as P_{tot} approaches infinity. With infinite P_{tot} (i.e., infinite γ_{c}), the average MSE converges to a positive constant.

- For all three MACs, when the number of sensors K increases from 4 to 8, the average MSE performance is improved.

- Compared to the orthogonal MAC with the same number of sensors, the coherent MAC performs better at low γ_{c} and worse at high γ_{c}.

- The hybrid MAC has performance lying between those of the coherent MAC and the orthogonal MAC with the same number of sensors. This is expected by the design philosophy of the hybrid MAC.

According to the expressions of the MSE, there are two kinds of distortion contributing to the final MSE: one is caused by channel noise (indicated by γ_{c} in ϵ) and the other by observation noise (indicated by γ_{o} in ϵ). Next, two estimation performance indicators are established for the above two kinds of distortion. First, setting $\sigma_v^2 = 0$ (i.e., $\gamma_{\mathrm{o}} = \infty$) gives $\mathbf{\Sigma}_{\bar{v}} = \mathbf{0}$ and the MSE distortion becomes

$$\epsilon = \left[\sigma_s^{-2} + \bar{\mathbf{h}}^{\top} \left(\mathbf{\Sigma}_{\bar{\omega}}\right)^{-1} \bar{\mathbf{h}}\right]^{-1} = \sigma_s^2 \left(1 + 2\alpha\gamma_{\mathrm{c}}\right)^{-1}. \tag{3.18}$$

The parameter α indicates the impact of channel noise on the MSE performance. The larger α is, the lesser the impact is. On the other hand, setting $\sigma_\omega^2 = 0$ (i.e., $\gamma_{\mathrm{c}} = \infty$) gives $\mathbf{\Sigma}_{\bar{\omega}} = \mathbf{0}$ and the MSE distortion is

$$\epsilon = \left[\sigma_s^{-2} + \bar{\mathbf{h}}^{\top} \left(\mathbf{\Sigma}_{\bar{\mathbf{v}}}\right)^{-1} \bar{\mathbf{h}}\right]^{-1} = \sigma_s^2 \left(1 + \beta\gamma_{\mathrm{o}}\right)^{-1}. \tag{3.19}$$

In this case, the parameter β indicates the impact of observation noise on the MSE performance. The larger β is, the lesser the impact is.

In the following, the expectations of these two parameters over channel realizations, $\mathcal{E}\{\alpha\}$ and $\mathcal{E}\{\beta\}$, are evaluated to explore the long-term effects of channel noise and observation noise on the MSE performance. $\mathcal{E}\{\alpha\}$ and $\mathcal{E}\{\beta\}$ are named as the channel noise suppression capability indicator and the observation noise suppression capability indicator, respectively. In general, with the same number of sensors, different MACs yield different values of $\mathcal{E}\{\alpha\}$ and $\mathcal{E}\{\beta\}$, implying different capabilities of channel noise suppression and observation noise suppression.

For the coherent MAC,

$$\mathcal{E}_{\mathrm{coh}}\{\alpha\} = \mathcal{E}\left\{\left(\sum_{i=1}^{K} \frac{r_i}{\sqrt{K}}\right)^2\right\} \tag{3.20}$$

and

$$\mathcal{E}_{\mathrm{coh}}\{\beta\} = \mathcal{E}\left\{\frac{\left(\sum_{i=1}^{K} \frac{r_i}{\sqrt{K}}\right)^2}{\frac{1}{K}\left(\sum_{i=1}^{K} r_i^2\right)}\right\}. \tag{3.21}$$

For the orthogonal MAC,

$$\mathcal{E}_{\mathrm{orth}}\{\alpha\} = \mathcal{E}\left\{\sum_{i=1}^{K} \frac{r_i^2}{K}\right\} = 1 \tag{3.22}$$

and

$$\mathcal{E}_{\text{orth}}\{\beta\} = K. \tag{3.23}$$

For the hybrid MAC,

$$\mathcal{E}_{\text{hyb}}\{\alpha\} = \mathcal{E}\left\{\sum_{n=1}^{N}\left(\sum\nolimits_{i\in\Omega_n}\frac{r_i}{\sqrt{K}}\right)^2\right\} \tag{3.24}$$

and

$$\mathcal{E}_{\text{hyb}}\{\beta\} = \mathcal{E}\left\{\sum_{n=1}^{N}\frac{\left(\sum_{i\in\Omega_n}\frac{r_i}{\sqrt{K}}\right)^2}{\frac{1}{K}\left(\sum_{i\in\Omega_n}r_i^2\right)}\right\}. \tag{3.25}$$

As $K\to\infty$, according to the central limit theorem, $\sum_{i=1}^{K}\frac{r_i}{\sqrt{K}}$ is a Gaussian random variable with mean $\sqrt{K}\mathcal{E}\{r_i\}$ and variation $\mathcal{D}\{r_i\}$. Since r_i is a Rayleigh distributed random variable with pdf $f_{r_i}(r_i) = 2r_i\exp(-r_i^2)$, it follows that $\mathcal{E}\{r_i\} = \sqrt{\frac{\pi}{4}}$ and $\mathcal{D}\{r_i\} = 1-\frac{\pi}{4}$. Thus

$$\mathcal{E}_{\text{coh}}\{\alpha\} = \frac{K\pi}{4} + 1 - \frac{\pi}{4} \approx 0.78K, \tag{3.26}$$

$$\mathcal{E}_{\text{coh}}\{\beta\} = \frac{\mathcal{E}\left\{\left(\sum_{i=1}^{K}\frac{r_i}{\sqrt{K}}\right)^2\right\}}{\mathcal{E}\{r_i^2\}} = \frac{K\pi}{4} + 1 - \frac{\pi}{4} \approx 0.78K. \tag{3.27}$$

Similarly, it can be shown that

$$\mathcal{E}_{\text{hyb}}\{\alpha\} = \frac{K\pi}{4N} + 1 - \frac{\pi}{4} \approx \frac{0.78}{N}K, \tag{3.28}$$

$$\mathcal{E}_{\text{hyb}}\{\beta\} = \frac{N^2\mathcal{E}\left\{\left(\sum_{i\in\Omega_n}\frac{r_i}{\sqrt{K}}\right)^2\right\}}{\mathcal{E}\{r_i^2\}} = \frac{K\pi}{4} + N\left(1-\frac{\pi}{4}\right) \approx 0.78K. \tag{3.29}$$

Table 3.1 $\mathcal{E}\{\alpha\}$ and $\mathcal{E}\{\beta\}$ for the coherent, orthogonal and hybrid MACs.

Type of MAC	$\mathcal{E}\{\alpha\}$	$\mathcal{E}\{\beta\}$
Coherent	$0.78K$	$0.78K$
Orthogonal	1	K
Hybrid	$\frac{0.78}{N}K$	$0.78K$

The values of $\mathcal{E}\{\alpha\}$ and $\mathcal{E}\{\beta\}$ for the coherent, orthogonal and hybrid MACs are summarized in Table 3.1. Based on the above two kinds of distortion, the observations of the average MSE can be explained as follows:

- Increasing the total transmitted power P_{tot} can only decrease the distortion caused by the channel noise. With infinite P_{tot}, the distortion caused by the channel noise vanishes and the average MSE converges to $\mathcal{E}\{\sigma_s^2 (1+\beta\gamma_{\text{o}})^{-1}\}$.

- As long as at least one of $\mathcal{E}\{\alpha\}$ and $\mathcal{E}\{\beta\}$ increases as K increases, the final average MSE benefits from using more sensors. For all the three MACs discussed here, this condition is satisfied.

- Compared to the orthogonal MAC with the same number of sensors, the coherent MAC has a much larger $\mathcal{E}\{\alpha\}$ (especially for large K) and a slightly smaller $\mathcal{E}\{\beta\}$. This means that the coherent MAC is much better at suppressing channel noise while a little worse at suppressing observation noise. As a result, the coherent MAC performs better at low γ_{c}, where channel noise is dominant, and performs worse at high γ_{c}, where observation noise is dominant. The reason that the orthogonal MAC suffers much more from channel noise is that there are K channel noise components in the orthogonal MAC, while there is only one channel noise component in the coherent MAC.

- The hybrid MAC has a channel noise suppression capability between those of the coherent and orthogonal MACs and the same observation noise suppression capability as that of the coherent MAC. In general, the average MSE of the hybrid MAC lies between those of the coherent and orthogonal MACs.

3.5.2 Bandwidth and Feedback Requirements

The bandwidth requirement for each MAC is directly related to the number of required orthogonal channels. For the coherent, orthogonal and hybrid MAC (with N groups) with K sensors, the numbers of orthogonal channels are 1, K and N. The coherent MAC is the most bandwidth efficient since only one channel is used. In addition, for the hybrid MAC, N can be fixed to a small value to save bandwidth.

In terms of feedback requirement, there is no need of any information feedback in the orthogonal MAC. For the coherent MAC, due to the requirement of coherent combination of signals from all the sensors to be transmitted on one channel, channel phases need to be

transmitted from the FC to the sensors. The exact number of bits used for such information feedback depends on the capability of the feedback channel and the required accuracy, but this is certainly a large amount of overhead. For the hybrid MAC, although more than one orthogonal channels are used and coherent combination is only required among signals transmitted on the same channel, the amount of channel information feedback from the FC to the sensors is still the same as that of the coherent MAC.

3.5.3 Outage Probability

Regarding estimation performance criteria in WSNs, beside the average MSE, another criterion, the diversity order of the outage probability, has also been proposed to evaluate the reliability of the estimation system. As defined in [22], the outage probability $\mathcal{P}_{D_0}$ of an estimation system is

$$\mathcal{P}_{D_0} = \text{Prob}\left\{\epsilon > D_0\right\}, \tag{3.30}$$

where D_0 is a predefined threshold. The lower $\mathcal{P}_{D_0}$ is, the more reliable the estimation system is.

In the orthogonal MAC, according to Theorem 3.1 in [22], for a sufficiently large but finite K and $D_0 > D_\infty$, the outage probability asymptotically converges to (as K increases) $\exp\left[-KI_\eta\left(a\right)\right]$, where D_∞ is the average MSE achieved by infinite K and $I_\eta\left(a\right)$ is a function of $\eta = \gamma_c / \left(1 + \frac{1}{\gamma_o}\right)$ and $a = \sigma_s^2 / \left(D_0 P_{\text{tot}}\right)$. It can be seen that K plays the role of estimation diversity order in that the outage probability decreases exponentially with K. In [22], it has also been shown by simulation results that the outage probability curve illustrates a diversity order of K approximately even for small values of K.

On the other hand, although the coherent MAC has favourable average MSE performance, namely high estimation accuracy, it cannot provide such diversity gain by using more sensors. The estimation diversity order of the coherent MAC is always 1.

However, as revealed in the following simulation results, in the opinion of the author of this thesis, the performance criterion of using the diversity order of the outage probability is not very meaningful to indicate the estimation reliability. According to Figures 3.5, 3.6 and 3.7, one has the following observations:

- For all values of K, D_0 and γ_c, the orthogonal MAC always has a fixed diversity order

that is proportional to K, which is consistent with the conclusion in [22].

- When D_0 is high (e.g., 0.01), in the γ_c range from 0 dB to 50 dB, the coherent MAC has the same diversity order as that of the orthogonal MAC, even for a small value $K = 2$. In addition, the coherent MAC reaches the same $\mathcal{P}_{D_0}$ with a smaller γ_c compared to that of the orthogonal MAC. The larger K is, the bigger the gap between the γ_c's of the two MACs for the same $\mathcal{P}_{D_0}$ is.

- As D_0 decreases (e.g., 0.005 and 0.002), for the coherent MAC with small K working in high γ_c range, a fixed diversity order cannot be maintained and the curves become flat. With $D_0 = 0.005$, the coherent MAC with $K = 8$ can reach $\mathcal{P}_{D_0}$ smaller than 10^{-4} before the curve becomes flat, while with $D_0 = 0.002$, the $\mathcal{P}_{D_0}$ curve becomes flat at about 10^{-2}.

In general, the diversity order of the coherent MAC is only 1, but this doesn't mean that the coherent MAC provides lower estimation reliability than the orthogonal MAC. If the estimation system works with large K and in a low γ_c range, since the coherent MAC can reach a very low outage probability at γ_c much smaller than that of the orthogonal MAC (for example, the gap is more than 10 dB for $K = 16$ and $D_0 = 0.005$), it may provide a higher reliability compared to the orthogonal MAC.

In the remaining part of this thesis, only the average MSE is adopted as the estimation performance criterion and the diversity order of the outage probability will not be discussed any further. More accurate and efficient performance criteria can be established in the future to evaluate the estimation reliability.

3.6 Summary

In this chapter, three important MACs, the coherent, orthogonal and hybrid MACs, are studied and compared in terms of estimation performance and bandwidth and feedback requirements. The coherent MAC is the most bandwidth efficient and has significant advantage in the average MSE performance at low to moderate γ_c. The main problem of this MAC is the requirement of a large amount of feedback. In contrast, the orthogonal MAC requires no feedback but large transmission bandwidth. In terms of the average MSE, it only

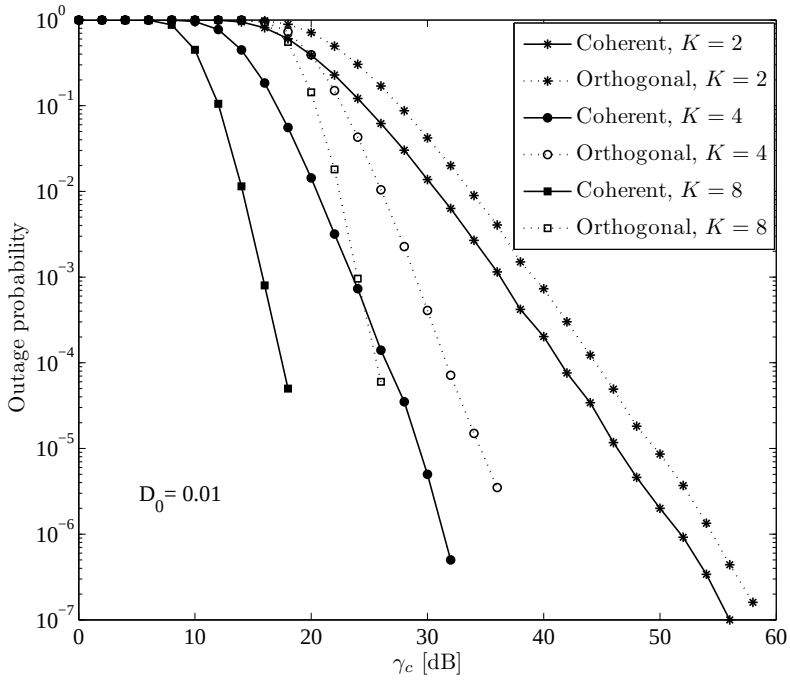

Figure 3.5 Outage probabilities of the coherent and orthogonal MACs ($D_0 = 0.01$, $\gamma_o = 20$ dB).

outperforms the coherent MAC a little at high γ_c. The hybrid MAC is a tradeoff between the coherent and orthogonal MACs, and both of its average MSE performance and bandwidth requirement lie between those of the other two MACs. In addition, as shown in the last subsection, due to its limitation in indicating the estimation reliability, the performance criterion of outage probability's diversity order will not be used in this thesis.

In the next chapter, a novel semi-orthogonal MAC will be proposed and studied. Similar to the hybrid MAC, this MAC provides a solution for scenarios that a small number of orthogonal channels are shared by more sensors. However, it is a better tradeoff between the coherent and orthogonal MACs when the average MSE performance and the feedback overhead are considered. By using more sensors, the semi-orthogonal MAC can achieve the same average MSE performance as that of the coherent MAC, while only a small amount of feedback is required in the semi-orthogonal MAC.

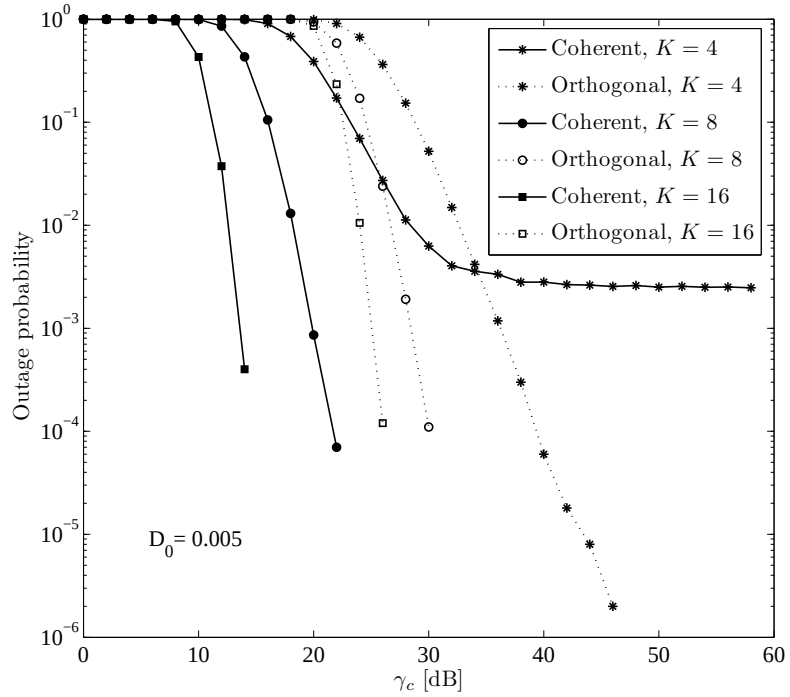

Figure 3.6 Outage probabilities of the coherent and orthogonal MACs ($D_0 = 0.005$, $\gamma_o = 20$ dB).

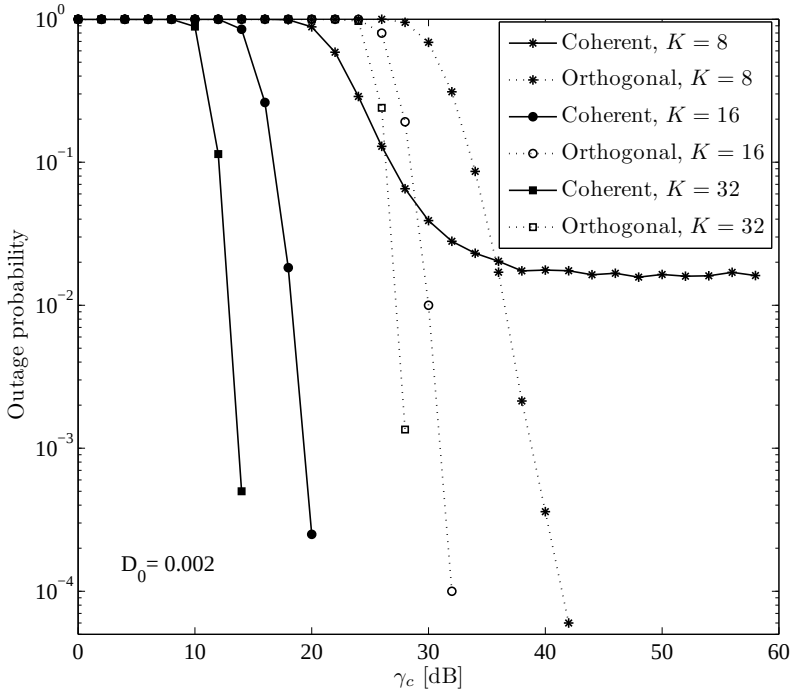

Figure 3.7 Outage probabilities of the coherent and orthogonal MACs ($D_0 = 0.002$, $\gamma_o = 20$ dB).

4. The Proposed Semi-orthogonal MAC

4.1 Introduction

In the previous chapter, three popular MACs were studied and compared. The coherent MAC has the best average MSE performance and is the most bandwidth efficient. However, to obtain coherent combination in the coherent MAC, the channel phase information needs to be transmitted from the FC to the sensors, which represents a large amount of feedback. On the other hand, the orthogonal MAC removes the requirement of feedback, but it consumes larger transmission bandwidth. In addition, its final average MSE suffers more from channel noise compared to the coherent MAC.

Motivated from the above discussion, this chapter focuses on the design of a wireless sensor network in order to improve the average MSE estimation performance under both bandwidth and power constraints. Specially, considered is a scenario where there are N (a small number due to bandwidth constraint) orthogonal channels that are shared by K sensors, where $K \geq N$, for transmitting the sensors' observations to the FC. An obvious approach to the above design problem is sensor grouping, and the hybrid MAC discussed in the previous chapter is one solution. In such a hybrid MAC, all sensors are divided into groups and the coherent MAC is used for sensors within each group, whereas the orthogonal MAC is used across different groups. A flexible tradeoff between the coherent and orthogonal MACs can therefore be obtained by changing the number of groups and the number of sensors in each group. However, in the hybrid MAC, to obtain coherent combination in each group, the same amount of channel information feedback from the FC to the sensors as that of the coherent MAC is still required.

In a sharp contrast to the hybrid MAC, the sensor grouping proposed in this chapter is such that sensors in one group transmit on one orthogonal channel without any channel

phase compensation at the transmitter. This means that the signals from sensors within one group are directly superimposed instead of coherently combined as in the hybrid MAC. To distinguish from the other MACs discussed before, the proposed MAC shall be called a semi-orthogonal MAC. In the previous chapter, two indicators of estimation performance were established based on the MSE distortion: the channel noise suppression capability indicator and the observation noise suppression capability indicator. These two performance indicators are also used in this chapter to investigate the estimation performances of the proposed semi-orthogonal MAC.

The proposed semi-orthogonal MAC can be implemented with either *fixed* or *adaptive* sensor grouping. In fixed sensor grouping, each sensor transmits on fixed orthogonal channels. In general, more than one orthogonal channel can be allocated to one sensor. However, it shall be shown that such channel allocation causes correlation among the equivalent channel responses[1] and degrades the estimation performance. As such, fixed sensor grouping should be done in such a way that the groups are disjoint. It is shown that, under the same bandwidth and power constraints and when the number of sensors K approaches infinity, the semi-orthogonal MAC has the same channel noise suppression capability but two times the observation noise suppression capability when compared to the orthogonal MAC.

For adaptive sensor grouping, sensors are grouped according to the ranges (i.e., sub-regions) that their channel phases fall into. It is shown that, compared to fixed sensor grouping, the MSE performance of the semi-orthogonal MAC with adaptive grouping is improved by a large margin. In fact the performance of the semi-orthogonal MAC with adaptive grouping is very close to the performance of the hybrid MAC under the same bandwidth and power constraints and the same number of sensors. It should be emphasized again that channel information feedback is not required in the semi-orthogonal MAC with adaptive sensor grouping. The only extra cost for implementing the proposed semi-orthogonal MAC is a few bits of feedback information from the FC to the sensors to indicate channel allocation. This amount of feedback overhead is significantly smaller than what required for channel information in the coherent and hybrid MACs. It shall also be demonstrated that $N = 4$ is the optimum setting that gives the best tradeoff between bandwidth consumption and

[1]The definition and meaning of equivalent channel responses will be made clearer in Section 4.2.

estimation performance.

4.2 System Model

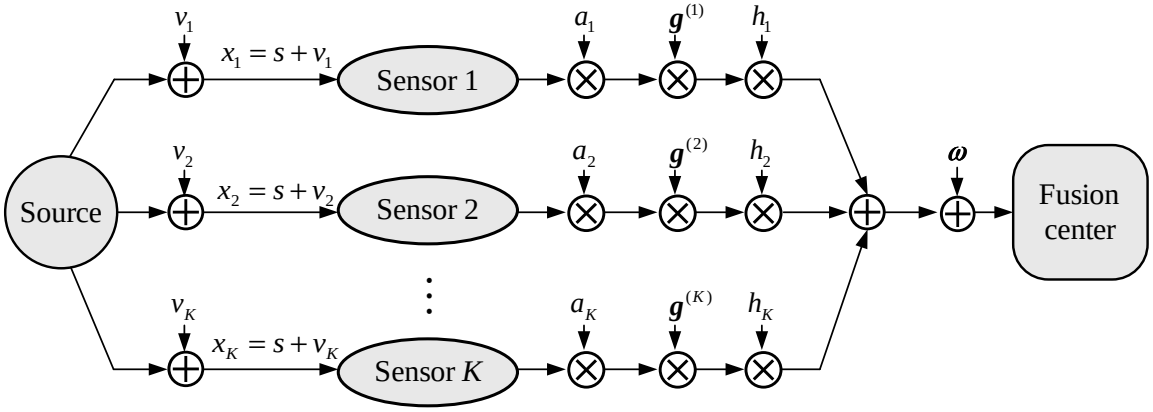

Figure 4.1 System model of a wireless sensor network using the proposed semi-orthogonal MAC.

Figure 4.1 illustrates the wireless sensor network with the proposed semi-orthogonal MAC. There are K sensors that are used to monitor a source signal s and communicate their observations to a FC over N orthogonal channels. The observation of the ith sensor can be expressed as

$$x_i = s + v_i, \quad 1 \leq i \leq K, \tag{4.1}$$

where the source signal s and observation noise v_i are treated as random variables with zero mean and variances σ_s^2 and σ_v^2, respectively. Using analog modulation, the ith sensor simply amplifies x_i with a gain a_i and transmits the result to the FC according to a length-N vector $\mathbf{g}^{(i)} = \left[g_1^{(i)}, g_2^{(i)}, \ldots, g_N^{(i)}\right]$, whose element is either 0 or 1. The set of $\mathbf{g}^{(i)}$'s gives an allocation of N orthogonal channels to K sensors. For the ith sensor, if the nth element of $\mathbf{g}^{(i)}$ is 1, then the ith sensor transmits on the nth orthogonal channel.[2]

At the FC, the received signal on the nth orthogonal channel is

$$y_n = \left[\sum_{i=1}^{K} a_i \left(s + v_i\right) g_n^{(i)} h_i\right] + \omega_n, \quad n = 1, 2, \ldots, N, \tag{4.2}$$

[2]This allocation is similar to the transmission in an overloaded code-division multiple access (CDMA) systems [31, 32] if one views vector $\mathbf{g}^{(i)}$ as the signature vector of sensor i.

where ω_n's are the i.i.d. (over n) complex AWGN components with zero mean and variance σ_ω^2. Note that it is assumed that the orthogonal channels assigned for a particular sensor have the same response. This assumption is reasonable because typically the orthogonal channels are composed of adjacent frequency bands or time slots and the wireless channel is assumed to change slowly.

Equation (4.2) can be rewritten as

$$y_n = \left(\sum_{i=1}^{K} a_i g_n^{(i)} h_i\right) s + \left(\sum_{i=1}^{K} a_i v_i g_n^{(i)} h_i\right) + \omega_n = \hat{h}_n s + \hat{v}_n + \omega_n, \tag{4.3}$$

where $\hat{h}_n = \sum_{i=1}^{K} a_i g_n^{(i)} h_i$ and $\hat{v}_n = \sum_{i=1}^{K} a_i v_i g_n^{(i)} h_i$ are defined as the *equivalent* channel response and *equivalent* observation noise of the nth orthogonal channel, respectively. Since y_n is complex, while s is real, the phase of the equivalent channel response $\hat{h}_n$ is compensated to obtain

$$\begin{aligned}
\bar{y}_n &= \mathcal{R}\left\{\frac{\hat{h}_n^*}{\left|\hat{h}_n\right|} y_n\right\} \qquad (4.4)\\
&= \left|\sum_{i=1}^{K} a_i g_n^{(i)} h_i\right| s + \mathcal{R}\left\{\frac{\left(\sum_{i=1}^{K} a_i g_n^{(i)} h_i^*\right)\left(\sum_{i=1}^{K} a_i v_i g_n^{(i)} h_i\right)}{\left|\sum_{i=1}^{K} a_i g_n^{(i)} h_i\right|}\right\} + \mathcal{R}\left\{\frac{\left(\sum_{i=1}^{K} a_i g_n^{(i)} h_i^*\right)\omega_n}{\left|\sum_{i=1}^{K} a_i g_n^{(i)} h_i\right|}\right\}\\
&= \bar{h}_n s + \bar{v}_n + \bar{\omega}_n.
\end{aligned}$$

The above phase compensation discards halves of observation noise and channel noise. It is pointed out that the phase compensation of the equivalent channel response is performed at the FC. Therefore no phase information is needed at the sensors and feedback of channel phase information is not required.

Let $\bar{\mathbf{y}} = [\bar{y}_1, \bar{y}_2, \ldots, \bar{y}_N]^\top$, $\bar{\mathbf{h}} = \left[\bar{h}_1, \bar{h}_2, \ldots, \bar{h}_N\right]^\top$, $\bar{\mathbf{v}} = [\bar{v}_1, \bar{v}_2, \ldots, \bar{v}_N]^\top$ and $\bar{\boldsymbol{\omega}} = [\bar{\omega}_1, \bar{\omega}_2, \ldots, \bar{\omega}_N]^\top$. Then one has

$$\bar{\mathbf{y}} = \bar{\mathbf{h}} s + \bar{\mathbf{v}} + \bar{\boldsymbol{\omega}}. \tag{4.5}$$

The LMMSE estimator is adopted at the FC. Accordingly, the estimate of s based on $\bar{\mathbf{y}}$ is

$$\check{s} = \sigma_s^2 \bar{\mathbf{h}}^\top \left(\sigma_s^2 \bar{\mathbf{h}} \bar{\mathbf{h}}^\top + \boldsymbol{\Sigma}_{\bar{\mathbf{v}}} + \boldsymbol{\Sigma}_{\bar{\omega}}\right)^{-1} \bar{\mathbf{y}}, \tag{4.6}$$

where

$$\mathbf{\Sigma}_{\bar{\mathbf{v}}} = \mathcal{E}\left\{\bar{\mathbf{v}}\bar{\mathbf{v}}^{\top}\right\} = \left\{\theta_{n,l} = \sigma_v^2 \sum_{i=1}^{K} a_i^2 g_n^{(i)} g_l^{(i)} t_{ni} t_{li}; \quad n,l = 1,2,\ldots,N\right\}, \tag{4.7}$$

$$t_{ni} = \mathcal{R}\left\{h_i\right\} \frac{\mathcal{R}\left\{\hat{h}_n\right\}}{\left|\hat{h}_n\right|} + \mathcal{I}\left\{h_i\right\} \frac{\mathcal{I}\left\{\hat{h}_n\right\}}{\left|\hat{h}_n\right|}, \tag{4.8}$$

and

$$\mathbf{\Sigma}_{\bar{\omega}} = \mathcal{E}\left\{\bar{\boldsymbol{\omega}}\bar{\boldsymbol{\omega}}^{\top}\right\} = \mathrm{diag}\left(\frac{\sigma_\omega^2}{2}, \frac{\sigma_\omega^2}{2}, \ldots, \frac{\sigma_\omega^2}{2}\right). \tag{4.9}$$

The corresponding MSE distortion is

$$\epsilon = \left[\sigma_s^{-2} + \bar{\mathbf{h}}^{\top}\left(\mathbf{\Sigma}_{\bar{\mathbf{v}}} + \mathbf{\Sigma}_{\bar{\omega}}\right)^{-1}\bar{\mathbf{h}}\right]^{-1}. \tag{4.10}$$

4.3 Semi-orthogonal MAC with Fixed Sensor Grouping

In this section, for simplicity, it is assumed that the number of sensors that transmit on each orthogonal channel is the same for all channels and the number of orthogonal channels used by each sensor is the same for all sensors. Furthermore, the total transmitted power is equally allocated among sensors and orthogonal channels. Let K_1 $(0 \leq K_1 \leq K)$ denote the number of sensors transmitting on each orthogonal channel. Then the gain is $a_i = \bar{a} = \sqrt{\frac{P_{\mathrm{tot}}}{NK_1(\sigma_s^2+\sigma_v^2)}}$.

As mentioned in Chapter 3, two indicators of estimation performance can be obtained based on the expression of the MSE distortion. First, setting $\sigma_v^2 = 0$ gives $\mathbf{\Sigma}_{\bar{\mathbf{v}}} = \mathbf{0}$ and the MSE distortion becomes

$$\epsilon = \left[\sigma_s^{-2} + \bar{\mathbf{h}}^{\top}\left(\mathbf{\Sigma}_{\bar{\omega}}\right)^{-1}\bar{\mathbf{h}}\right]^{-1} = \sigma_s^2\left(1 + 2\alpha\gamma_{\mathrm{c}}\right)^{-1}, \tag{4.11}$$

where $\alpha = \sum_{n=1}^{N}\left|\frac{\sum_{i=1}^{K} g_n^{(i)} h_i}{\sqrt{NK_1}}\right|^2$. The parameter α indicates the impact of channel noise on the MSE performance. The larger α is, the lesser the impact is.

On the other hand, setting $\sigma_\omega^2 = 0$ gives $\mathbf{\Sigma}_{\bar{\omega}} = \mathbf{0}$ and the MSE distortion is

$$\epsilon = \left[\sigma_s^{-2} + \bar{\mathbf{h}}^{\top}\left(\mathbf{\Sigma}_{\bar{\mathbf{v}}}\right)^{-1}\bar{\mathbf{h}}\right]^{-1} = \sigma_s^1\left(1 + \beta\gamma_{\mathrm{o}}\right)^{-1}, \tag{4.12}$$

where $\beta = \sigma_v^2\bar{\mathbf{h}}^{\top}\left(\mathbf{\Sigma}_{\bar{\mathbf{v}}}\right)^{-1}\bar{\mathbf{h}}$. In this case, the parameter β indicates the impact of observation noise on the MSE performance. The larger β is, the lesser the impact is. In next section, the performance of the proposed semi-orthogonal MAC will be investigated in terms of the expectations of these two parameters, $\mathcal{E}\left\{\alpha\right\}$ and $\mathcal{E}\left\{\beta\right\}$.

4.3.1 Correlation Analysis of the Equivalent Channel Responses

When assigning N orthogonal channels to K sensors, where $K \geq N$, an obvious question arises: *Should more than one orthogonal channel be assigned to a single sensor and will this improve the MSE performance of distributed estimation?* To answer this question, let's examine a simple scenario where there are two orthogonal channels with K_1 sensors transmitting on each of them. The gain in this case is $a_i = \bar{a} = \sqrt{\frac{P_{\text{tot}}}{2K_1(\sigma_s^2+\sigma_v^2)}}$. Note that there are $M = \max(2K_1 - K, 0)$ sensors that transmit on both orthogonal channels. Treating the equivalent channel responses $\hat{h}_1 = \bar{a}\sum_{i=1}^{K} g_1^{(i)} h_i$ and $\hat{h}_2 = \bar{a}\sum_{i=1}^{K} g_2^{(i)} h_i$ as random variables, the correlation coefficient between $\hat{h}_1$ and $\hat{h}_2$ is computed as

$$\rho = \frac{\mathcal{E}\left\{\hat{h}_1 \hat{h}_2^*\right\}}{\sqrt{\mathcal{D}\left(\hat{h}_1\right)}\sqrt{\mathcal{D}\left(\hat{h}_2\right)}} = \frac{M}{K_1}. \tag{4.13}$$

If there is no sensor transmitting on both orthogonal channels, $M = 0$ and the above correlation coefficient will be zero. However, such scenario requires that $K = 2K_1$ and all K sensors are equally divided into 2 disjoint groups with sensors in each group transmitting on one orthogonal channel.

Next, define $\tilde{h}_1 = \frac{1}{\sqrt{2K_1}}\sum_{i=1}^{K} g_1^{(i)} h_i = \frac{m_1}{\sqrt{2}} \mathrm{e}^{j\phi_1}$ and $\tilde{h}_2 = \frac{1}{\sqrt{2K_1}}\sum_{i=1}^{K} g_2^{(i)} h_i = \frac{m_2}{\sqrt{2}} \mathrm{e}^{j\phi_2}$. Then $\alpha = \left|\tilde{h}_1\right|^2 + \left|\tilde{h}_2\right|^2 = \frac{1}{2}\left(m_1^2 + m_2^2\right)$.

To obtain the expression for β, first one has

$$\begin{aligned}
\theta_{1,2} &= \sigma_v^2 \bar{a}^2 \sum_{i=1}^{K} g_1^{(i)} \left(\mathcal{R}\left\{h_i\right\}\cos\phi_1 + \mathcal{I}\left\{h_i\right\}\sin\phi_1\right) g_2^{(i)} \left(\mathcal{R}\left\{h_i\right\}\cos\phi_2 + \mathcal{I}\left\{h_i\right\}\sin\phi_2\right) \\
&= \frac{\sigma_v^2 P_{\text{tot}}}{\sigma_s^2+\sigma_v^2}\left[\cos\phi_1\cos\phi_2\left(\sum_{i=1}^{K}\frac{g_1^{(i)}g_2^{(i)}}{2K_1}\mathcal{R}^2\left\{h_i\right\}\right) + \sin\phi_1\sin\phi_2\left(\sum_{i=1}^{K}\frac{g_1^{(i)}g_2^{(i)}}{2K_1}\mathcal{I}^2\left\{h_i\right\}\right)\right. \\
&\quad \left. + \left(\cos\phi_1\sin\phi_2 + \sin\phi_1\cos\phi_2\right)\left(\sum_{i=1}^{K}\frac{g_1^{(i)}g_2^{(i)}}{2K_1}\mathcal{R}\left\{h_i\right\}\mathcal{I}\left\{h_i\right\}\right)\right].
\end{aligned} \tag{4.14}$$

When K and K_1 approach infinity, one has $\sum_{i=1}^{K}\frac{g_1^{(i)}g_2^{(i)}}{2K_1}\mathcal{R}^2\left\{h_i\right\} = \frac{M}{2K_1}\mathcal{E}\left\{\mathcal{R}^2\left\{h_i\right\}\right\} = \frac{\rho}{2}\frac{1}{2} = \frac{\rho}{4}$, $\sum_{i=1}^{K}\frac{g_1^{(i)}g_2^{(i)}}{2K_1}\mathcal{I}^2\left\{h_i\right\} = \frac{\rho}{4}$, and $\sum_{i=1}^{K}\frac{g_1^{(i)}g_2^{(i)}}{2K_1}\mathcal{R}\left\{h_i\right\}\mathcal{I}\left\{h_i\right\} = 0$. It then follows that

$$\theta_{1,2} = \frac{\sigma_v^2 P_{\text{tot}}}{\sigma_s^2+\sigma_v^2}\frac{\rho}{4}\left(\cos\phi_1\cos\phi_2 + \sin\phi_1\sin\phi_2\right) = \frac{\sigma_v^2 P_{\text{tot}}}{\sigma_s^2+\sigma_v^2}\frac{\rho}{4}\cos\left(\phi_1 - \phi_2\right). \tag{4.15}$$

Similarly, one can show that $\theta_{2,1} = \theta_{1,2} = \frac{\sigma_v^2 P_{\text{tot}}}{\sigma_s^2+\sigma_v^2}\frac{\rho_{nl}}{4}\cos(\phi_1 - \phi_2)$ and $\theta_{1,1} = \theta_{2,2} = \frac{\sigma_v^2 P_{\text{tot}}}{4(\sigma_s^2+\sigma_v^2)}$. Therefore,

$$\begin{aligned}\beta &= \begin{bmatrix} \left|\tilde{h}_1\right| & \left|\tilde{h}_2\right| \end{bmatrix} \begin{bmatrix} \frac{1}{4} & \frac{\rho\cos(\phi_1-\phi_2)}{4} \\ \frac{\rho\cos(\phi_1-\phi_2)}{4} & \frac{1}{4} \end{bmatrix}^{-1} \begin{bmatrix} \left|\tilde{h}_1\right| \\ \left|\tilde{h}_2\right| \end{bmatrix} \\ &= \frac{2\left[m_1^2 - 2\rho\cos(\phi_1-\phi_2)\, m_1 m_2 + m_2^2\right]}{1-\rho^2\cos^2(\phi_1-\phi_2)}. \end{aligned} \tag{4.16}$$

With the above expressions of α and β, Appendix 7.1 shows that their expectations are given by

$$\begin{aligned}&\mathcal{E}\{\alpha\} \\ &= \frac{2(1-\rho^2)^2}{\pi}\int_1^0 \frac{(\rho^2x^2)^2}{\sqrt{1-x^2}}\left[\mathrm{F}\left(1,3,2,1-\rho^2x^2\right) + 2\mathrm{F}\left(1,3,\frac{5}{2},\rho^2x^2\right)\right]\mathrm{d}x + \frac{(1-\rho^2)^2}{\pi} \\ &\quad \int_1^0 \frac{\rho^2x^2}{\sqrt{1-x^2}}\left[\left(1+3\rho^2x^2\right)\mathrm{F}\left(1,3,3,1-\rho^2x^2\right) + 4\left(1+\rho^2x^2\right)\mathrm{F}\left(1,3,\frac{3}{2},\rho^2x^2\right)\right]\mathrm{d}x,\end{aligned} \tag{4.17}$$

and

$$\begin{aligned}&\mathcal{E}\{\beta\} \\ &= \frac{4(1-\rho^2)^2}{\pi}\int_1^0 \frac{(\rho^2x^2)^2}{(1-\rho^2x^2)\sqrt{1-x^2}}\left[2\mathrm{F}\left(1,3,2,1-\rho^2x^2\right) + \frac{4}{3}\mathrm{F}\left(1,3,\frac{5}{2},\rho^2x^2\right)\right]\mathrm{d}x \\ &\quad + \frac{4(1-\rho^2)^2}{\pi}\int_1^0 \frac{\rho^2x^2}{\sqrt{1-x^2}}\left[\mathrm{F}\left(1,3,3,1-\rho^2x^2\right) + 4\mathrm{F}\left(1,3,\frac{3}{2},\rho^2x^2\right)\right]\mathrm{d}x,\end{aligned} \tag{4.18}$$

where $\mathrm{F}(\alpha,\beta,\gamma,z)$ is the Gauss hypergeometric function [33].

At this point, the connection between the correlation among the equivalent channel responses of the orthogonal channels and the capabilities of channel noise suppression and observation noise suppression has been established for $N = 2$ and K approaching infinity. Figure 4.2 plots the expressions in (4.17) and (4.18) versus ρ together with the values obtained by simulation for $N = 2$. As can be seen, $\mathcal{E}\{\alpha\}$ is basically a constant while $\mathcal{E}\{\beta\}$ is a monotonically-decreasing function of ρ. This means that, while the correlation among the equivalent channel responses barely affects the channel noise suppression capability, it reduces the observation noise suppression capability. Overall, the correlation among the equivalent channel responses degrades the estimation performance, and hence should

be avoided. This can be done by not assigning more than one orthogonal channel to each sensor.

Simulation results for the more general cases of $N > 2$ and finite numbers of sensors are provided next to verify the above conclusions. For $N > 2$, it is not easy to determine channel allocation among sensors and perform the corresponding correlation analysis among the equivalent channel responses of the orthogonal channels. Nevertheless, the following general channel allocation scheme shall be investigated. Assume that K is an integer multiple of N. If $\frac{(n-1)K}{N} + K_1 \leq K$, then the nth orthogonal channel is shared by sensors with indices in the set of $\left\{\frac{(n-1)K}{N} + 1, \ldots, \frac{(n-1)K}{N} + K_1\right\}$. If $\frac{(n-1)K}{N} + K_1 > K$, then the set of sensor indices is $\left\{1, \ldots, \frac{(n-1)K}{N} + K_1 - K\right\} \cup \left\{\frac{(n-1)K}{N} + 1, \ldots, K\right\}$. As long as $K_1 > \frac{K}{N}$, some sensors will transmit on more than one orthogonal channel and the correlation among the equivalent channel responses of orthogonal channels is not zero. As K_1 increases from $\frac{K}{N}$ to K, more and more sensors transmit on more than one orthogonal channel and the correlation among the equivalent channel responses increases from 0 to 1. Therefore K_1 can be used to approximately indicate the level of correlation among the equivalent channel responses. As shown in Figure 4.3, for the three settings of ($N = 2$, $K = 16$), ($N = 4$, $K = 32$) and ($N = 8$, $K = 64$), as K_1 increases $\mathcal{E}\{\alpha\}$ basically stays the same, while $\mathcal{E}\{\beta\}$ decreases, although not monotonically. As expected, $\mathcal{E}\{\beta\}$ takes on the largest value when $K_1 = \frac{K}{N}$.

From the above theoretical derivations and simulation results, in the rest of this thesis, only one orthogonal channel is assigned to each sensor. In other words, all sensors are divided into disjoint groups and those sensors in the same group transmit on one orthogonal channel. For convenience, allocation of orthogonal channels is indicated by $\{\Omega_n\}_{n=1}^{N}$, where Ω_n is the index set of sensors that transmit on the nth orthogonal channel.

4.3.2 Estimation Performance with Fixed Sensor Grouping

Fixed sensor grouping considered in this section means that the orthogonal channel used by each sensor, once assigned, does not change during the communication phase. Considered is the same channel allocation scheme with zero correlation among the equivalent channel responses as described in Section 4.3.1, i.e., $K_1 = \frac{K}{N}$ and $\Omega_n = \left\{\frac{(n-1)K}{N} + 1, \ldots, \frac{nK}{N}\right\}$. In this case, with equal power allocation, the gain is $a_i = \bar{a} = \sqrt{\frac{P_{\text{tot}}}{K(\sigma_s^2+\sigma_v^2)}}$.

Compared in Figure 4.4 are the average MSE distortions achieved by the orthogonal,

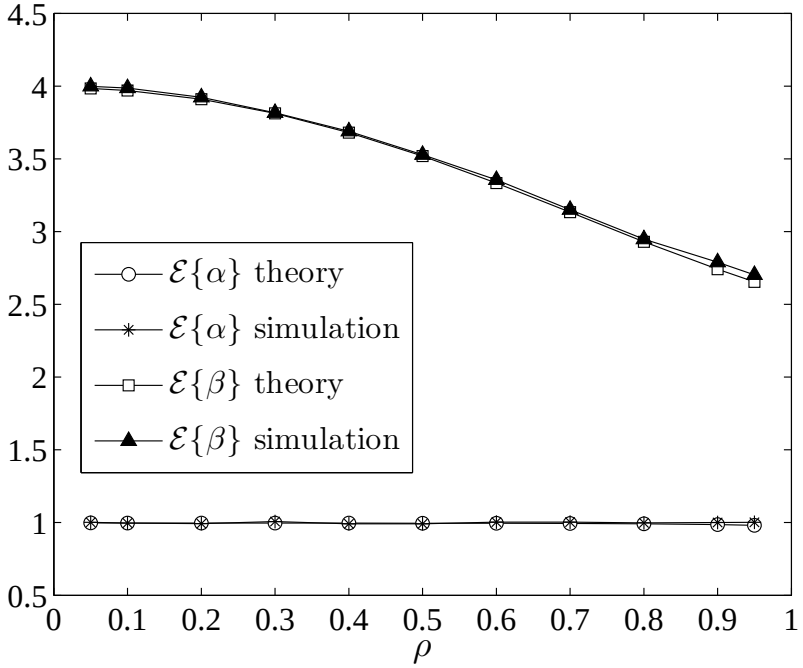

Figure 4.2 $\mathcal{E}\{\alpha\}$ and $\mathcal{E}\{\beta\}$ as functions of ρ.

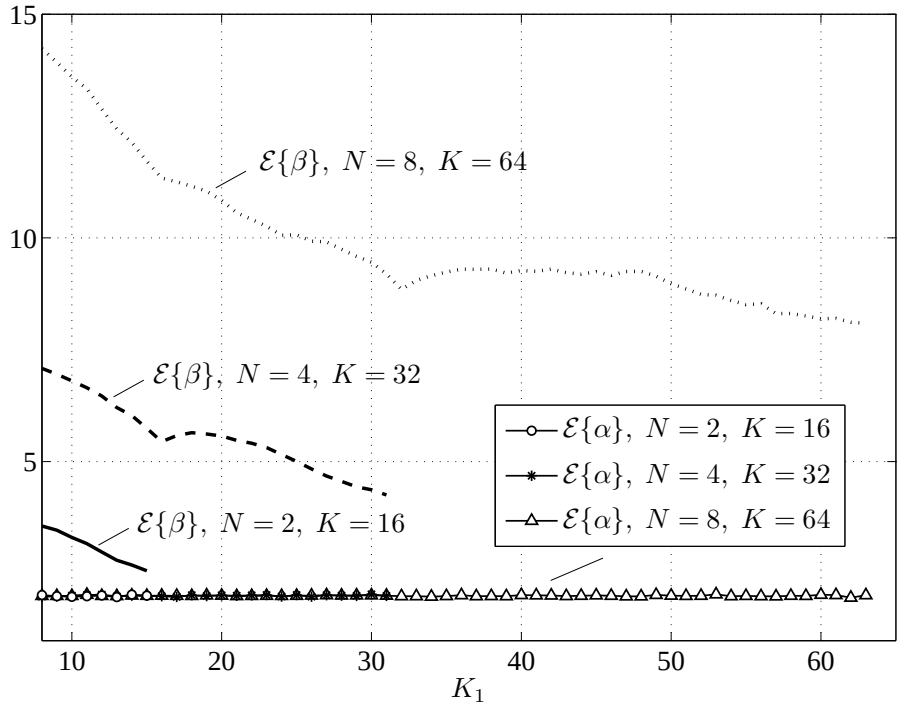

Figure 4.3 $\mathcal{E}\{\alpha\}$ and $\mathcal{E}\{\beta\}$ as functions of K_1.

coherent and the proposed semi-orthogonal MACs. Each point in these figures is obtained by averaging over 10,000 independent channel realizations. In all of the three MACs, there are K sensors, while the numbers of orthogonal channels (which translate proportionally to the amounts of bandwidth) are: K, 1, and N for the orthogonal, coherent, and semi-orthogonal MACs, respectively. Throughout this thesis, unless stated otherwise, the total transmitted power is the same for all MACs.

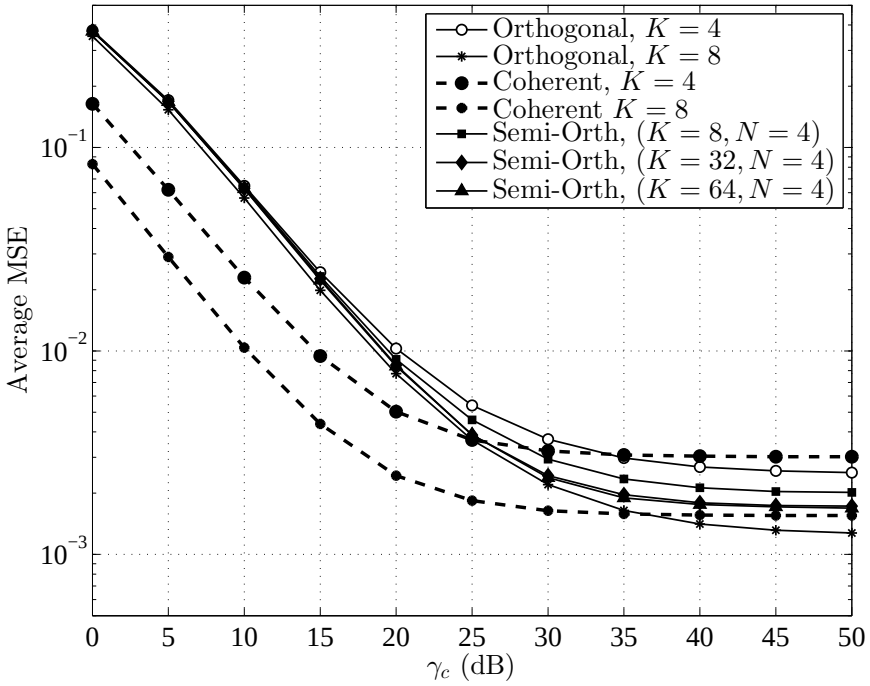

Figure 4.4 Average MSE performance of the orthogonal, coherent and semi-orthogonal MACs: $\gamma_o = 20$ dB.

Compared to the coherent MAC with the same number of sensors, the semi-orthogonal MAC consumes more bandwidth and has worse MSE performance. However, the advantage of the coherent MAC comes at the expensive price of channel phase information feedback, which is not needed in the semi-orthogonal MAC.

With the same number of orthogonal channels but using more sensors, the semi-orthogonal MAC outperforms the orthogonal MAC, especially at high γ_c. As the number of sensors increases, the performance of the semi-orthogonal MAC is enhanced but the performance improvement due to using each extra sensor reduces. The average MSE asymptotically converges to a lower bound as K goes to infinity. This is similar to the orthogonal MAC. The

most significant improvement occurs when K increases from 4 (one time of N) to 16 (4 times of N). When K is larger than 32 (8 times of N), the performance improvement due to increasing K is almost negligible.

Before closing this section, a more detailed performance comparison between the orthogonal MAC and the proposed semi-orthogonal MAC is carried out. The comparison is done for a fixed number of N orthogonal channels (i.e., fixed transmission bandwidth). For the parameter α, in the orthogonal MAC with N sensors, $\mathcal{E}_{\text{orth}}\{\alpha\} = 1$, whereas in the semi-orthogonal MAC with K sensors, one has $\mathcal{E}_{\text{semi}}\{\alpha\} = \mathcal{E}\left\{\sum_{n=1}^{N}\left|\frac{\sum_{i\in\Omega_n} h_i}{\sqrt{K}}\right|^2\right\} = 1$, which is the same as that in the orthogonal MAC. This means that both the semi-orthogonal MAC and the orthogonal MAC have the same channel noise suppression capability.

For the parameter β, it is a constant N in the orthogonal MAC for any channel realization. On the other hand, in the semi-orthogonal MAC,

$$\beta = \sum_{n=1}^{N}\beta_n = \sum_{n=1}^{N}\frac{\left|\sum_{i\in\Omega_n} a_i h_i\right|^2}{\sum_{i\in\Omega_n} a_i^2\left(\mathcal{R}\{h_i\}\frac{\mathcal{R}\{\hat{h}_n\}}{|\hat{h}_n|} + \mathcal{I}\{h_i\}\frac{\mathcal{I}\{\hat{h}_n\}}{|\hat{h}_n|}\right)^2}. \tag{4.19}$$

The value of β depends on the instantaneous channel realization, and it is a random variable. The pdf of β was obtained by simulation and is plotted in Figure 4.5 for various values of $\frac{K}{N}$. The corresponding mean values of β are shown in Table 4.1.

Table 4.1 Values of $\mathcal{E}_{\text{semi}}\{\beta\}$ with $N = 4$.

K	4	8	16	32	64	128
$\mathcal{E}_{\text{semi}}\{\beta\}$	4	5.3	6.4	7.1	7.5	7.8

Figure 4.5 clearly shows that, as long as $\frac{K}{N} > 1$, there is a high probability that the value of β is larger than $N = 4$. Furthermore, the larger the ratio $\frac{K}{N}$ is, the more likely β takes on a larger value. In fact, it can be shown that when $K \to \infty$, β follows a gamma distribution with parameters $a = N$ and $b = 2$. The proof is as follows.

Recall that

$$\beta_n = \frac{\left|\sum_{i\in\Omega_n}\sqrt{\frac{N}{K}}h_i\right|^2}{\frac{N}{K}\sum_{i\in\Omega_n}\left(\mathcal{R}\{h_i\}\frac{\mathcal{R}\{\hat{h}_n\}}{|\hat{h}_n|} + \mathcal{I}\{h_i\}\frac{\mathcal{I}\{\hat{h}_n\}}{|\hat{h}_n|}\right)^2}, \tag{4.20}$$

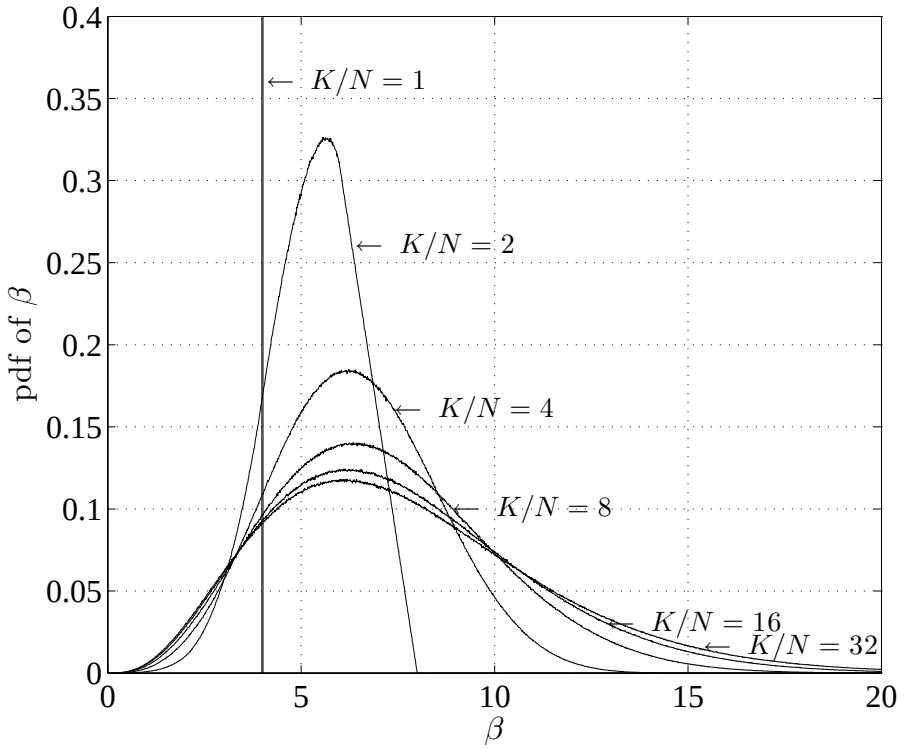

Figure 4.5 pdf of parameter β with $N = 4$.

and β_n's are independent to each other.

Let $\tilde{h}_n = \sum_{i\in\Omega_n} \sqrt{\frac{N}{K}} h_i = m_n \mathrm{e}^{j\phi_n}$. Then $\tilde{h}_n$ is a circularly symmetric complex Gaussian random variables with zero mean and variance 1. The numerator of β_n, $\left|\tilde{h}_n\right|^2$, is of exponential distribution with parameter $\lambda = 1$, whose pdf is

$$f_{\left|\tilde{h}_n\right|^2}\left(\left|\tilde{h}_n\right|^2\right) = \exp\left(-\left|\tilde{h}_n\right|^2\right). \tag{4.21}$$

Since $\hat{h}_n$ has the same phase as $\tilde{h}_n$, so the denominator of β_n turns to

$$\begin{aligned} & \frac{N}{K}\sum\nolimits_{i\in\Omega_n} \left(\mathcal{R}\left\{h_i\right\}\cos\phi_n + \mathcal{I}\left\{h_i\right\}\sin\phi_n\right)^2 \\ = \; & \left(\frac{N}{K}\sum\nolimits_{i\in\Omega_n} \mathcal{R}^2\left\{h_i\right\}\right)\cos^2\phi_n + \left(\frac{N}{K}\sum\nolimits_{i\in\Omega_n} \mathcal{I}^2\left\{h_i\right\}\right)\sin^2\phi_n \\ & +2\left(\frac{N}{K}\sum\nolimits_{i\in\Omega_n} \mathcal{R}\left\{h_i\right\}\mathcal{I}\left\{h_i\right\}\right)\cos\phi_n\sin\phi_n. \end{aligned} \tag{4.22}$$

When $K \to \infty$, according to the strong law of large numbers, (4.22) turns to

$$\begin{aligned} & \mathcal{E}\left\{\mathcal{R}^2\left\{h_i\right\}\right\}\cos^2\phi_n + \mathcal{E}\left\{\mathcal{I}^2\left\{h_i\right\}\right\}\sin^2\phi_n + 2\mathcal{E}\left\{\mathcal{R}\left\{h_i\right\}\mathcal{I}\left\{h_i\right\}\right\}\cos\phi_n\sin\phi_n \\ = \; & \frac{1}{2}\cos^2\phi_n + \frac{1}{2}\sin^2\phi_n = \frac{1}{2}. \end{aligned} \tag{4.23}$$

Therefore, when $K \to \infty$, $\beta_n = 2\left|\tilde{h}_n\right|^2$ is exponentially distributed with parameter $\lambda = 2$, whose pdf is

$$f_{\beta_n}\left(\beta_n\right) = \frac{1}{2}\exp\left(\frac{\beta_n}{2}\right),\ \beta_n \geq 0. \tag{4.24}$$

Finally, it is well known that the sum of N independent and identically distributed (i.i.d.) exponential random variables with parameter $\lambda = 2$ is a gamma random variable with parameters $a = N$ and $b = 2$. For completeness, the pdf of the gamma distribution is as follows:

$$f_\beta\left(\beta\right) = \frac{\beta^{a-1}}{\Gamma\left(a\right)b^a}\exp\left(-\frac{\beta}{b}\right), \quad \beta \geq 0,\ a > 0,\ b > 0, \tag{4.25}$$

where $\Gamma\left(a\right) = \int_0^\infty x^{a-1}\mathrm{e}^{-x}\mathrm{d}x$ is the gamma function. If a is an integer, then $\Gamma\left(a\right) = (a-1)!$.

As a result, the upper bound of $\mathcal{E}_{\text{semi}}\left\{\beta\right\}$ is $2N$. Thus, compared to the orthogonal MAC, the semi-orthogonal MAC has a better observation noise suppression capability, but it is bounded by two times the observation noise suppression capability of the orthogonal MAC.

In summary, when the number of orthogonal channels is fixed, the semi-orthogonal MAC has the same channel noise suppression capability and greater observation noise suppression capability when compared to the orthogonal MAC. This clearly explains why the semi-orthogonal MAC outperforms the orthogonal MAC, especially at high γ_{c} where observation noise is dominant.

4.4 Semi-Orthogonal MAC with Adaptive Sensor Grouping

Recall that the expressions of α and β in the semi-orthogonal MAC with disjoint sensor grouping and equal power allocation are as follows:

$$\alpha = \sum_{n=1}^{N}\alpha_n = \sum_{n=1}^{N}\left|\sum\nolimits_{i\in\Omega_n}\frac{h_i}{\sqrt{K}}\right|^2, \tag{4.26}$$

$$\beta = \sum_{n=1}^{N} \beta_n = \sum_{n=1}^{N} \frac{\left| \sum_{i \in \Omega_n} \frac{h_i}{\sqrt{K}} \right|^2}{\sum_{i \in \Omega_n} \frac{1}{K} \left(\mathcal{R}\{h_i\} \frac{\mathcal{R}\{\hat{h}_n\}}{|\hat{h}_n|} + \mathcal{I}\{h_i\} \frac{\mathcal{I}\{\hat{h}_n\}}{|\hat{h}_n|} \right)^2}. \tag{4.27}$$

It can be seen that α is a sum of α_n's, where each α_n is affected only by the channel responses of sensors transmitting on the nth orthogonal channel. Therefore α_n can be interpreted as an indicator of the channel noise suppression capability of the nth orthogonal channel. Similarly, β_n, which is also affected only by the channel responses of sensors transmitting on the nth orthogonal channel, can be interpreted as the indicator of the observation noise suppression capability of the nth orthogonal channel. This simple observation suggests that if all sensors can be properly grouped according to their channel responses, larger α_n and β_n can be obtained for each orthogonal channel and thus the overall channel noise suppression and observation noise suppression capabilities of the semi-orthogonal MAC will be improved.

4.4.1 Grouping Sensors Based on the Instantaneous Channel Responses

Intuitively, sensors with channel responses of similar phases should be grouped together to get better channel noise suppression and observation noise suppression. Will this "similar phase" grouping strategy work and how to define "similar phase"? To answer this question, examine a scenario that one sensor with channel response of magnitude 1 and phase 0 transmits on an orthogonal channel. Both the indicators of the channel noise suppression and observation noise suppression of this orthogonal channel are 1. Next, add another sensor with channel response of magnitude r ($r < 1$) and phase ϑ ($0 \leq \vartheta \leq \pi$) to form a group[3]. Then the two indicators of this orthogonal channel change to:

$$\alpha_n = (r\cos\vartheta + 1)^2 + (r\sin\vartheta)^2 = r^2 + 2r\cos\vartheta + 1, \tag{4.28}$$

$$\beta_n = \frac{r^2 + 2r\cos\vartheta + 1}{(\cos\phi)^2 + (r\cos\vartheta\cos\phi + r\sin\vartheta\sin\phi)^2}, \tag{4.29}$$

where ϕ is the phase of the equivalent channel response and $\tan\phi = \frac{r\sin\vartheta}{r\cos\vartheta+1}$.

If $\alpha_n > 1$, the added sensor is said to be *constructive* for channel noise suppression and if $\beta_n > 1$, the added sensor is *constructive* for observation noise suppression. Note that if

[3]If the channel response of the added sensor is of magnitude larger than 1, then it can be taken as the first sensor and the other sensor is taken as the added sensor.

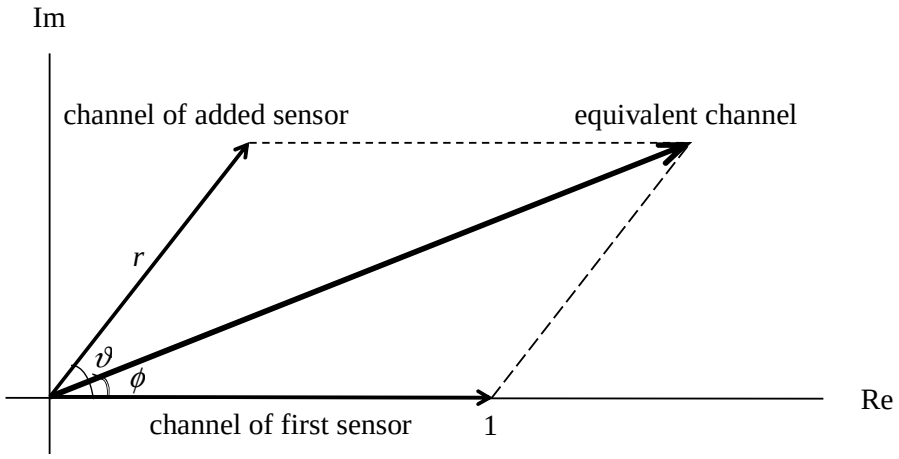

Figure 4.6 The channel responses of the original and added sensors.

the added sensor transmits on an orthogonal channel alone, then $\alpha_n = r^2$ and $\beta_n = 1$. This means that if the added sensor is constructive, sensor grouping improves performance of individual sensors (i.e., without being grouped).

In order to see if the added sensor is constructive for channel noise suppression and/or observation noise suppression, it is straightforward to show from (4.28) and (4.29) that

$$\begin{cases} \alpha_n > 1, & \text{if } 0 \le \vartheta < \arccos\left(-\frac{r}{2}\right) \\ \alpha_n \le 1, & \text{if } \arccos\left(-\frac{r}{2}\right) \le \vartheta \le \pi \end{cases} \tag{4.30}$$

and

$$\begin{cases} \beta_n > 1, & \text{if } 0 \le \vartheta < \arccos\left(-r\right) \\ \beta_n \le 1, & \text{if } \arccos\left(-r\right) \le \vartheta \le \pi \end{cases} \tag{4.31}$$

The above analysis leads to the following three regions of ϑ (see Figure 4.7):

- If ϑ is in region A, i.e., $0 \le \vartheta < \arccos\left(-\frac{r}{2}\right)$, the added sensor is constructive for both channel noise suppression and observation noise suppression. Note that region A includes $\left[0, \frac{\pi}{2}\right]$, regardless of the value of r.

- If ϑ is in region B, i.e., $\arccos\left(-\frac{r}{2}\right) \le \vartheta < \arccos\left(-r\right)$, the added sensor is destructive for channel noise suppression, but constructive for observation noise suppression.

- If ϑ is in region C, i.e., $\arccos\left(-r\right) \le \vartheta < \pi$, the added sensor is destructive for both channel noise suppression and observation noise suppression.

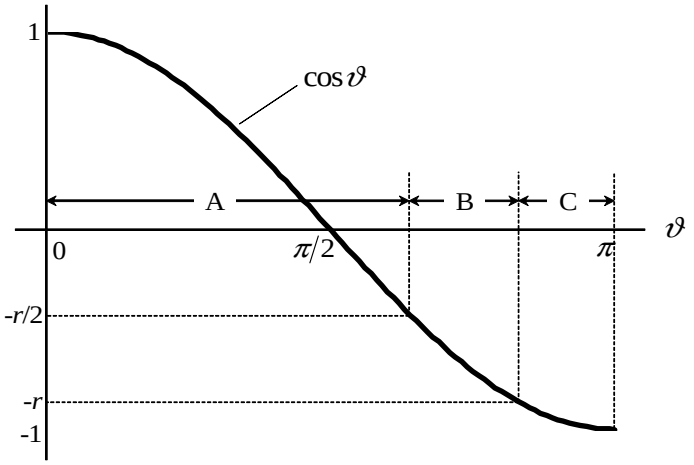

Figure 4.7 Three regions of ϑ.

At this point, the question raised at the beginning of this subsection has been answered for grouping two sensors. In summary, if the phase difference between the channel responses of the two sensors is in the region of $\left[0, \frac{\pi}{2}\right]$, sensor grouping is beneficial. However if the phase difference is larger than $\frac{\pi}{2}$, grouping sensors on the same orthogonal channel may be destructive for either channel noise suppression or observation noise suppression, or for both of them, and sensor grouping may give worse performance.

Now consider a WSN using the proposed semi-orthogonal MAC with $N = 2$. If the whole phase region of 2π is partitioned into 2 equal sub-regions (each of length π), then grouping the sensors with channel phases in the same sub-region to transmit on the same orthogonal channel might not always be beneficial. However, for the WSN using the proposed semi-orthogonal MAC with $N \geq 4$, if the whole phase region is partitioned into N equal sub-regions (each of length $\frac{2\pi}{N}$), then grouping the sensors with channel phases in the same sub-region always picks constructive sensors in one group and therefore performance improvement is guaranteed. This is analyzed in more detail for $N = 4$ and $N > 4$ in the following subsections.

4.4.2 Performance Analysis for $N = 4$

With $N = 4$, the simplest partition of the 2π phase into 4 sub-regions is $\left[0, \frac{\pi}{2}\right)$, $\left[\frac{\pi}{2}, \pi\right)$, $\left[\pi, \frac{3\pi}{2}\right)$ and $\left[\frac{3\pi}{2}, 2\pi\right)$. Focusing on the sub-region $\left[0, \frac{\pi}{2}\right)$, define

$$\tilde{h}_1 = \sum\nolimits_{i \in \Omega_1} \frac{h_i}{\sqrt{K}}. \tag{4.32}$$

Let $h_i = x + jy$, then x and y are real *positive* (one-sided) Gaussian random variables with the same pdf of $\frac{2}{\sqrt{\pi}}\exp\left(-x^2\right),\ x > 0$. It is simple to show that the mean and variance of both x and y are $\mu_x = \mu_y = \frac{1}{\sqrt{\pi}}$ and $\sigma_x^2 = \sigma_y^2 = \frac{1}{2} - \frac{1}{\pi}$, respectively. As $K \to \infty$, according to the central limit theorem, $\tilde{h}_1$ is a complex Gaussian random variable with i.i.d. real and imaginary parts. Let $\tilde{h}_1 = \tilde{x} + j\tilde{y}$. Then it is simple to show that $\tilde{x}$ and $\tilde{y}$ are i.i.d. real Gaussian random variables with mean $\mu = \frac{\sqrt{K}}{4\sqrt{\pi}}$ and variance $\sigma^2 = \frac{1}{8} - \frac{1}{4\pi}$. It then follows that

$$\mathcal{E}\left\{\alpha_1\right\} = \mathcal{E}\left\{\tilde{x}^2 + \tilde{y}^2\right\} = 2(\mu^2 + \sigma^2). \tag{4.33}$$

To compute $\mathcal{E}\left\{\beta_1\right\}$, let $m = \sqrt{\tilde{x}^2 + \tilde{y}^2}$ and $\phi = \arctan\left(\frac{\tilde{y}}{\tilde{x}}\right)$. Then m and ϕ are independent. One has

$$\begin{aligned}
\mathcal{E}\left\{\beta_1\right\} &= \mathcal{E}\left\{\frac{m^2}{\sum_{i\in\Omega_1}\frac{1}{K}\left[\mathcal{R}\left\{h_i\right\}\cos\phi + \mathcal{I}\left\{h_i\right\}\sin\phi\right]^2}\right\} \qquad (4.34)\\
&= \mathcal{E}\left\{\frac{4m^2}{\mathcal{E}\left\{\mathcal{R}^2\left\{h_i\right\}\right\}\cos^2\phi + \mathcal{E}\left\{\mathcal{I}^2\left\{h_i\right\}\right\}\sin^2\phi + 2\mathcal{E}\left\{\mathcal{R}\left\{h_i\right\}\right\}\mathcal{E}\left\{\mathcal{I}\left\{h_i\right\}\right\}\cos\phi\sin\phi}\right\}\\
&= \frac{4\mathcal{E}\left\{m^2\right\}}{\sigma_x^2 + \mu_x^2 + 2\mu_x^2\cos\phi\sin\phi} = \frac{8(\sigma^2+\mu^2)}{\sigma_x^2 + \mu_x^2 + 2\mu_x^2\cos\phi\sin\phi}
\end{aligned}$$

As $K \to \infty$, ϕ can be substituted by $\frac{\pi}{4}$ (see Appendix 7.2). Then one has $\mathcal{E}\left\{\beta_1\right\} = \frac{8\sigma^2+8\mu^2}{\sigma_x^2+2\mu_x^2}$.

Obviously, the same results apply for the other 3 sub-regions. Thus, for the semi-orthogonal MAC with adaptive sensor grouping and $N = 4$, one obtains

$$\mathcal{E}\left\{\alpha\right\} = \sum_{n=1}^{4}\mathcal{E}\left\{\alpha_n\right\} = 8\mu^2 + 8\sigma^2 = \frac{K}{2\pi} + 1 - \frac{2}{\pi} \approx 0.16K, \tag{4.35}$$

$$\mathcal{E}\left\{\beta\right\} = \sum_{n=1}^{4}\mathcal{E}\left\{\beta_n\right\} = \frac{32\sigma^2 + 32\mu^2}{\sigma_x^2 + 2\mu_x^2} = \frac{\frac{2K}{\pi} + 4 - \frac{8}{\pi}}{\frac{1}{2} + \frac{1}{\pi}} \approx 0.78K. \tag{4.36}$$

Table 4.2 compares $\mathcal{E}\left\{\alpha\right\}$ and $\mathcal{E}\left\{\beta\right\}$ among different MACs under a fixed number of sensors, K. To put these numbers in perspective, the number of orthogonal channels, N, required by each type of MAC is also indicated. The theoretical and simulation results of $\mathcal{E}\left\{\alpha\right\}$ and $\mathcal{E}\left\{\beta\right\}$ are shown in Figures. 4.8 and 4.9, respectively. Observe that when K is large enough, the theoretical results agree with the simulation results. For small K, the simulation result is better than the theoretical result for $\mathcal{E}\left\{\alpha\right\}$ of the semi-orthogonal MAC with fixed

sensor grouping. As for $\mathcal{E}\{\beta\}$, there are differences between the theoretical and simulation results of the hybrid MAC, and the semi-orthogonal MAC (with either fixed or adaptive sensor grouping). This observation suggests that for these three MACs, a sufficiently large number of sensors is required to achieve the asymptotic performance.

Table 4.2 Asymptotic performance in terms of $\mathcal{E}\{\alpha\}$ and $\mathcal{E}\{\beta\}$.

Type of MAC	$\mathcal{E}\{\alpha\}$	$\mathcal{E}\{\beta\}$	Number of orthogonal channels, N
Coherent	$0.78K$	$0.78K$	1
Orthogonal	1	K	K
Hybrid ($N = 4$)	$0.20K$	$0.78K$	4
semi-orthogonal, fixed grouping ($N = 4$)	1	8	4
semi-orthogonal, adaptive grouping ($N = 4$)	$0.16K$	$0.78K$	4

For the semi-orthogonal MAC with adaptive sensor grouping and $N = 4$, as $K \to \infty$, $\mathcal{E}\{\alpha\}$ and $\mathcal{E}\{\beta\}$ increases in the order of K, and thus the average MSE distortion finally goes to zero. This phenomenon is the same as those of both the coherent and hybrid MACs. However, for the orthogonal MAC and the semi-orthogonal MAC with fixed sensor grouping, the average MSE distortion converges to a fixed value as K increases. This is because at least one of $\mathcal{E}\{\alpha\}$ and $\mathcal{E}\{\beta\}$ cannot be increased when K increases.

The semi-orthogonal MAC with adaptive sensor grouping can achieve the same performance at low γ_c and even better performance at high γ_c as compared to the coherent MAC. However, the semi-orthogonal MAC requires 4 times the number of orthogonal channels and about 5 times the number of sensors. Nevertheless, it does not require channel phase information feedback. Furthermore, the semi-orthogonal MAC with adaptive sensor grouping can performs very close to the hybrid MAC. According to the simulation results in Figure 4.8, for $\mathcal{E}\{\alpha\}$, the semi-orthogonal MAC is better for small K but worse for large K. With

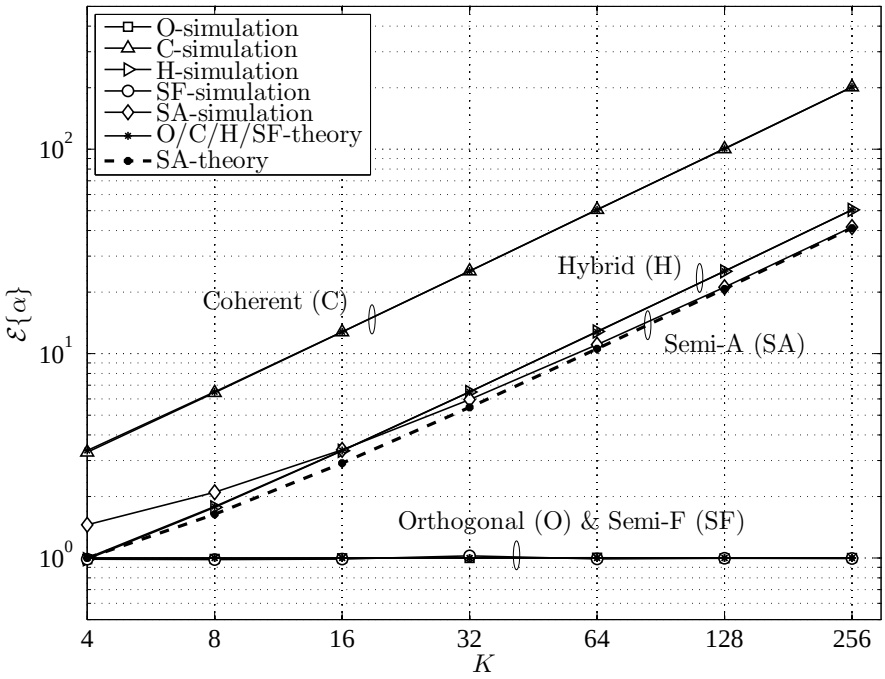

Figure 4.8 Simulation and theoretical results of $\mathcal{E}\{\alpha\}$.

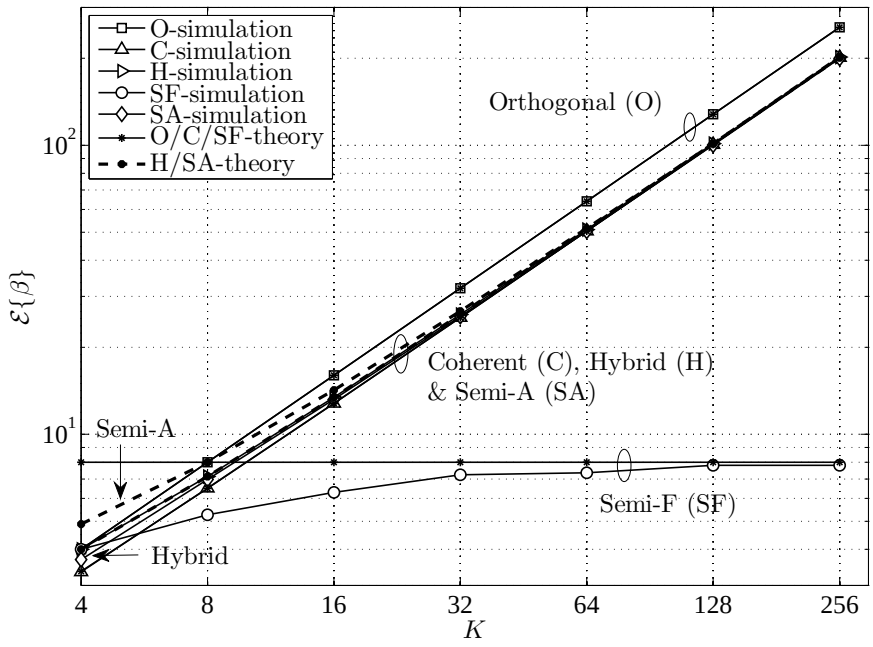

Figure 4.9 Simulation and theoretical results of $\mathcal{E}\{\beta\}$.

about $K = 16$, the two MACs have the same $\mathcal{E}\{\alpha\}$. For $\mathcal{E}\{\beta\}$, the semi-orthogonal MAC performs nearly the same as the hybrid MAC for all values of K. Again, it is important to point out that channel phase information feedback is needed in the hybrid MAC.

Regarding the bandwidth requirement (in terms of the number of orthogonal channels), the hybrid and semi-orthogonal MACs are much more efficient than the orthogonal MAC. The coherent MAC is the most bandwidth efficient since only one channel is used. For the orthogonal MAC and the semi-orthogonal MAC with fixed sensor grouping, no feedback of channel phases from the FC to the sensors is required. For the coherent MAC, due to the requirement of coherent combination among sensors, channel phases need to be transmitted from the FC to the sensors. The exact number of bits used for such information feedback depends on the capability of the feedback channel and the required accuracy, but this is certainly a large amount of overhead. For the hybrid MAC, although only coherent combination among sensors in each group is required, the amount of channel information feedback from the FC to the sensors is still the same as that of the coherent MAC. For the semi-orthogonal MAC with adaptive sensor grouping, the FC needs to inform sensors the orthogonal channels to transmit on. For each sensor, only $\log_2 N$ bits are needed. This is a much smaller amount of feedback, especially when the semi-orthogonal MAC is most suitable to be deployed, in application scenarios with limited bandwidth resources.

Finally, the simulation results of average MSE achieved by the 5 MACs under comparison are plotted in Figure 4.10. When $K = N = 4$, the coherent MAC obviously outperforms the other 4 MACs at low γ_c, which is due to its outstanding capability on channel noise suppression. In this case, the hybrid MAC and the semi-orthogonal MAC with fixed sensor grouping are equivalent to the orthogonal MAC. The semi-orthogonal MAC with adaptive sensor grouping performs a little better than the orthogonal MAC.

With K increasing from $K = 4$ to $K = 16$, the performance improvements are significant, except for the semi-orthogonal MAC with fixed sensor grouping. In particular, the performance of the semi-orthogonal MAC with adaptive sensor grouping is the same as that of the hybrid MAC, which is consistent with the theoretical derivation, and it is between those of the orthogonal MAC and the coherent MAC.

When K is further increased to $K = 80$, the performance of the semi-orthogonal MAC

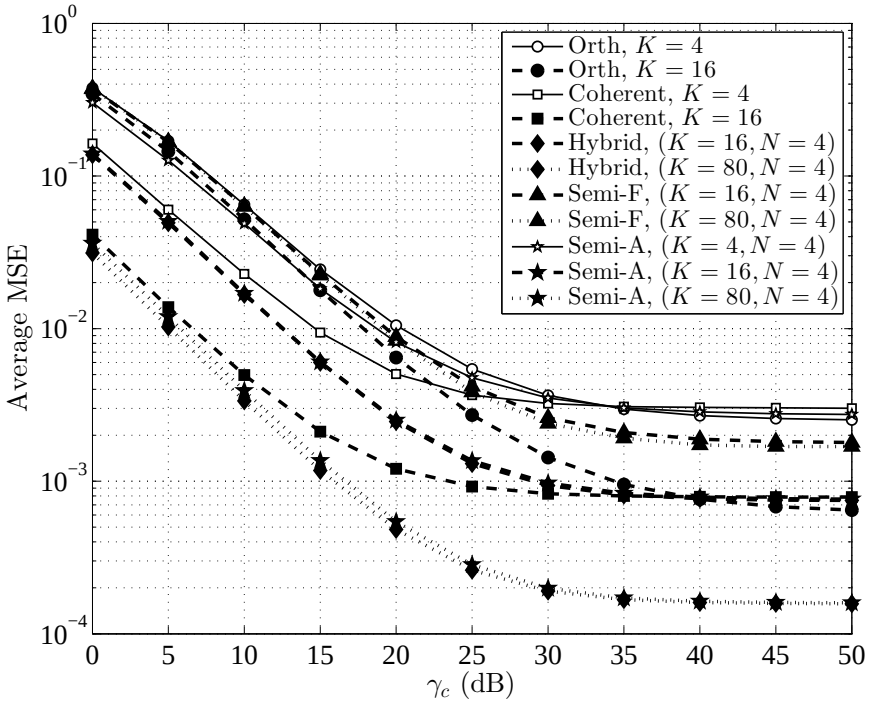

Figure 4.10 Comparison of the average MSE distortions among five different MACs. Note that in the figure's legend, "Semi-F" and "Semi-A" mean the proposed semi-orthogonal MAC with fixed and adaptive sensor grouping strategies, respectively.

with fixed sensor grouping stays nearly the same as the performance with $K = 16$. On the other hand, the performance of the semi-orthogonal MAC with adaptive sensor grouping improves significantly. The semi-orthogonal MAC with adaptive sensor grouping and $K = 80$ achieves the same (at low γ_c) or even better (at high γ_c) performance compared to the coherent MAC with $K = 16$. In addition, with $K = 80$, the hybrid MAC only slightly outperforms the semi-orthogonal MAC at low γ_c. All the simulation results match with the theoretical analysis presented before.

4.4.3 Performance Analysis for $N > 4$

In this case, the nth sub-region of the phase partition is $[\vartheta_1, \vartheta_2)$, where $\vartheta_1 = \frac{2\pi(n-1)}{N}$ and $\vartheta_2 = \frac{2\pi n}{N}$. Given that the probability that the phase of a channel response falls into a specific sub-region is $1/N$, the joint pdf of x and y is simply

$$f_{x,y}(x, y) = \frac{N}{\pi} \exp\left[-\left(x^2 + y^2\right)\right], \tag{4.37}$$

where $x > 0$ and $x \tan \vartheta_1 < y < x \tan \vartheta_2$. Based on this joint pdf, it is simple to show that when $K \to \infty$, the means and variances of x and y are

$$\mu_x = \frac{N}{2\sqrt{\pi}} \cos\left(\frac{\vartheta_1 + \vartheta_2}{2}\right) \sin\left(\frac{\pi}{N}\right), \ \mu_y = \frac{N}{2\sqrt{\pi}} \sin\left(\frac{\vartheta_1 + \vartheta_2}{2}\right) \sin\left(\frac{\pi}{N}\right),$$

$$\sigma_x^2 = \frac{N}{4\pi} \cos\left(\vartheta_1 + \vartheta_2\right) \sin\left(\frac{2\pi}{N}\right) + \frac{1}{2} - \mu_x^2, \ \sigma_y^2 = -\frac{N}{4\pi} \cos\left(\vartheta_1 + \vartheta_2\right) \sin\left(\frac{2\pi}{N}\right) + \frac{1}{2} - \mu_y^2,$$

and

$$\mathcal{E}\left\{xy\right\} = \frac{N}{4\pi} \sin\left(\vartheta_1 + \vartheta_2\right) \sin\left(\frac{2\pi}{N}\right).$$

Let $\tilde{h}_n = \sum_{i \in \Omega_n} \frac{h_i}{\sqrt{K}} = \tilde{x}_n + j\tilde{y}_n = m_n e^{j\phi_n}$. Then according to the central limit theorem when $K \to \infty$, $\tilde{x}_n$ and $\tilde{y}_n$ are i.i.d Gaussian random variables with means and variances

$$\mu_{\tilde{x}} = \mu_{\tilde{y}} = \frac{\sqrt{K}}{N} \mu_x, \ \sigma_{\tilde{x}}^2 = \sigma_{\tilde{y}}^2 = \frac{\sigma_x^2}{N}.$$

It then follows that

$$\mathcal{E}\left\{\alpha_n\right\} = \mathcal{E}\left\{\tilde{x}_n^2 + \tilde{y}_n^2\right\} = 2(\mu_{\tilde{x}}^2 + \sigma_{\tilde{x}}^2) = \frac{2K\mu_x^2}{N^2} + \frac{1 - 2\mu_x^2}{N} = \frac{1}{N} + \frac{(K-N)}{4\pi} \sin^2\left(\frac{\pi}{N}\right). \quad (4.38)$$

Therefore,

$$\mathcal{E}\left\{\alpha\right\} = \sum_{n=1}^{N} \mathcal{E}\left\{\alpha_n\right\} = 1 + \frac{N\left(K-N\right)}{4\pi} \sin^2\left(\frac{\pi}{N}\right) \approx \left[\frac{N}{4\pi} \sin^2\left(\frac{\pi}{N}\right)\right] K. \quad (4.39)$$

On the other hand,

$$\mathcal{E}\left\{\beta_n\right\} = \frac{N\mathcal{E}\left\{\alpha_n\right\}}{(\mu_x^2 + \sigma_x^2)\cos^2\phi_n + \left(\mu_y^2 + \sigma_y^2\right)\sin^2\phi_n + 2\mathcal{E}\left\{xy\right\}\cos\phi_n \sin\phi_n} = \frac{N\mathcal{E}\left\{\alpha_n\right\}}{\kappa}. \quad (4.40)$$

Similar to the case with $N = 4$, as $K \to \infty$, ϕ_n can be substituted by $\frac{\vartheta_1 + \vartheta_2}{2}$. Then κ can be

shown to take on the following value:

$$\begin{aligned}
\kappa &= \left[\frac{N}{4\pi}\cos\left(\vartheta_1+\vartheta_2\right)\sin\left(\frac{2\pi}{N}\right)+\frac{1}{2}\right]\cos^2\left(\frac{\vartheta_1+\vartheta_2}{2}\right) \\
&\quad +\left[-\frac{N}{4\pi}\cos\left(\vartheta_1+\vartheta_2\right)\sin\left(\frac{2\pi}{N}\right)+\frac{1}{2}\right]\sin^2\left(\frac{\vartheta_1+\vartheta_2}{2}\right) \\
&\quad +2\frac{N}{4\pi}\sin\left(\vartheta_1+\vartheta_2\right)\sin\left(\frac{2\pi}{N}\right)\cos\left(\frac{\vartheta_1+\vartheta_2}{2}\right)\sin\left(\frac{\vartheta_1+\vartheta_2}{2}\right) \\
&= \frac{1}{2}+\frac{N}{4\pi}\cos\left(\vartheta_1+\vartheta_2\right)\sin\left(\frac{2\pi}{N}\right)\left[\cos^2\left(\frac{\vartheta_1+\vartheta_2}{2}\right)-\sin^2\left(\frac{\vartheta_1+\vartheta_2}{2}\right)\right] \\
&\quad +\frac{N}{4\pi}\sin^2\left(\vartheta_1+\vartheta_2\right)\sin\left(\frac{2\pi}{N}\right) \\
&= \frac{1}{2}+\frac{N}{4\pi}\cos^2\left(\vartheta_1+\vartheta_2\right)\sin\left(\frac{2\pi}{N}\right)+\frac{N}{4\pi}\sin^2\left(\vartheta_1+\vartheta_2\right)\sin\left(\frac{2\pi}{N}\right) \\
&= \frac{1}{2}+\frac{N}{4\pi}\sin\left(\frac{2\pi}{N}\right).
\end{aligned} \tag{4.41}$$

Therefore

$$\mathcal{E}\left\{\beta\right\}=\sum_{n=1}^{N}\mathcal{E}\left\{\beta_n\right\}=\frac{N+\frac{N^2(K-N)}{4\pi}\sin^2\left(\frac{\pi}{N}\right)}{\frac{1}{2}+\frac{N}{4\pi}\sin\left(\frac{2\pi}{N}\right)}\approx\left[\frac{N^2\sin^2\left(\frac{\pi}{N}\right)}{2\pi+N\sin\left(\frac{2\pi}{N}\right)}\right]K. \tag{4.42}$$

The theoretical quantities $\frac{\mathcal{E}\{\alpha\}}{K}$ and $\frac{\mathcal{E}\{\beta\}}{K}$ are plotted versus N for the semi-orthogonal MAC with adaptive sensor grouping and a sufficient large K ($K = 128N$) in Figure 4.11, where the simulation results are also provided to verify the theoretical derivations. As can be seen, as N increases from 4, $\frac{\mathcal{E}\{\alpha\}}{K}$ decreases while $\frac{\mathcal{E}\{\beta\}}{K}$ stays nearly the same. Therefore with a fixed K, if N increase, which means more orthogonal channels and each with fewer sensors transmitting on, the channel noise suppression capability degrades, while the observation noise suppression capability is practically unchanged. The degradation of the channel noise suppression capability due to having more orthogonal channels is reasonable, because with more orthogonal channels, more channel noise components are introduced at the FC. On the other hand, the observation noise suppression capability is determined only by the number of sensors, independent of the number of orthogonal channels.

Figure 4.11 also provides the results for $N = 2$. Compared to $N = 4$, although there are fewer orthogonal channels and thus fewer channel noise components for $N = 2$, using $N = 2$ has almost the same channel noise suppression capability as using $N = 4$. In addition, the observation noise suppression capability for $N = 2$ is much weaker than that for $N = 4$.

These phenomenons are consistent with the analysis in Section 4.4.1. In general, $N = 4$ is the optimum choice for the semi-orthogonal MAC with adaptive sensor grouping, which achieves the best MSE performance while requiring the least transmission bandwidth.

The qualities $\frac{\mathcal{E}\{\alpha\}}{K}$ and $\frac{\mathcal{E}\{\beta\}}{K}$ are also plotted in Figure 4.11 for the hybrid MAC. The advantage of the hybrid MAC over the semi-orthogonal MAC with adaptive sensor grouping is most obvious for $N = 2$. Again, this is because with $N = 2$, destructive superposition of signals from two sensors exists in the semi-orthogonal MAC, while it is never the case in the hybrid MAC. As N increases, the sub-regions of channel phases become narrow, and the direct superposition behaves more and more like the coherent combination. For $N = 8$, the two MACs have nearly the same performance.

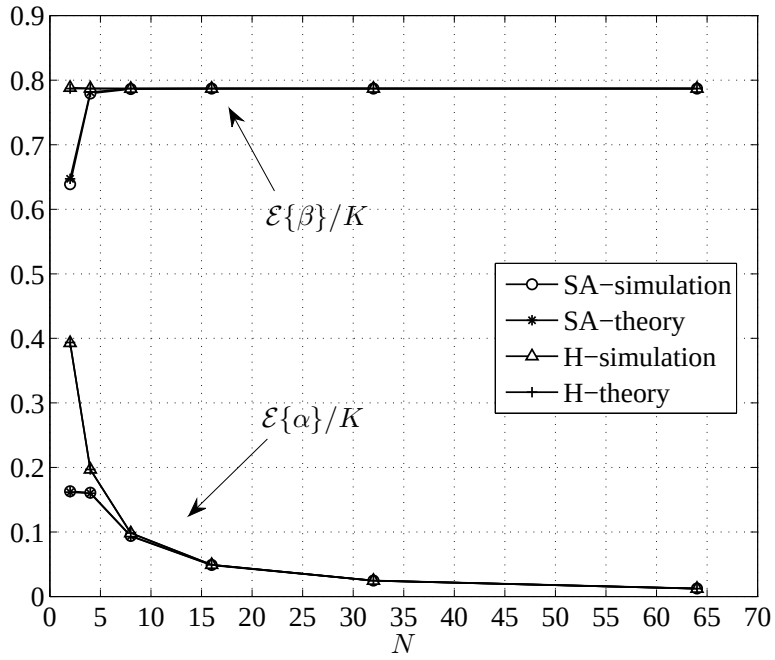

Figure 4.11 Plots of $\frac{\mathcal{E}\{\alpha\}}{K}$ and $\frac{\mathcal{E}\{\beta\}}{K}$, by simulation and theoretical analysis.

Finally, the average MSE performances of the semi-orthogonal MAC with adaptive sensor grouping are compared for $N = 4$ and $N = 8$. As shown in Figure 4.12, at low γ_c, for the network with $K = 80$, using $N = 8$ can't achieve the same performance as using $N = 4$. If K increases to 140 for $N = 8$, then the performance is the same as that of having $N = 4$ and $K = 80$. This is consistent with the previous theoretical and simulation results, which

are $\frac{\mathcal{E}\{\alpha\}}{K} \approx 0.16$ for $N = 4$ and $\frac{\mathcal{E}\{\alpha\}}{K} \approx 0.094$ for $N = 8$.

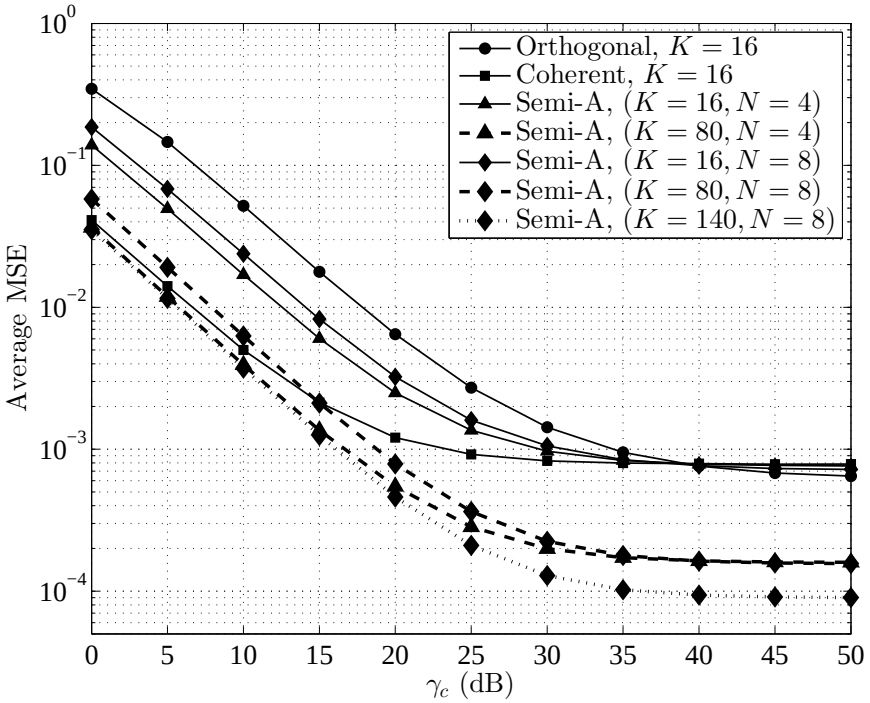

Figure 4.12 Performance comparison in terms of the average MSE for $N > 4$.

4.5 Summary

For WSNs consisting of a sufficient large number of sensors but operating under limited bandwidth resource, a novel semi-orthogonal MAC has been proposed to provide multiple access for K sensors via N orthogonal channels, where $K \geq N$. Based on a combination of channel noise suppression capability and observation noise suppression capability, this chapter thoroughly analyzed the average MSE performance of the semi-orthogonal MAC with either fixed or adaptive sensor grouping. Compared to the orthogonal MAC operating under the same bandwidth, the semi-orthogonal MAC with fixed sensor grouping has the same channel noise suppression capability, but twice the observation noise suppression capability as K approaches infinity. This is achieved with no requirement of information feedback from the FC to sensors. For the semi-orthogonal MAC with adaptive sensor grouping, the average MSE performance improvement over the orthogonal MAC is even more significant. For a fixed total transmission power, the average MSE of the semi-orthogonal MAC with adaptive sensor grouping decreases to zero as K approaches infinity, breaking through the lower bound

in the orthogonal MAC. The semi-orthogonal MAC with adaptive sensor grouping performs very close to the hybrid MAC under the same bandwidth and number of sensors. However, the amount of information feedback required by the semi-orthogonal MAC is significantly smaller than that of the hybrid MAC. For the semi-orthogonal MAC with adaptive sensor grouping, setting $N = 4$ gives the optimum tradeoff between bandwidth consumption and estimation performance.

5. Scaling Law and the Improved Power Allocation of the Semi-orthogonal MAC

5.1 Introduction

In the previous two chapters, the average MSE performance of the semi-orthogonal MAC was studied based on a combination of two performance indicators: the channel noise suppression capability, $\mathcal{E}\{\alpha\}$, and the observation noise suppression, $\mathcal{E}\{\beta\}$. Although the final average MSE is strongly related to $\mathcal{E}\{\alpha\}$ and $\mathcal{E}\{\beta\}$, unfortunately, there is no direct and simple relationship between $\{\mathcal{E}\{\alpha\}, \mathcal{E}\{\beta\}\}$ and the average MSE. As a result, many observations and conclusions regarding the average MSE performance of interested MACs were mainly obtained based on simulation results.

Although it seems very complicated, if not impossible, to derive the exact expression of the average MSE of the proposed semi-orthogonal MAC, some of its properties can still be studied and analyzed. In the first part of this chapter, one important property of the average MSE, namely the achieved scaling law, is investigated. In particular, the scaling laws of different cases of the semi-orthogonal MAC, including the orthogonal MAC as a special case, are established. It is shown that only the semi-orthogonal MAC with adaptive sensor grouping can achieve the optimal scaling law of $1/K$ of the estimation system using wireless sensor networks as defined in this thesis. As a reference, the coherent MAC can also achieve the optimal scaling law, but it requires a large amount of feedback.

In all previous chapters, the estimation is conducted under equal power allocation. In fact, the total transmitted power can be divided and allocated to the sensors according to their channel responses as well as the levels of observation noise and channel noise, to achieve smaller instantaneous MSE. In the second part of this chapter, the issues of power allocation in each sensor group and among sensor groups will be studied. In each sensor group, since

the optimal power allocation is too difficult to obtain, two improved strategies are provided for scenarios with different γ_c and γ_o ranges. Among the sensor groups, an optimal power allocation solution is obtained based on the convex optimization theory. It is pointed out that to implement the improved power allocation, extra feedback from the FC to the sensors is required. Since one advantage of the semi-orthogonal MAC is requiring a small amount of feedback, it is important to assess whether the performance improvement brought by the improved power allocation is worth the extra feedback overhead. This issue is also discussed at the end of this chapter.

Recall the expression of MSE in the semi-orthogonal MAC:

$$\epsilon = \left[\sigma_s^{-2} + \sum_{n=1}^{N} \frac{\left| \sum_{i \in \Omega_n} a_i h_i \right|^2}{\left(\sum_{i \in \Omega_n} a_i^2 t_{ni}^2 \right) \sigma_v^2 + \frac{\sigma_\omega^2}{2}} \right]^{-1}, \tag{5.1}$$

where $t_{ni} = x_i \cos \phi_n + y_i \sin \phi_n$. x_i and y_i are the real and imaginary parts of h_i, and ϕ_n is the phase of the equivalent channel response on the nth orthogonal channel $\hat{h}_n = \sum_{i \in \Omega_n} a_i h_i$. In this chapter, for simplicity, assume $\sigma_s^2 = 1$.

5.2 Scaling Law of the Average MSE

As defined in [19], the scaling law, denoted by the symbol $\sim$, means "asymptotic equivalence". More precisely, the scaling law is written as

$$f_1(K) \sim f_2(K) \tag{5.2}$$

which simply means that $\lim_{K \to \infty} f_1(K) / f_2(K) = c$, for some constant $c > 0$. In the specific case of estimation in WSNs, the scaling law can be used to describe the decaying trend achieved by the average MSE as the scale of the WSNs, i.e., the number of sensors K, increases.

According to Theorem 1 in [19], the lower bound of MSE distortion that can be achieved in a sensor network with Gaussian statistical assumptions is consisted of two parts. For sensor networks with one scalar source signal, such as the one that is studied in this thesis, the first part of the distortion scales like $1/K$. As a result, no matter how the second part of the distortion behaves, the optimal scaling law achieved by a sensor network with Gaussian statistical assumptions and one scalar source signal is $1/K$. This conclusion applies to both

analog and digital transmissions. It has been proved that the coherent MAC is an example of analog transmission which can achieve such an optimal scaling law. In the following, the scaling laws achieved by different cases of the semi-orthogonal MAC are investigated.

With equal power allocation, i.e., $a_i = \bar{a} = \sqrt{P_{\text{tot}}/\left[K\left(\sigma_s^2 + \sigma_v^2\right)\right]}$, equation (5.1) turns to

$$\epsilon = \left[1 + \sum_{n=1}^{N} \frac{\left|\sum_{i\in\Omega_n} \frac{h_i}{\sqrt{K}}\right|^2}{\left(\sum_{i\in\Omega_n} \frac{t_{ni}^2}{K}\right)\frac{1}{\gamma_{\text{o}}} + \frac{1}{2\gamma_{\text{c}}}\left(1 + \frac{1}{\gamma_{\text{o}}}\right)}\right]^{-1}. \tag{5.3}$$

In the following, for simplicity, define $\gamma_{\text{c}}' = \gamma_{\text{c}}/\left(1 + \frac{1}{\gamma_{\text{o}}}\right)$.

5.2.1 Orthogonal MAC

The orthogonal MAC is a special case of the semi-orthogonal MAC. In this case, $N = K$ and

$$\epsilon = \left(1 + \sum_{i=1}^{K} \frac{|h_i|^2}{\frac{|h_i|^2}{\gamma_{\text{o}}} + \frac{K}{2\gamma_{\text{c}}'}}\right)^{-1}. \tag{5.4}$$

A lower bound of the average MSE of the orthogonal MAC is

$$\begin{aligned} \mathcal{E}\{\epsilon\} &\geq \left(1 + \sum_{i=1}^{K} \mathcal{E}\left\{\frac{|h_i|^2}{\frac{|h_i|^2}{\gamma_{\text{o}}} + \frac{K}{2\gamma_{\text{c}}'}}\right\}\right)^{-1} = \left(1 + K\mathcal{E}\left\{\gamma_{\text{o}} - \frac{\frac{K\gamma_{\text{o}}}{2\gamma_{\text{c}}'}}{\frac{|h_1|^2}{\gamma_{\text{o}}} + \frac{K}{2\gamma_{\text{c}}'}}\right\}\right)^{-1} \\ &\geq \left(1 + K\gamma_{\text{o}} - \frac{\frac{K^2\gamma_{\text{o}}}{2\gamma_{\text{c}}'}}{\frac{\mathcal{E}\{|h_1|^2\}}{\gamma_{\text{o}}} + \frac{K}{2\gamma_{\text{c}}'}}\right)^{-1} = \left(1 + \frac{1}{\frac{1}{K\gamma_{\text{o}}} + \frac{1}{2\gamma_{\text{c}}'}}\right)^{-1}. \end{aligned} \tag{5.5}$$

The above lower bound decreases as K increases. However, it converges to a constant value of $(1 + 2\gamma_{\text{c}}')^{-1}$ when $K \to \infty$. Thus, the optimal scaling law of analog Gaussian sensor networks studied in this thesis, which states that the average MSE behaves as $1/K$, is not achieved by the orthogonal MAC. This result is explained as follows. As analyzed in the previous two chapters, there are two kinds of distortion contributing to the average MSE: one is caused by observation noise and the other by channel noise. Usually, the distortion due to observation noise is independent of the communication resources (e.g., power, bandwidth) and typically deceases like $1/K$. The distortion due to channel noise may be decreased by using more sensors, power and/or bandwidth. Only when both distortions decease as $1/K$, the optimal scaling law can be achieved by the overall average MSE. For the orthogonal MAC, as $K \to \infty$, the distortion caused by observation noise, indicated by γ_{o} in $\mathcal{E}\{\epsilon\}$, can

be reduced to zero, while the distortion caused by channel noise, indicated by γ_c, is bounded away from zero. In fact, in this case, only increasing power can drive the average MSE to zero.

5.2.2 Semi-Orthogonal MAC with Fixed Sensor Grouping

With sensor grouping, N is fixed to a small value to save bandwidth. For fixed sensor grouping (FSG), K sensors are divided into N disjoint groups such that $\Omega_n = \{(n-1)(K/N)+1, \ldots, n(K/N)\}$ and the sensors in each group transmit on one orthogonal channel. In this case, K is an integer multiple of N. The strategy of FSG means that the orthogonal channel used by each sensor, once assigned, does not change during the communication phase. As a result, no feedback of channel information is required in this scheme.

Based on equation (5.3), a lower bound on the average MSE of the semi-orthogonal MAC with FSG can be found as

$$\mathcal{E}\{\epsilon\} \geq \mathcal{E}\left\{\left(1+\sum_{n=1}^{N}\frac{\left|\sum_{i\in\Omega_n}\frac{h_i}{\sqrt{K}}\right|^2}{\frac{1}{2\gamma_c'}}\right)^{-1}\right\} = \left(1+\sum_{n=1}^{N}\frac{\mathcal{E}\left\{\left|\sum_{i\in\Omega_n}\frac{h_i}{\sqrt{K}}\right|^2\right\}}{\frac{1}{2\gamma_c'}}\right)^{-1}. \tag{5.6}$$

Since $\sum_{i\in\Omega_n} h_i/\sqrt{K}$ is a complex Gaussian random variable with zero mean and variance $1/N$, the lower bound turns to

$$\mathcal{E}\{\epsilon\} \geq \left(1+\sum_{n=1}^{N}\frac{\frac{1}{N}}{\frac{1}{2\gamma_c'}}\right)^{-1} = (1+2\gamma_c')^{-1}. \tag{5.7}$$

The above lower bound is a constant independent of K. Thus, similar to the orthogonal MAC, the optimal scaling law of $1/K$ cannot be achieved by the semi-orthogonal MAC with FSG.

5.2.3 Semi-Orthogonal MAC with Adaptive Sensor Grouping

For the adaptive sensor grouping (ASG), the sensors are grouped based on the phases of their channel responses. To this end, the whole phase region of 2π are partitioned into N equal sub-regions (each of length $2\pi/N$), and the sensors with channel phases in the same sub-region are assigned to transmit on the same orthogonal channel. In this case, feedback of orthogonal channel allocation from the FC to the sensors is required. For each sensor,

$\log_2 N$ bits are needed, which is a much smaller amount of feedback compared to the channel phase information required in the coherent MAC, especially when N is small.

The scaling law achieved by the semi-orthogonal MAC with ASG is stated in the following theorem.

Theorem 1. *The average MSE achieved by the semi-orthogonal MAC with ASG scales like* $1/K$ *when* $K \to \infty$*, i.e.,*

$$\lim_{K\to\infty} K\mathcal{E}\left\{\epsilon\right\} = c, \tag{5.8}$$

for some constant $c > 0$*.*

Proof. The strong law of large numbers [34] is used to obtain $\mathcal{E}\left\{\epsilon\right\}$ as $K \to \infty$. First, equation (5.3) is rewritten in the following form:

$$\epsilon = \left\{1 + \sum_{n=1}^{N} \frac{\frac{K_n^2}{K}\left[\left(\sum_{i\in\Omega_n}\frac{x_i}{K_n}\right)^2 + \left(\sum_{i\in\Omega_n}\frac{y_i}{K_n}\right)^2\right]}{\frac{K_n}{K}\left(\sum_{i\in\Omega_n}\frac{t_{ni}^2}{K_n}\right)\frac{1}{\gamma_o} + \frac{1}{2\gamma_c'}}\right\}^{-1}, \tag{5.9}$$

where x_i and y_i are, respectively, the real and imaginary parts of h_i, and K_n is the size of Ω_n. When $K \to \infty$, $K_n \to K/N$ (which is also infinity). Then it follows from the strong law of large numbers that when $K_n \to \infty$ one has $\sum_{i\in\Omega_n} x_i/K_n \xrightarrow{a.e.} \mathcal{E}\left\{x_i\right\}$, $\sum_{i\in\Omega_n} y_i/K_n \xrightarrow{a.e.} \mathcal{E}\left\{y_i\right\}$ and $\sum_{i\in\Omega_n} t_{ni}^2/K_n \xrightarrow{a.e.} \mathcal{E}\left\{t_{ni}^2\right\}$. It then follows that

$$\epsilon \xrightarrow{a.e.} \left[1 + \sum_{n=1}^{N} \frac{\frac{K}{N^2}\left(\mathcal{E}^2\left\{x_i\right\} + \mathcal{E}^2\left\{y_i\right\}\right)}{\frac{1}{N}\mathcal{E}\left\{t_{ni}^2\right\}\frac{1}{\gamma_o} + \frac{1}{2\gamma_c'}}\right]^{-1}. \tag{5.10}$$

As $K \to \infty$, all sensor groups have identical distributions of channel responses. Therefore, (5.10) turns to

$$\epsilon \xrightarrow{a.e.} \left[1 + \frac{N\frac{K}{N^2}\left(\mathcal{E}^2\left\{x_i\right\} + \mathcal{E}^2\left\{y_i\right\}\right)}{\frac{1}{N}\mathcal{E}\left\{t_{ni}^2\right\}\frac{1}{\gamma_o} + \frac{1}{2\gamma_c'}}\right]^{-1} = \left[1 + K\frac{\left(\mathcal{E}^2\left\{x_i\right\} + \mathcal{E}^2\left\{y_i\right\}\right)}{\mathcal{E}\left\{t_{ni}^2\right\}\frac{1}{\gamma_o} + \frac{N}{2\gamma_c'}}\right]^{-1}. \tag{5.11}$$

For the ASG scheme, the channel responses in sensor group n have i.i.d. distribution of

$$\frac{N}{\pi}\exp\left[-\left(x_i^2 + y_i^2\right)\right], \quad \frac{2\left(n-1\right)\pi}{N} \le \varphi_i < \frac{2n\pi}{N}, \tag{5.12}$$

where φ_i is the phase of h_i. Based on this distribution function, one has

$$\mathcal{E}\left\{x_i\right\} = \tfrac{N}{2\sqrt{\pi}}\cos\alpha\sin\beta,\ \mathcal{E}\left\{y_i\right\} = \tfrac{N}{2\sqrt{\pi}}\sin\alpha\sin\beta,$$

$$\mathcal{E}\left\{x_i^2\right\} = \tfrac{N}{4\pi}\cos 2\alpha\sin 2\beta + \tfrac{1}{2},\ \mathcal{E}\left\{y_i^2\right\} = -\tfrac{N}{4\pi}\cos 2\alpha\sin 2\beta + \tfrac{1}{2},$$

$$\mathcal{E}\left\{x_i y_i\right\} = \tfrac{N}{4\pi}\sin 2\alpha\sin 2\beta,$$

where $\alpha = (2n-1)\,\pi/N$ and $\beta = \pi/N$.

In addition,

$$\begin{aligned} \mathcal{E}\left\{t_{ni}^2\right\} &= \mathcal{E}\left\{\left(x_i\cos\phi_n + y_i\sin\phi_n\right)^2\right\}, \\ &= \mathcal{E}\left\{x_i^2\right\}\cos^2\phi_n + \mathcal{E}\left\{y_i^2\right\}\sin^2\phi_n + 2\,\mathcal{E}\left\{x_i y_i\right\}\cos\phi_n\sin\phi_n, \end{aligned} \tag{5.13}$$

where ϕ_n is the phase of $\hat{h}_n$. It is easy to prove that when $K \to \infty$, ϕ_n approaches $\mathcal{E}\{\varphi_i\} = (2n-1)\,\pi/N$ with probability 1. Thus,

$$\mathcal{E}\left\{t_{ni}^2\right\} \xrightarrow{a.e.} \frac{1}{2} + \frac{N}{4\pi}\sin\left(\frac{2\pi}{N}\right). \tag{5.14}$$

Therefore, when $K \to \infty$,

$$\epsilon \xrightarrow{a.e.} \left\{1 + K\frac{\frac{N^2}{4\pi}\sin^2\left(\frac{\pi}{N}\right)}{\left[\frac{1}{2} + \frac{N}{4\pi}\sin\left(\frac{2\pi}{N}\right)\right]\frac{1}{\gamma_o} + \frac{N}{2\gamma_c'}}\right\}^{-1}. \tag{5.15}$$

Finally,

$$\lim_{K\to\infty} K\mathcal{E}\{\epsilon\} = \frac{\left[\frac{1}{2} + \frac{N}{4\pi}\sin\left(\frac{2\pi}{N}\right)\right]\frac{1}{\gamma_o} + \frac{N}{2\gamma_c'}}{\frac{N^2}{4\pi}\sin^2\left(\frac{\pi}{N}\right)}, \tag{5.16}$$

which is a constant.

□

5.2.4 Simulation Results

This subsection compares simulation results of the average MSE with the lower bounds and asymptotic approximation analytically derived in the previous subsections. Let $\gamma_o = 20$ dB and $\gamma_c = 25$ dB.

Figure 5.1 plots the average MSEs of the orthogonal MAC and the semi-orthogonal MAC with FSG versus the number of sensors, K. As K increases, the average MSEs of both MACs asymptotically converge to positive constants. For the semi-orthogonal MAC with FSG, the lower bound of $(1+2\gamma_c')^{-1}$ obtained in subsection 5.2.2 is quite loose for small values of K and N, but it becomes tighter when K and N get larger.

The scaling law achieved by the semi-orthogonal MAC with ASG is illustrated in Figure 5.2. In this figure, the average MSEs of the orthogonal and coherent MACs are also provided for comparison. Similar to the coherent MAC, the average MSE of the semi-orthogonal MAC with ASG appears as a straight line when K is large. Since the plots are in log-log fashion, a

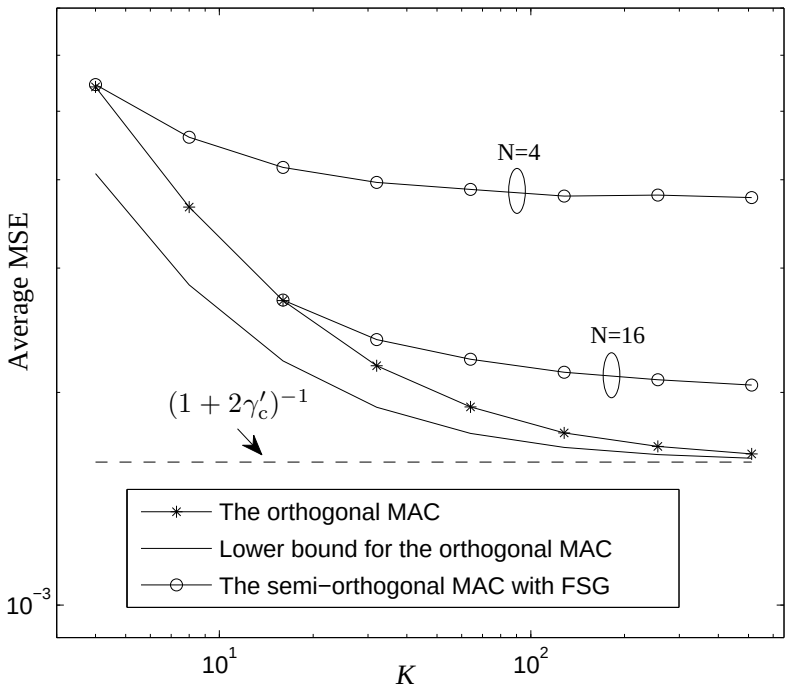

Figure 5.1 Average MSE and its lower bound for the orthogonal MAC and the semi-orthogonal MAC with FSG.

straight line means that the average MSE decays in an order of $1/K$ as K increases, showing that the optimal scaling law of the studied analog Gaussian sensor networks is achieved. In addition, it can be shown that the constant c of the ASG scheme (equation (5.16)) is larger than that of the coherent MAC. This means that the ASG scheme has a higher distortion compared to the coherent MAC with the same number of sensors. Therefore, while the semi-orthogonal MAC with ASG is as optimal as the coherent MAC in the scaling-law sense, it requires more sensors than the coherent MAC to achieve the same distortion. This fact is consistent with the simulation results in Chapter 4.

5.3 Improved Power Allocation

In all the previous chapters, the estimation is conducted under equal power allocation. In fact, the total transmit power can be divided and allocated to the sensors according to their channel responses and levels of observation noise and channel noise, as well as other factors, to obtain smaller instantaneous MSE. In this subsection, the improved power

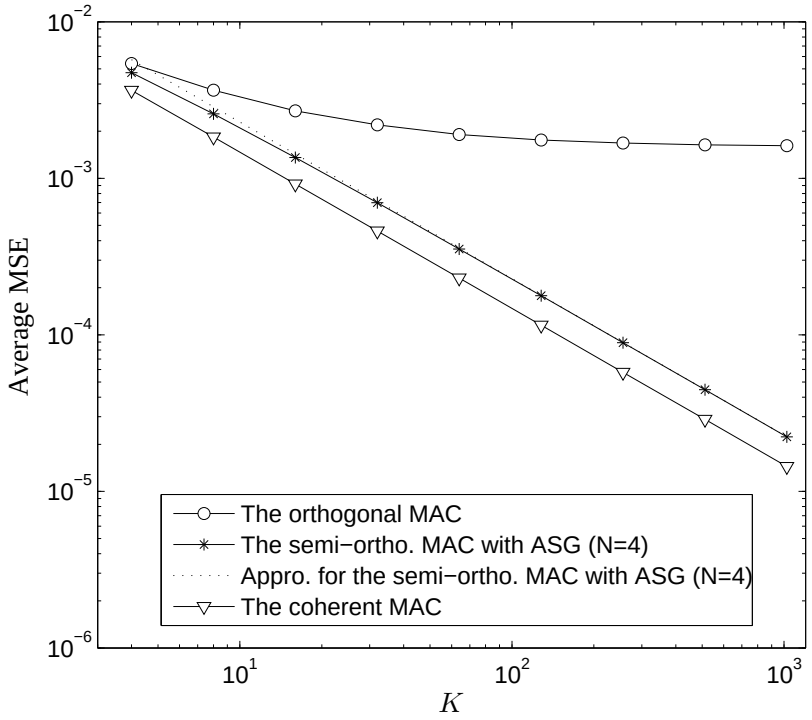

Figure 5.2 Average MSE and its approximation for the semi-orthogonal MAC with ASG.

allocation strategies will be investigated. The problem is addressed in two steps: First, power allocation in each sensor group will be studied. Then power allocation among sensor groups is examined. For the convenience of discussion, define the total transmitted power in the nth group as $P_n = \sum_{i \in \Omega_n} a_i^2 \left(\sigma_s^2 + \sigma_v^2\right)$ and the channel SNR on the nth orthogonal channel as $\gamma_{c_n} = P_n / \sigma_\omega^2$.

5.3.1 Power Allocation in Each Sensor Group

Assuming for the nth sensor group that $a_i = \tilde{a}_i \sqrt{P_n / (\sigma_s^2 + \sigma_v^2)}$. Then $\sum_{i\in\Omega_n} \tilde{a}_i^2 = 1$. Define

$$\begin{aligned} M_n &= \frac{\left(\sum_{i\in\Omega_n} a_i^2 t_{ni}^2\right)\sigma_v^2 + \frac{\sigma_\omega^2}{2}}{\left|\sum_{i\in\Omega_n} a_i h_i\right|^2} \\ &= \frac{1}{\gamma_{\mathrm{o}}} \frac{\sum_{i\in\Omega_n}\left[\tilde{a}_i x_i \left(\sum_{i\in\Omega_n}\tilde{a}_i x_i\right) + \tilde{a}_i y_i \left(\sum_{i\in\Omega_n}\tilde{a}_i y_i\right)\right]^2}{\left[\left(\sum_{i\in\Omega_n}\tilde{a}_i x_i\right)^2 + \left(\sum_{i\in\Omega_n}\tilde{a}_i y_i\right)^2\right]^2} \\ &\quad + \frac{1}{2\gamma_{\mathrm{c}_n}}\left(1 + \frac{1}{\gamma_{\mathrm{o}}}\right) \frac{1}{\left(\sum_{i\in\Omega_n}\tilde{a}_i x_i\right)^2 + \left(\sum_{i\in\Omega_n}\tilde{a}_i y_i\right)^2} \\ &= \frac{1}{\gamma_{\mathrm{o}}} A_n + \frac{1}{2\gamma_{\mathrm{c}_n}}\left(1 + \frac{1}{\gamma_{\mathrm{o}}}\right) B_n. \end{aligned} \tag{5.17}$$

The objective of the optimal power allocation in each sensor group is to minimize M_n with the constraint $\sum_{i\in\Omega_n} \tilde{a}_i^2 = 1$. In the following, A_n and B_n will be minimized separately first. After that, their effects on M_n in different scenarios will be analyzed.

Analysis on A_n

$$\begin{aligned} A_n &= \frac{\sum_{i\in\Omega_n}\left[\tilde{a}_i x_i \left(\sum_{i\in\Omega_n}\tilde{a}_i x_i\right) + \tilde{a}_i y_i \left(\sum_{i\in\Omega_n}\tilde{a}_i y_i\right)\right]^2}{\left[\left(\sum_{i\in\Omega_n}\tilde{a}_i x_i\right)^2 + \left(\sum_{i\in\Omega_n}\tilde{a}_i y_i\right)^2\right]^2} \\ &\geq \frac{\frac{1}{K_n}\left[\sum_{i\in\Omega_n}\tilde{a}_i x_i \left(\sum_{i\in\Omega_n}\tilde{a}_i x_i\right) + \tilde{a}_i y_i \left(\sum_{i\in\Omega_n}\tilde{a}_i y_i\right)\right]^2}{\left[\left(\sum_{i\in\Omega_n}\tilde{a}_i x_i\right)^2 + \left(\sum_{i\in\Omega_n}\tilde{a}_i y_i\right)^2\right]^2} = \frac{1}{K_n} \end{aligned} \tag{5.18}$$

If, and only if, $\tilde{a}_i x_i \left(\sum_{i\in\Omega_n}\tilde{a}_i x_i\right) + \tilde{a}_i y_i \left(\sum_{i\in\Omega_n}\tilde{a}_i y_i\right)$ is of the same value for every i in Ω_n, A_n can achieve its minimum value $1/K_n$. Unfortunately, it appears to be very complicated to solve the following problem[1],

$$\tilde{a}_i x_i \left(\sum_{i\in\Omega_n}\tilde{a}_i x_i\right) + \tilde{a}_i y_i \left(\sum_{i\in\Omega_n}\tilde{a}_i y_i\right) = c, \quad \text{for any } i \in \Omega_n. \tag{5.19}$$

In fact, a set of $\{\tilde{a}_i\}$ which makes $\tilde{a}_i x_i = c_1$ and $\tilde{a}_i y_i = c_2$ at the same time will guarantee that equation (5.19) holds. However it is impossible to obtain such a set of $\{\tilde{a}_i\}$ for any sets

[1] c, c_1 and c_2 indicate constants with any value.

of $\{x_i\}$ and $\{y_i\}$. Instead, a set of $\{\tilde{a}_i\}$ which tries to decrease deviations in sets $\{\tilde{a}_i x_i\}$ and $\{\tilde{a}_i y_i\}$ at the same time is analyzed[2], which is

$$\tilde{a}_i = \min\left\{\frac{1}{x_i},\ \frac{1}{y_i}\right\}. \tag{5.20}$$

Comparison between this set of $\{\tilde{a}_i\}$, which shall be called as the improved power allocation in the following, and that for equal power allocation in each group, which is $\left\{\tilde{a}_i = 1/\sqrt{K_n}\right\}$, is provided by simulation.

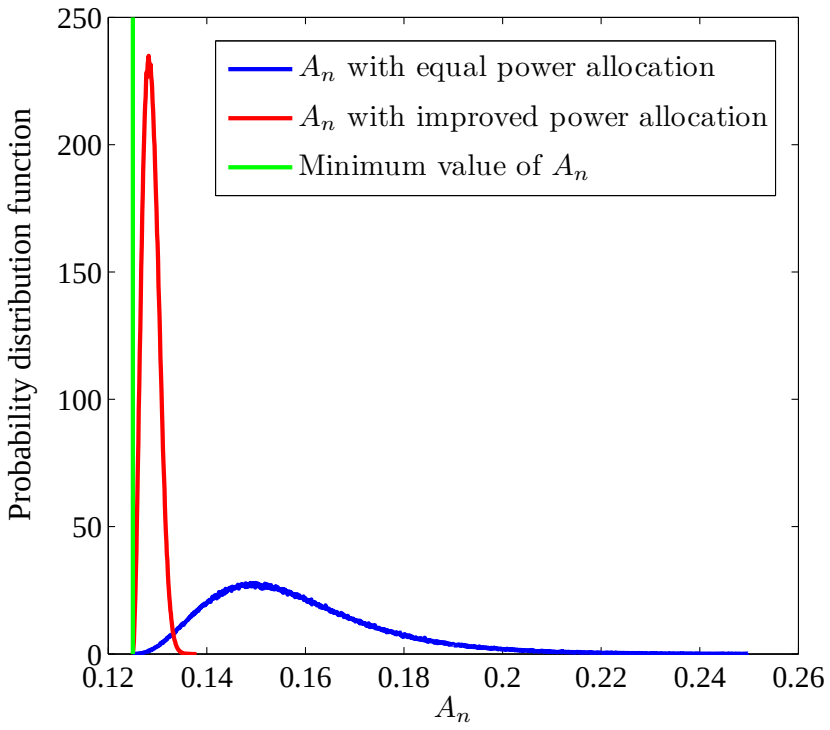

Figure 5.3 Probability distributions of A_n with equal power allocation and the improved power allocation ($K_n = 8$).

As shown in Figure 5.3, the distribution of A_n with the improved power allocation concentrates in a small range close to $1/K_n$, which is the minimum value of A_n. On the contrary, the distribution of A_n with equal power allocation spreads in a large range starting from $1/K_n$. This improved power allocation may be not the optimal power allocation that can be achieved, but it efficiently deceases distortion caused by observation noise in each sensor

[2]The vector with $\{\tilde{a}_i\}$ as elements will be normalized if it is not of Euclidean norm 1.

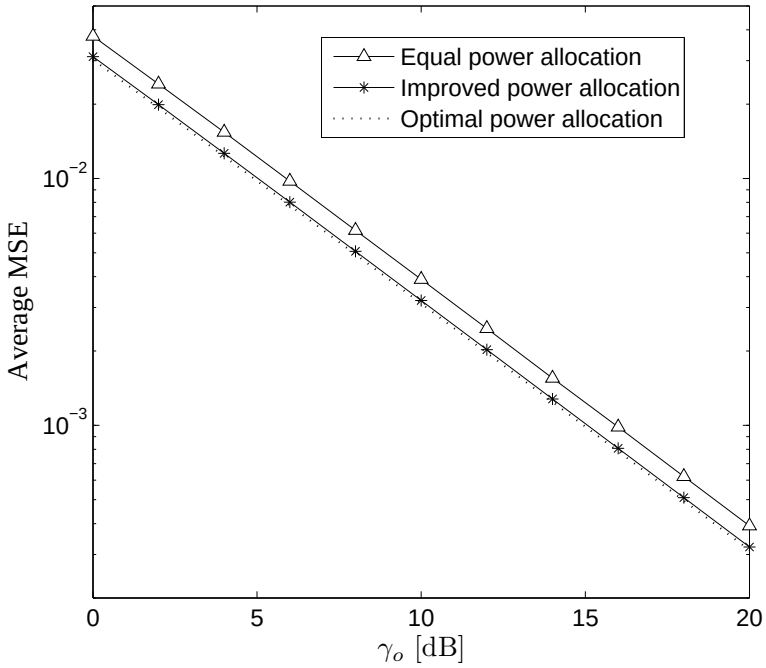

Figure 5.4 Average MSE comparison between equal power allocation and the improved power allocation for A_n ($N = 4, K = 32, \gamma_c = \infty$).

group. Let $\gamma_{c_n} = \infty$. Then the final average MSE is only caused by observation noise. In this case, as shown in Figure 5.4, there is a gap of about 1 dB between equal power allocation and the improved power allocation. In addition, the average MSE performance of the improved power allocation is nearly the same as that of the optimal power allocation[3].

Analysis on B_n

$$B_n = \frac{1}{\left(\sum_{i\in\Omega_n} \tilde{a}_i x_i\right)^2 + \left(\sum_{i\in\Omega_n} \tilde{a}_i y_i\right)^2} \tag{5.21}$$

Define $\tilde{\mathbf{a}} = [\tilde{a}_1, \tilde{a}_2, \ldots, \tilde{a}_{K_n}]$, $\mathbf{x} = [x_1, x_2, \ldots, x_{K_n}]$ and $\mathbf{y} = [y_1, y_2, \ldots, y_{K_n}]$. Then

$$B_n^{-1} = \tilde{\mathbf{a}}\left(\mathbf{x}^\intercal\mathbf{x} + \mathbf{y}^\intercal\mathbf{y}\right)\tilde{\mathbf{a}}^\intercal = \frac{\tilde{\mathbf{a}}\left(\mathbf{x}^\intercal\mathbf{x} + \mathbf{y}^\intercal\mathbf{y}\right)\tilde{\mathbf{a}}^\intercal}{\tilde{\mathbf{a}}\tilde{\mathbf{a}}^\intercal}. \tag{5.22}$$

B_n^{-1} is a Rayleigh quotient with maximum value $\lambda_{\max}$, where $\lambda_{\max}$ is the maximum eigenvalue of matrix $\mathbf{x}^\intercal\mathbf{x} + \mathbf{y}^\intercal\mathbf{y}$ and B_n^{-1} reaches that maximum at the corresponding eigenvector $\mathbf{v}_{\max}$

[3]The average MSE performance of the optimal power allocation is obtained by letting $A_n = 1/K_n$.

of matrix $\mathbf{x}^\intercal\mathbf{x} + \mathbf{y}^\intercal\mathbf{y}$. That is

$$\tilde{\mathbf{a}} = \mathbf{v}_{\max}. \tag{5.23}$$

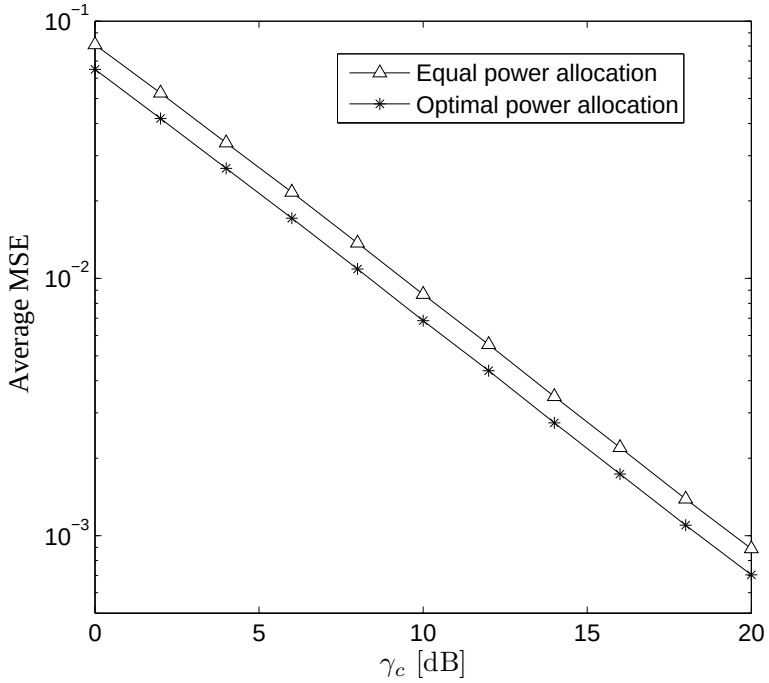

Figure 5.5 Average MSE comparison between equal power allocation and the optimal power allocation for B_n ($N = 4, K = 32, \gamma_o = \infty$).

Let $\gamma_o = \infty$. Then the final average MSE is only caused by channel noise. In this case, as shown in Fig. 5.5, there is a gap of about 1 dB between equal power allocation and the optimal power allocation.

Minimization of M_n

From (5.17), it is easy to know that:

- If $\gamma_o \ll \gamma_{c_n}$, then the distortion caused by channel noise can be ignored. In this case, (5.20) is recommended to provide improved power allocation for M_n instead of equal power allocation.

- If $\gamma_o \gg \gamma_{c_n}$, then the distortion caused by observation noise can be ignored. In this case, (5.23) is recommended to provide improved power allocation for M_n instead of equal power allocation.

- When γ_o is comparable to γ_{c_n}, a compromise between (5.20) and (5.23) maybe optimal for M_n. However, it is very complicated to obtain this optimal power allocation because A_n and B_n should be optimized simultaneously. In this case, for simplicity, equal power allocation is recommended.

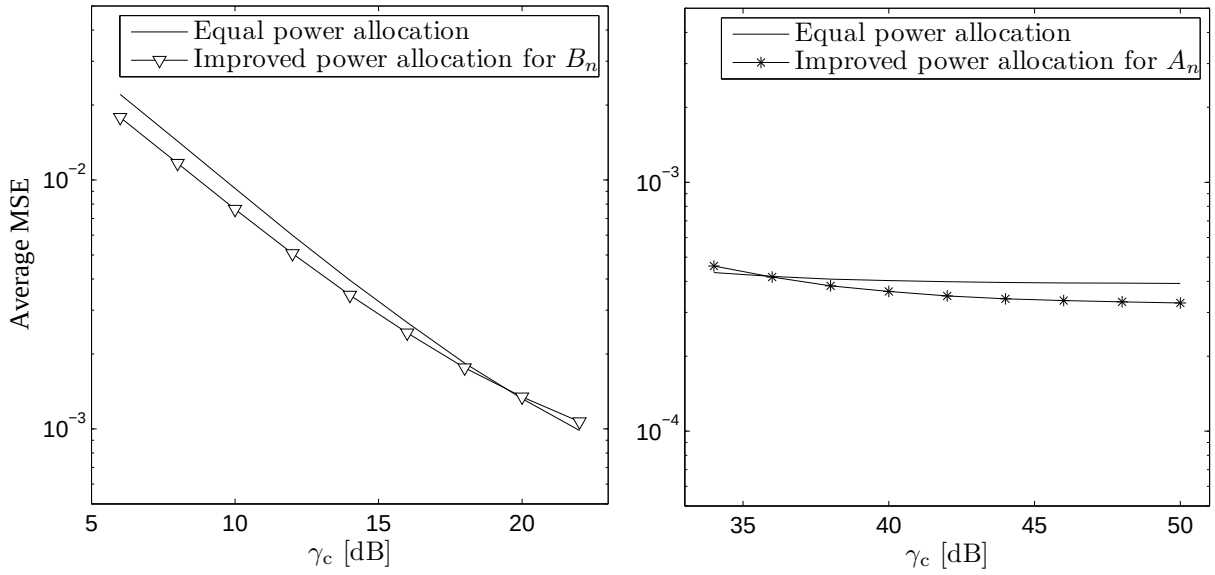

Figure 5.6 Average MSE comparison between equal power allocation and the improved power allocation for A_n and B_n ($N = 4, K = 32, \gamma_o = 20$ dB).

Take $\gamma_o = 20$ dB as an example. As shown in Figure 5.6, when $\gamma_c < 20$ dB, the recommended power allocation for B_n can provide better average MSE performance, while when $\gamma_c > 36$ dB, the recommended power allocation for A_n can provide better average MSE performance.

Note that, in all of the above three cases, the recommended power allocation does not depend on the value of P_n. As a result, power allocation among sensor groups can be done after $\{\tilde{a}_i\}$ has been fixed.

5.3.2 Power Allocation among Sensor Groups

Once $\{\tilde{a}_i\}$ is fixed, the MSE distortion can be expressed as

$$\epsilon = \left[\sigma_s^{-2} + \sum_{n=1}^{N} \frac{1}{\alpha_n + \beta_n / P_n}\right]^{-1}, \tag{5.24}$$

where $\alpha_n = A_n/\gamma_o$ and $\beta_n = \sigma_\omega^2 (1 + 1/\gamma_o) B_n/2$ are fixed. Then power allocation among sensor groups becomes a convex optimization problem as follows:

$$\begin{aligned} \min_{P_n} \quad & -\sum_{n=1}^{N} \frac{1}{\alpha_n + \beta_n/P_n}, \\ \text{s.t.} \quad & \sum_{n=1}^{N} P_n \leq P_{\text{tot}}, P_n \geq 0. \end{aligned} \tag{5.25}$$

The optimal power allocation for each sensor group can be obtained as follows (the detailed derivations can be found in Appendix 7.3):

Rank the sensor groups such that $\beta_1 \leq \beta_2 \leq \cdots \leq \beta_N$ and find the smallest $M' \leq N$ such that $f(M') \geq 1$, where

$$f(M) = \sqrt{\beta_M} \left(\frac{\sum_{n=1}^{M} \frac{\sqrt{\beta_n}}{\alpha_n}}{P_{\text{tot}} + \sum_{n=1}^{M} \frac{\beta_n}{\alpha_n}} \right). \tag{5.26}$$

Take $N_1 = M' - 1$. Then the first N_1 sensor groups are active and

$$P_n^{\text{opt}} = \begin{cases} \frac{1}{\alpha_n} \left(\sqrt{\frac{\beta_n}{\mu}} - \beta_n \right), & n \leq N_1 \\ 0, & n > N_1 \end{cases} \tag{5.27}$$

where

$$\mu = \left(\frac{\sum_{n=1}^{N_1} \frac{\sqrt{\beta_n}}{\alpha_n}}{P_{\text{tot}} + \sum_{n=1}^{N_1} \frac{\beta_n}{\alpha_n}} \right)^2. \tag{5.28}$$

Comparison of the average MSE performance between equal power allocation and the optimal power allocation among sensor groups is provided in Figure 5.7. For simplicity, P_n is equally allocated among sensors in each sensor group. Among sensor groups, the figure's legend "Equal power allocation" means P_{tot} is allocated in proportion to the number of sensors in each group, while "Optimal power allocation" means solution (5.27) is used. It can be seen that in low γ_c range (smaller than 25 dB), the optimal power allocation provides better average MSE performance. When γ_c becomes higher, the two power allocations have nearly the same performance.

At low γ_c, the intra sensor group power allocation solution (5.23) and the inter sensor groups power allocation solution (5.27) can be combined to further improve the average MSE performance. The simulation results are provided in Figure 5.8. Note that the figure's

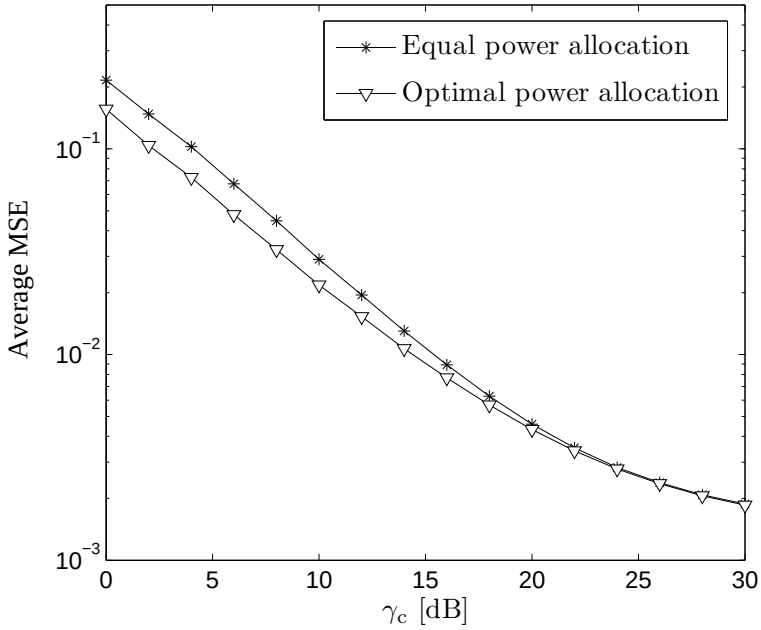

Figure 5.7 Average MSE comparison between equal power allocation and the optimal power allocation among sensor groups ($N = 4, K = 8, \gamma_o = 20$ dB).

legend "Equal power allocation" means P_{tot} is equally allocated to each sensor, "Optimal PA: intra for B_n" means only solution (5.23) is used in each sensor group, "Optimal PA: inter" means only solution (5.27) is used among sensor groups and "Optimal PA: intra+inter" means solution (5.23) and (5.27) are used together. It can be seen from the figure that when $\gamma_c < 15$ dB, the combined solution provides the best average MSE performance.

5.3.3 Overhead Required by the Improved Power Allocation

To calculate the improved power gain a_i for the ith sensor, not only the channel response of the ith sensor but also the channel responses of all other sensors are required. Therefore, a_i's should be calculated at the FC and then transmitted to the sensors. This brings extra feedback overhead to the estimation system. Note that one advantage of the semi-orthogonal MAC is that only a small amount of feedback is required. When adopting the improved power allocation in the semi-orthogonal MAC, the improvement in estimation performance and the increase in feedback overhead should be carefully balanced. For example, the power gains a_i's can be chosen from a set with finite discrete elements and the indices of the elements

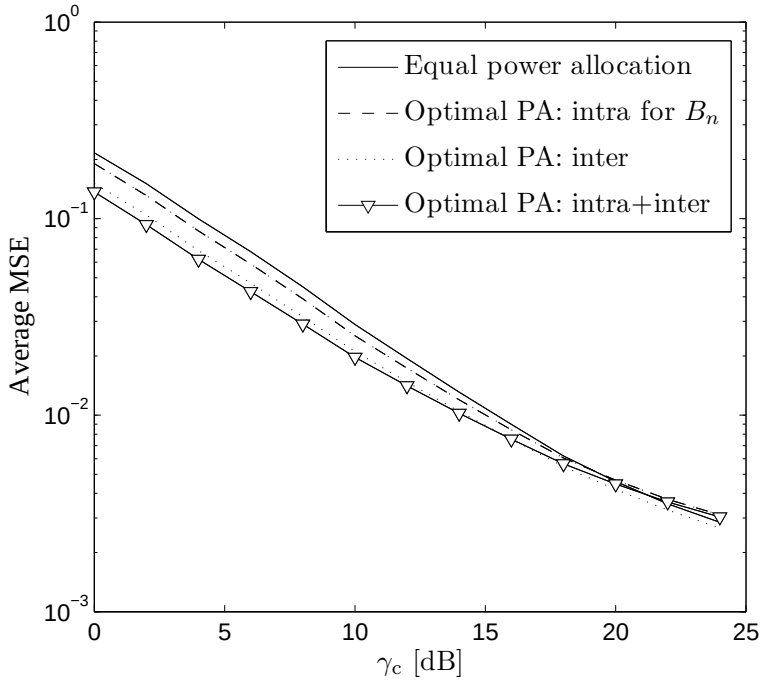

Figure 5.8 Average MSE comparison between equal power allocation and the optimal power allocation: intra sensor group and/or inter sensor groups ($N = 4, K = 8, \gamma_o = 20$ dB).

are transmitted to the sensors instead of the actual values of a_i's. Then the performance improvement and the extra feedback overhead can be balanced by changing the number of elements in the set. With more elements, more accurate a_i's can be provided to the sensors, which leads to larger performance improvement. However, in this case, more bits are required to transmit the indices of those elements.

5.4 Summary

In this chapter, the scaling laws achieved by different cases of the semi-orthogonal MAC are studied first. Similar to the orthogonal MAC, as the number of sensors K increases to infinity, the average MSE distortion of the semi-orthogonal MAC with FSG converges to a positive constant. On the contrary, the average MSE achieved by the semi-orthogonal MAC with ASG scales like $1/K$ when K is large enough. In other words, the ASG scheme achieves the optimal scaling law of the analog sensor network studied in this thesis. As a result, the average MSE of the semi-orthogonal MAC with ASG can be decreased to any level by using

more sensors.

In the second part of this chapter, the improved power allocations in each sensor group and among sensor groups are investigated. In each sensor group, the improved power allocations for the two extreme cases of "$\gamma_{\mathrm{o}} \ll \gamma_{\mathrm{c}_n}$" and "$\gamma_{\mathrm{o}} \gg \gamma_{\mathrm{c}_n}$" are provided, while equal power allocation is recommended when γ_{o} is comparable to γ_{c_n} for the simplicity of the estimation system. Among sensor groups, an optimal solution of assigning P_n's is obtained by the convex optimization theory, which provides better average MSE performance than equal power allocation, especially at low γ_{c}. In addition, since the improved power allocation requires extra feedback in the estimation system, the performance improvement and extra feedback brought by the improved power allocation should be carefully balanced when it is adopted together with the semi-orthogonal MAC.

6. Conclusions and Suggestions for Future Research

6.1 Conclusions

This thesis is concerned with distributed estimation in a Gaussian WSN with analog transmission. For a scenario in which a large number of sensors are deployed under limited bandwidth constraint, a novel semi-orthogonal MAC has been proposed to provide multiple access for K sensors via N orthogonal channels, where $K \geq N$. The K sensors are divided into N groups, and signals from sensors in each group are directly combined (opposed to be coherently combined) and transmitted on one orthogonal channel.

First, the performance of the semi-orthogonal MAC is studied under equal power allocation among sensors. Based on a combination of channel noise suppression capability and observation noise suppression capability, the average MSE performance of the proposed semi-orthogonal MAC with either fixed or adaptive sensor grouping is thoroughly analyzed. In fixed sensor grouping, each sensor is assigned to transmit on the same orthogonal channel during the entire process of communication. Compared to the orthogonal MAC operating under the same bandwidth, the semi-orthogonal MAC with fixed sensor grouping has the same channel noise suppression capability, but twice the observation noise suppression capability as K approaches infinity. This is achieved with no requirement of channel phase information feedback from the FC to sensors. In adaptive sensor grouping, the sensors are grouped based on the phases of their channel responses. In this case, the average MSE performance improvement of the semi-orthogonal MAC over the orthogonal MAC is even more significant. For a fixed total transmission power, the average MSE of the semi-orthogonal MAC with adaptive sensor grouping decreases to zero as K increases, breaking through the lower bound in the orthogonal MAC. The semi-orthogonal MAC with adaptive sensor

grouping performs very close to the hybrid MAC under the same bandwidth and number of sensors. However, in the semi-orthogonal MAC, only several bits of feedback per sensor are required to transmit the assignment of orthogonal channels, which is a significantly smaller amount than that of the hybrid MAC. In addition, for the semi-orthogonal MAC with adaptive sensor grouping, setting $N = 4$ practically gives the optimum tradeoff between bandwidth consumption and estimation performance.

In addition, one important property of the average MSE achieved by the semi-orthogonal MAC, the scaling law, is also analyzed in this thesis. The scaling law describes the decaying trend achieved by the average MSE as the scale of the WSNs, i.e., the number of sensors K, increases. Similar to the orthogonal MAC, the semi-orthogonal MAC with fixed sensor grouping requires no feedback from the FC to the sensors but fails to achieve the optimal scaling law of the analog Gaussian sensor network studied in this thesis. In contrast, for the semi-orthogonal MAC with adaptive sensor grouping, the optimal scaling law of $1/K$ can be achieved. This means that the estimation distortion can be decreased to an arbitrary low level by employing more sensors. The result on the optimal scaling law achieved by the semi-orthogonal MAC with adaptive sensor grouping is the same as that of the coherent MAC, but the former requires a much smaller amount of feedback than the latter.

In the last part of the thesis, improved power allocations for the semi-orthogonal MAC are investigated. The task is divided into two steps: first the power allocation in each sensor group is studied and then the power allocation among sensor groups is examined. In each sensor group, the improved power allocations for scenarios with different observation SNR and channel SNR ranges are provided. Among sensor groups, an optimal solution is obtained by the convex optimization theory, which provides better average MSE performance than equal power allocation, especially at low channel SNR. Since the improved power allocation requires extra feedback, the performance improvement and extra feedback required by the improved power allocation should be carefully balanced when it is adopted together with the semi-orthogonal MAC.

6.2 Suggestions for Future Research

In this thesis, a rather simple system model for distributed estimation in WSNs with analog transmission is considered. Specifically, the source signal is modelled as a scalar Gaussian random variable affected by an additive Gaussian observation noise. To facilitate performance analysis, a homogeneous assumption of identical observation noise variance for all sensors is made. Practical WSNs may vary from case to case. More complicated system models, such as the one with vector source signal, multiplicative noise and different observation and channel noise variances, are worthwhile to be considered in the future to better fit the reality.

In addition, the design of feedback transmission is also worth consideration. On one hand, the feedback information should be compressed to the least amount to save feedback transmission bandwidth. On the other hand, compression of feedback information may cause inaccuracy, which will degrade the estimation performance. How to balance between the feedback bandwidth requirement and the estimation performance is an important question to answer for practical application of WSNs. With different MACs, the feedback information is different and the sensitivity of the estimation performance to the accuracy of feedback is also different. This is an interesting topic for future study.

Another aspect of the estimation performance, the reliability, is briefly touched on in this thesis. The performance criterion using the diversity order of the outage probability has been shown to be quite inefficient to evaluate the reliability of the estimation system. Therefore, more efficient and accuracy performance criteria need to be established in the future for reliability evaluation and optimization.

A. Derivations of $\mathcal{E}\{\alpha\}$ and $\mathcal{E}\{\beta\}$ as Functions of ρ

Let $m_1 e^{j\phi_1} = r_1 + jt_1$ and $m_2 e^{j\phi_2} = r_2 + jt_2$. Then $m_1 = \sqrt{r_1^2 + t_1^2}$, $m_2 = \sqrt{r_2^2 + t_2^2}$, $\phi_1 = \arctan\left(\frac{t_1}{r_1}\right)$, $\phi_2 = \arctan\left(\frac{t_2}{r_2}\right)$. According to the central limit theorem, $m_1 e^{j\phi_1}$ and $m_2 e^{j\phi_2}$ are two complex Gaussian random variables with zero mean and unit variance. Furthermore, the correlation coefficient between $m_1 e^{j\phi_1}$ and $m_2 e^{j\phi_2}$ is ρ. Thus the joint pdf of r_1, r_2, t_1 and t_2 is

$$f(r_1, t_1, r_2, t_2) = c^2 \exp\left\{-\frac{r_1^2 + t_1^2 - 2\rho(r_1 r_2 + t_1 t_2) + r_2^2 + t_2^2}{1-\rho^2}\right\}, \quad c = \frac{1}{\pi\sqrt{1-\rho^2}}. \tag{A.1}$$

Also,

$$J = \begin{vmatrix} \frac{\partial m_1}{\partial r_1} & \frac{\partial m_1}{\partial t_1} & \frac{\partial m_1}{\partial r_2} & \frac{\partial m_1}{\partial t_2} \\ \frac{\partial m_2}{\partial r_1} & \frac{\partial m_2}{\partial t_1} & \frac{\partial m_2}{\partial r_2} & \frac{\partial m_2}{\partial t_2} \\ \frac{\partial \phi_1}{\partial r_1} & \frac{\partial \phi_1}{\partial t_1} & \frac{\partial \phi_1}{\partial r_2} & \frac{\partial \phi_1}{\partial t_2} \\ \frac{\partial \phi_2}{\partial r_1} & \frac{\partial \phi_2}{\partial t_1} & \frac{\partial \phi_2}{\partial r_2} & \frac{\partial \phi_2}{\partial t_2} \end{vmatrix} = \begin{vmatrix} \frac{r_1}{m_1} & \frac{t_1}{m_1} & 0 & 0 \\ 0 & 0 & \frac{r_2}{m_2} & \frac{t_2}{m_2} \\ -\frac{t_1}{m_1^2} & \frac{r_1}{m_1^2} & 0 & 0 \\ 0 & 0 & -\frac{t_2}{m_2^2} & \frac{r_2}{m_2^2} \end{vmatrix} = -\frac{1}{m_1 m_2}. \tag{A.2}$$

It then follows that

$$\begin{aligned} f(m_1, m_2, \phi_1, \phi_2) &= \frac{f(r_1, t_1, r_2, t_2)}{|J|} \\ &= c^2 m_1 m_2 \exp\left\{-\frac{m_1^2 - 2\rho m_1 m_2 \cos(\phi_1 - \phi_2) + m_2^2}{1-\rho^2}\right\}. \end{aligned} \tag{A.3}$$

Let $x = \cos(\phi_1 - \phi_2)$ and $y = \phi_2$. Then

$$J = \begin{vmatrix} \frac{\partial x}{\partial \phi_1} & \frac{\partial x}{\partial \phi_2} \\ \frac{\partial y}{\partial \phi_1} & \frac{\partial y}{\partial \phi_2} \end{vmatrix} = \begin{vmatrix} -\sin(\phi_1 - \phi_2) & \sin(\phi_1 - \phi_2) \\ 0 & 1 \end{vmatrix} = -\sin(\phi_1 - \phi_2),$$

$$\begin{aligned} &f(m_1, m_2, x, y) \\ &= \frac{2f(m_1, m_2, \phi_1, \phi_2)}{|J|} = \frac{2c^2 m_1 m_2}{\sqrt{1-x^2}} \exp\left\{-\frac{m_1^2 - 2\rho m_1 m_2 x + m_2^2}{1-\rho^2}\right\}, \end{aligned} \tag{A.4}$$

and

$$\begin{aligned} f\left(m_1, m_2, x\right) &= 2\pi f\left(m_1, m_2, x, y\right) \\ &= \frac{4m_1 m_2}{\pi\left(1-\rho^2\right)\sqrt{1-x^2}} \exp\left\{-\frac{m_1^2 - 2\rho m_1 m_2 x + m_2^2}{1-\rho^2}\right\}. \end{aligned} \tag{A.5}$$

Next,

$$\begin{aligned} \mathcal{E}\left\{\alpha\right\} &= \mathcal{E}\left\{m_1^2 + m_2^2\right\} \\ &= \frac{4}{\pi\left(1-\rho^2\right)} \int_0^\infty \int_0^\infty \int_1^{-1} \frac{\left(m_1^2 + m_2^2\right) m_1 m_2}{\sqrt{1-x^2}} \\ &\qquad \exp\left\{-\frac{m_1^2 - 2\rho m_1 m_2 x + m_2^2}{1-\rho^2}\right\} \mathrm{d}x\mathrm{d}m_1\mathrm{d}m_2 \\ &= \frac{4}{\pi\left(1-\rho^2\right)} \int_1^{-1} \frac{1}{\sqrt{1-x^2}} \int_0^\infty m_2 \exp\left\{-\frac{\left(1-\rho^2 x^2\right) m_2^2}{1-\rho^2}\right\} \Lambda\left(x, m_2\right) \mathrm{d}m_2\mathrm{d}x, \end{aligned} \tag{A.6}$$

where

$$\begin{aligned} \Lambda\left(x, m_2\right) &= \int_0^\infty \left(m_1^2 + m_2^2\right) m_1 \exp\left\{-\frac{\left(m_1 - \rho m_2 x\right)^2}{1-\rho^2}\right\} \mathrm{d}m_1 \\ &= \int_{-\rho m_2 x}^\infty \left[\begin{array}{l} y^3 + 3\rho x m_2 y^2 + \left(1 + 3\rho^2 x^2\right) \\ m_2^2 y + \rho x\left(1 + \rho^2 x^2\right) m_2^3 \end{array}\right] \exp\left\{-\frac{y^2}{1-\rho^2}\right\} \mathrm{d}y. \end{aligned} \tag{A.7}$$

If $-1 < x < 0$, then

$$\begin{aligned} &\Lambda\left(x, m_2\right) \\ &= \int_{-\rho m_2 x}^\infty \left[\begin{array}{l} y^3 + 3\rho x m_2 y^2 + \left(1 + 3\rho^2 x^2\right) \\ m_2^2 y + \rho x\left(1 + \rho^2 x^2\right) m_2^3 \end{array}\right] \exp\left\{-\frac{y^2}{1-\rho^2}\right\} \mathrm{d}y \\ &= \frac{\left(1-\rho^2\right)^2}{2} \Gamma\left(2, \frac{\rho^2 x^2 m_2^2}{1-\rho^2}\right) + \frac{3\rho x m_2 \left(1-\rho^2\right)^{\frac{3}{2}}}{2} \Gamma\left(\frac{3}{2}, \frac{\rho^2 x^2 m_2^2}{1-\rho^2}\right) \\ &\quad + \frac{\left(1 + 3\rho^2 x^2\right) m_2^2 \left(1-\rho^2\right)}{2} \Gamma\left(1, \frac{\rho^2 x^2 m_2^2}{1-\rho^2}\right) \\ &\quad + \frac{\rho x\left(1 + \rho^2 x^2\right) m_2^3 \left(1-\rho^2\right)^{\frac{1}{2}}}{2} \Gamma\left(\frac{1}{2}, \frac{\rho^2 x^2 m_2^2}{1-\rho^2}\right). \end{aligned} \tag{A.8}$$

If $0 < x < 1$, then

$$
\begin{aligned}
&\Lambda\left(x, m_2\right) \qquad (A.9)\\
&= \int_{-\rho m_2 x}^{\infty} \left[\begin{array}{l} y^3 + 3\rho x m_2 y^2 + \left(1 + 3\rho^2 x^2\right) \\ m_2^2 y + \rho x \left(1 + \rho^2 x^2\right) m_2^3 \end{array} \right] \exp\left\{ -\frac{y^2}{1-\rho^2} \right\} \mathrm{d}y \\
&= \frac{\left(1-\rho^2\right)^2}{2} \Gamma\left(2, \frac{\rho^2 x^2 m_2^2}{1-\rho^2}\right) + \frac{3\rho x m_2 \left(1-\rho^2\right)^{\frac{3}{2}}}{2} \Gamma\left(\frac{3}{2}, \frac{\rho^2 x^2 m_2^2}{1-\rho^2}\right) \\
&\quad + \frac{\left(1 + 3\rho^2 x^2\right) m_2^2 \left(1-\rho^2\right)}{2} \Gamma\left(1, \frac{\rho^2 x^2 m_2^2}{1-\rho^2}\right) \\
&\quad + \frac{\rho x \left(1 + \rho^2 x^2\right) m_2^3 \left(1-\rho^2\right)^{\frac{1}{2}}}{2} \Gamma\left(\frac{1}{2}, \frac{\rho^2 x^2 m_2^2}{1-\rho^2}\right) \\
&\quad + 3\rho x m_2 \left(1-\rho^2\right)^{\frac{3}{2}} \gamma\left(\frac{3}{2}, \frac{\rho^2 x^2 m_2^2}{1-\rho^2}\right) \\
&\quad + \rho x \left(1 + \rho^2 x^2\right) m_2^3 \left(1-\rho^2\right)^{\frac{1}{2}} \gamma\left(\frac{1}{2}, \frac{\rho^2 x^2 m_2^2}{1-\rho^2}\right).
\end{aligned}
$$

The functions $\gamma\left(a, x\right)$ and $\Gamma\left(a, x\right)$ are incomplete gamma functions [33]. Since $\frac{\left(1-\rho^2\right)^2}{2} \Gamma\left(2, \frac{\rho^2 x^2 m_2^2}{1-\rho^2}\right)$ and $\frac{\rho x \left(1+\rho^2 x^2\right) m_2^3 \left(1-\rho^2\right)^{\frac{1}{2}}}{2} \Gamma\left(\frac{1}{2}, \frac{\rho^2 x^2 m_2^2}{1-\rho^2}\right)$ are odd functions of x and the integral with respect to x is from -1 to 1, the two terms integrate to zero. Then one has

$$
\begin{aligned}
&\mathcal{E}\left\{\alpha\right\} \qquad (A.10)\\
&= \frac{4}{\pi\left(1-\rho^2\right)} \int_{-1}^{0} \frac{1}{\sqrt{1-x^2}} \int_{0}^{\infty} m_2 \exp\left\{ -\frac{\left(1-\rho^2 x^2\right) m_2^2}{1-\rho^2} \right\} \Lambda_{-}\left(x, m_2\right) \mathrm{d}m_2 \mathrm{d}x \\
&\quad + \frac{4}{\pi\left(1-\rho^2\right)} \int_{0}^{1} \frac{1}{\sqrt{1-x^2}} \int_{0}^{\infty} m_2 \exp\left\{ -\frac{\left(1-\rho^2 x^2\right) m_2^2}{1-\rho^2} \right\} \Lambda_{+}\left(x, m_2\right) \mathrm{d}m_2 \mathrm{d}x,
\end{aligned}
$$

where

$$
\begin{aligned}
&\Lambda_{-}\left(x, m_2\right) \qquad (A.11)\\
&= \frac{\left(1-\rho^2\right)^2}{2} \Gamma\left(2, \frac{\rho^2 x^2 m_2^2}{1-\rho^2}\right) + \frac{\left(1 + 3\rho^2 x^2\right) m_2^2 \left(1-\rho^2\right)}{2} \Gamma\left(1, \frac{\rho^2 x^2 m_2^2}{1-\rho^2}\right),
\end{aligned}
$$

$$
\begin{aligned}
&\Lambda_{+}\left(x, m_2\right) \qquad (A.12)\\
&= \frac{\left(1-\rho^2\right)^2}{2} \Gamma\left(2, \frac{\rho^2 x^2 m_2^2}{1-\rho^2}\right) + \frac{\left(1 + 3\rho^2 x^2\right) m_2^2 \left(1-\rho^2\right)}{2} \Gamma\left(1, \frac{\rho^2 x^2 m_2^2}{1-\rho^2}\right) \\
&\quad + 3\rho x m_2 \left(1-\rho^2\right)^{\frac{3}{2}} \gamma\left(\frac{3}{2}, \frac{\rho^2 x^2 m_2^2}{1-\rho^2}\right) \\
&\quad + \rho x \left(1 + \rho^2 x^2\right) m_2^3 \left(1-\rho^2\right)^{\frac{1}{2}} \gamma\left(\frac{1}{2}, \frac{\rho^2 x^2 m_2^2}{1-\rho^2}\right).
\end{aligned}
$$

One also can compute

$$\begin{aligned}
&\int_0^\infty m_2 \exp\left\{-\frac{(1-\rho^2x^2)\,m_2^2}{1-\rho^2}\right\}\Gamma\left(2,\frac{\rho^2x^2m_2^2}{1-\rho^2}\right)\mathrm{d}m_2 \qquad (A.13)\\
&= \int_0^\infty m_2 \exp\left\{-\frac{(1-\rho^2x^2)\,m_2^2}{1-\rho^2}\right\}\int_{\frac{\rho^2x^2m_2^2}{1-\rho^2}}^\infty \mathrm{e}^{-t}t\mathrm{d}t\mathrm{d}m_2\\
&= \int_0^\infty \mathrm{e}^{-t}t\int_0^{\frac{\sqrt{(1-\rho^2)t}}{\rho|x|}} m_2 \exp\left\{-\frac{(1-\rho^2x^2)\,m_2^2}{1-\rho^2}\right\}\mathrm{d}m_2\mathrm{d}t\\
&= \frac{1-\rho^2}{2\,(1-\rho^2x^2)}\int_0^\infty \mathrm{e}^{-t}t\gamma\left(1,\frac{(1-\rho^2x^2)\,t}{\rho^2x^2}\right)\mathrm{d}t\\
&= \frac{1-\rho^2}{2\,(1-\rho^2x^2)}\frac{1-\rho^2x^2}{\rho^2x^2}\Gamma(3)\left(1+\frac{1-\rho^2x^2}{\rho^2x^2}\right)^{-3}\mathrm{F}\left(1,3,2,1-\rho^2x^2\right)\\
&= \left(1-\rho^2\right)\left(\rho^2x^2\right)^2\mathrm{F}\left(1,3,2,1-\rho^2x^2\right),
\end{aligned}$$

and similarly,

$$\begin{aligned}
&\int_0^\infty m_2 \exp\left\{-\frac{(1-\rho^2x^2)\,m_2^2}{1-\rho^2}\right\}m_2^2\,\Gamma\left(1,\frac{\rho^2x^2m_2^2}{1-\rho^2}\right)\mathrm{d}m_2 \qquad (A.14)\\
&\qquad = \frac{\left(1-\rho^2\right)^2\left(\rho^2x^2\right)}{2}\mathrm{F}\left(1,3,3,1-\rho^2x^2\right),
\end{aligned}$$

$$\begin{aligned}
&\int_0^\infty m_2 \exp\left\{-\frac{(1-\rho^2x^2)\,m_2^2}{1-\rho^2}\right\}m_2\,\gamma\left(\frac{3}{2},\frac{\rho^2x^2m_2^2}{1-\rho^2}\right)\mathrm{d}m_2 \qquad (A.15)\\
&\qquad = \frac{2\left(1-\rho^2\right)^{\frac{3}{2}}\left(\rho^2x^2\right)^{\frac{3}{2}}}{3}\mathrm{F}\left(1,3,\frac{5}{2},\rho^2x^2\right),
\end{aligned}$$

$$\begin{aligned}
&\int_0^\infty m_2 \exp\left\{-\frac{(1-\rho^2x^2)\,m_2^2}{1-\rho^2}\right\}m_2^3\,\gamma\left(\frac{1}{2},\frac{\rho^2x^2m_2^2}{1-\rho^2}\right)\mathrm{d}m_2 \qquad (A.16)\\
&\qquad = 2\left(1-\rho^2\right)^{\frac{5}{2}}\left(\rho^2x^2\right)^{\frac{1}{2}}\mathrm{F}\left(1,3,\frac{3}{2},\rho^2x^2\right),
\end{aligned}$$

where $\mathrm{F}(\alpha,\beta,\gamma,z)$ is the Gauss hypergeometric function [33]. Thus

$$\begin{aligned}
&\mathcal{E}\{\alpha\} \qquad (A.17)\\
&= \frac{4\left(1-\rho^2\right)^2}{\pi}\int_0^1 \frac{\left(\rho^2x^2\right)^2}{\sqrt{1-x^2}}\left[\mathrm{F}\left(1,3,2,1-\rho^2x^2\right)+2\mathrm{F}\left(1,3,\frac{5}{2},\rho^2x^2\right)\right]\mathrm{d}x\\
&\quad +\frac{2\left(1-\rho^2\right)^2}{\pi}\int_0^1 \frac{\rho^2x^2}{\sqrt{1-x^2}}\left[\begin{array}{l}\left(1+3\rho^2x^2\right)\mathrm{F}\left(1,3,3,1-\rho^2x^2\right)\\ +4\left(1+\rho^2x^2\right)\mathrm{F}\left(1,3,\frac{3}{2},\rho^2x^2\right)\end{array}\right]\mathrm{d}x.
\end{aligned}$$

Similarly,

$$\begin{aligned}
\mathcal{E}\left\{\beta\right\} &= \mathcal{E}\left\{\frac{2\left[m_1^2 - 2\rho\cos\left(\phi_1-\phi_2\right)m_1m_2 + m_2^2\right]}{1-\rho^2\cos^2\left(\phi_1-\phi_2\right)}\right\} \qquad (A.18)\\
&= \frac{8\left(1-\rho^2\right)}{\pi}\times\int_0^\infty\int_0^\infty\int_{-1}^1 \frac{\left(m_1^2 - 2\rho x m_1m_2 + m_2^2\right)m_1m_2}{\left(1-\rho^2x^2\right)\sqrt{1-x^2}} \\
&\qquad\qquad \exp\left\{-\frac{m_1^2 - 2\rho m_1m_2x + m_2^2}{1-\rho^2}\right\}\mathrm{d}x\mathrm{d}m_1\mathrm{d}m_2 \\
&= \frac{4\left(1-\rho^2\right)^2}{\pi}\int_0^1 \frac{\left(\rho^2x^2\right)^2}{\left(1-\rho^2x^2\right)\sqrt{1-x^2}}\left[\begin{array}{l}\mathrm{F}\left(1,3,2,1-\rho^2x^2\right)\\ +\frac{4}{3}\mathrm{F}\left(1,3,\frac{5}{2},\rho^2x^2\right)\end{array}\right]\mathrm{d}x \\
&\quad +\frac{4\left(1-\rho^2\right)^2}{\pi}\int_0^1 \frac{\rho^2x^2}{\sqrt{1-x^2}}\left[\mathrm{F}\left(1,3,3,1-\rho^2x^2\right) + 4\mathrm{F}\left(1,3,\frac{3}{2},\rho^2x^2\right)\right]\mathrm{d}x.
\end{aligned}$$

B. Proof of $\phi = \frac{\pi}{4}$ when $K \to \infty$

Let τ be the deviation of ϕ from $\frac{\pi}{4}$. Referring to Figure B.1, for any small τ_0, one has

$$\mathrm{P}\left(|\tau| \le \tau_0\right) = \mathrm{P}\left\{(\tilde{x}, \tilde{y}) \text{ in the shaded area}\right\} \ge \mathrm{P}\left\{(\tilde{x}, \tilde{y}) \text{ in the circle}\right\} \tag{B.1}$$

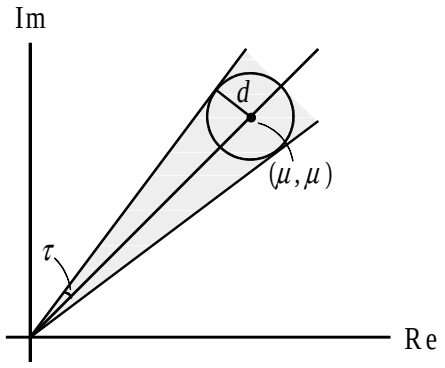

Figure B.1 Integral area of τ.

Because of the circular symmetry property of zero-mean complex Gaussian random variables and that the magnitude of a zero-mean complex Gaussian random variable is Rayleigh distributed, one has

$$\mathrm{P}\left\{(\tilde{x}, \tilde{y}) \text{ in the circle}\right\} = \int_0^d \frac{r}{2\sigma^2} \exp\left(-\frac{r^2}{4\sigma^2}\right) \mathrm{d}r = 1 - \exp\left(-\frac{d^2}{4\sigma^2}\right) \tag{B.2}$$

where $d = \mu \sin\tau_0 = \frac{\sqrt{K}}{4\sqrt{\pi}} \sin\tau_0$. As $K \to \infty$, $\exp\left(-\frac{d^2}{4\sigma^2}\right)$ goes to zero, thus $\mathrm{P}\left\{(\tilde{x}, \tilde{y}) \text{ in the circle}\right\}$ goes to 1 and $\mathrm{P}\left(|\tau| \le \tau_0\right)$ also goes to 1. It follows that ϕ can be substituted by $\frac{\pi}{4}$.

C. Derivation of P_n^{opt}

The convex optimization problem is

$$\begin{aligned} \min_{P_n} \quad & -\sum_{n=1}^{N} \frac{1}{\alpha_n + \beta_n/P_n}, \\ \text{s.t.} \quad & \sum_{n=1}^{N} P_n \leq P_{\text{tot}}, P_n \geq 0. \end{aligned} \tag{C.1}$$

This problem can be solved using the same techniques as in [22] and [35]. First, the Lagrangian L associated with this optimization problem is:

$$L = -\sum_{n=1}^{N} \frac{1}{\alpha_n + \beta_n/P_n} + \mu \left(\sum_{n=1}^{N} P_n - P_{\text{tot}} \right) - \sum_{n=1}^{N} \lambda_n P_n, \tag{C.2}$$

which leads to the following Karush-Kuhn-Tucker (KKT) conditions:

$$\begin{aligned} P_n &\geq 0, \quad \forall n, \\ P_{\text{tot}} - \sum_{n=1}^{N} P_n &\geq 0, \\ \lambda_n &\geq 0, \quad \forall n, \\ \mu &\geq 0, \\ \lambda_n P_n &= 0, \quad \forall n, \\ \mu \left(P_{\text{tot}} - \sum_{n=1}^{N} P_n \right) &= 0, \\ -\frac{1}{\alpha_n P_n + \beta_n} + \frac{\alpha_n P_n}{(\alpha_n P_n + \beta_n)^2} + \mu - \lambda_n &= 0, \quad \forall n. \end{aligned} \tag{C.3}$$

If $\mu = 0$, then according to equation (C.3), one has

$$\lambda_n = -\frac{\beta_n}{(\alpha_n P_n + \beta_n)^2} < 0. \tag{C.4}$$

Therefore $\mu \neq 0$ and

$$P_{\text{tot}} = \sum_{n=1}^{N} P_n. \tag{C.5}$$

For those sensors with $P_n > 0$, $\lambda_n = 0$ holds, then according to equation (C.3), $\frac{\beta_n}{(\alpha_n P_n + \beta_n)^2} = \mu$. Thus

$$P_n = \frac{1}{\alpha_n} \left(\sqrt{\frac{\beta_n}{\mu}} - \beta_n \right)^+, \tag{C.6}$$

where $(x)^+$ equals 0 where x is less than zero, and otherwise equals x. Once μ is fixed, as long as $\mu\beta_n < 1$, the corresponding sensor is active.

Next, the indices of active sensors are determined. Rank the sensors such that $\beta_1 \leq \beta_2 \leq \cdots \leq \beta_N$, and assume the first N_1 sensors are active, then

$$\sum_{n=1}^{N_1} \frac{1}{\alpha_n} \left(\sqrt{\frac{\beta_n}{\mu}} - \beta_n \right) = P_{\text{tot}}, \tag{C.7}$$

which leads to

$$\mu = \left(\frac{\sum_{n=1}^{N_1} \frac{\sqrt{\beta_n}}{\alpha_n}}{P_{\text{tot}} + \sum_{n=1}^{N_1} \frac{\beta_n}{\alpha_n}} \right)^2. \tag{C.8}$$

To solve the cut-off index N_1, which is obviously determined by the relative magnitudes between $\mu\beta_n$ and 1, introduce the function

$$f(M) = \sqrt{\mu\beta_M} = \sqrt{\beta_M} \left(\frac{\sum_{n=1}^{M} \frac{\sqrt{\beta_n}}{\alpha_n}}{P_{\text{tot}} + \sum_{n=1}^{M} \frac{\beta_n}{\alpha_n}} \right). \tag{C.9}$$

Solving the threshold N_1 is equivalent to finding N_1 such that $f(N_1) < 1$ and $f(N_1 + 1) \geq 1$. It can be proved that such a N_1 is unique and always exists unless $f(M) < 1$ for all $1 \leq M \leq N$ in which case $N_1 = N$ and all sensors are active.

Proof. It is easy to show that

$$f(1) = \frac{\frac{\beta_1}{\alpha_1}}{P_{\text{tot}} + \frac{\beta_1}{\alpha_1}} < 1. \tag{C.10}$$

Then find the smallest $M' \leq N$ such that $f(M') \geq 1$. It is claimed that $f(M) \geq 1$ for any $M \geq M'$. This can be proved by showing that if $f(M) \geq 1$, then $f(M+1) \geq 1$. Suppose

$f(M) \geq 1$ for some $M' \leq M \leq N$, then one has

$$\begin{aligned} f(M+1) &= \sqrt{\beta_{M+1}} \left(\frac{\sum_{n=1}^{M+1} \frac{\sqrt{\beta_n}}{\alpha_n}}{P_{\text{tot}} + \sum_{n=1}^{M+1} \frac{\beta_n}{\alpha_n}} \right) \\ &= \frac{\sqrt{\beta_{M+1}} \left(\sum_{n=1}^{M} \frac{\sqrt{\beta_n}}{\alpha_n} \right) + \frac{\beta_{M+1}}{\alpha_{M+1}}}{P_{\text{tot}} + \left(\sum_{n=1}^{M} \frac{\beta_n}{\alpha_n} \right) + \frac{\beta_{M+1}}{\alpha_{M+1}}} \geq \frac{\sqrt{\beta_M} \left(\sum_{n=1}^{M} \frac{\sqrt{\beta_n}}{\alpha_n} \right) + \frac{\beta_{M+1}}{\alpha_{M+1}}}{P_{\text{tot}} + \left(\sum_{n=1}^{M} \frac{\beta_n}{\alpha_n} \right) + \frac{\beta_{M+1}}{\alpha_{M+1}}} \geq 1, \end{aligned} \tag{C.11}$$

where the last inequality is due to the fact that

$$\frac{a+b}{c+b} > 1, \quad \text{if } \{a > c,\, a > 0,\, b > 0,\, c > 0\}.$$

Next make the following identifications

$$a = \sqrt{\beta_M} \left(\sum_{n=1}^{M} \frac{\sqrt{\beta_n}}{\alpha_n} \right),\; b = \frac{\beta_{M+1}}{\alpha_{M+1}},\; c = P_{\text{tot}} + \left(\sum_{n=1}^{M} \frac{\beta_n}{\alpha_n} \right)$$

and use the fact that $f(M) = \frac{a}{c} > 1$. Since $f(M) > 1$ for any $M \geq M'$, it follows that there is a unique N_1 satisfying $f(N_1) < 1$ and $f(N_1 + 1) \geq 1$, and $N_1 = M' - 1$. The proof is complete. □

References

[1] D. Culler, D. Estrin, and M. Srivastava, "Guest editors' introduction: Overview of sensor networks," *Computer*, vol. 37, pp. 41–49, Aug. 2004.

[2] Z. Q. Luo, M. Gastpar, J. Liu, and A. Swami, "Distributed signal processing in sensor networks," *IEEE Signal Proces. Magaz.*, vol. 23, pp. 14–15, Jul. 2006.

[3] P. Willett, P. F. Swaszek, and R. S. Blum, "The good, bad, and ugly: Distributed detection of a known signal in dependent Gaussian noise," *IEEE Trans. Signal Process.*, vol. 48, pp. 3266–3279, Dec. 2000.

[4] R. Viswanathan and P. K. Varshney, "Distributed detection with multiple sensors: Part I-fundamentals," *Proc. IEEE*, vol. 85, pp. 54–63, Jan. 1997.

[5] R. Blum, S. Kassam, and H. Poor, "Distributed detection with multiple sensors: Part II-advanced topics," *Proc. IEEE*, vol. 85, pp. 64–79, Jan. 1997.

[6] J.-J. Xiao and Z.-Q. Luo, "Universal decentralized detection in a bandwidth-constrained sensor network," *IEEE Trans. Signal Process.*, vol. 53, pp. 2617–2624, Aug. 2005.

[7] J.-F. Chamberland and V. V. Veeravalli, "Decentralized detection in sensor networks," *IEEE Trans. Signal Process.*, vol. 51, pp. 407–416, Feb. 2003.

[8] R. R. Tenny and J. Nils R. Sandell, "Detection with distributed sensors," *IEEE Trans. on Aerospace and Electronic Systems*, vol. AES-17, pp. 501–510, July 1981.

[9] I. Y. Hoballah and P. K. Varshney, "Distributed Bayesian signal detection," *IEEE Trans. Inform. Theory*, vol. 35, pp. 995–1000, Sept. 1989.

[10] A. R. Reibman and L. W. Nolte, "Optimal detection and performance of distributed sensor systems," *IEEE Trans. on Aerospace and Electronic Systems*, vol. AES-23, pp. 24–30, Jan. 1987.

[11] S. Thomopoulos, R. Viswanathan, and D. Bougoulias, "Optimal distributed decision fusion," *IEEE Trans. on Aerospace and Electronic Systems*, vol. 25, pp. 761–765, Sept. 1989.

[12] T. Berger, Z. Zhang, and H. Viswanathan, "The CEO problem," *IEEE Trans. Inform. Theory*, vol. 42, pp. 887–902, May 1996.

[13] H. Viswanathan and T. Berger, "The quadratic Gaussian CEO problem," *IEEE Trans. Inform. Theory*, vol. 43, pp. 1549–1559, Sep. 1997.

[14] Y. Oohama, "The rate-distortion function for the quadratic Gaussian CEO problem," *IEEE Trans. Inform. Theory*, vol. 44, pp. 1057–1070, May 1998.

[15] A. Ribeiro and G. B. Giannakis, "Bandwidth-constrained distributed estimation for wireless sensor network-part I: Gaussian case," *IEEE Trans. Signal Process.*, vol. 54, pp. 1131–1143, Mar. 2006.

[16] A. Ribeiro and G. B. Giannakis, "Bandwidth-constrained distributed estimation for wireless sensor network-part II: Unknown probability density function," *IEEE Trans. Signal Process.*, vol. 54, pp. 2784–2796, July 2006.

[17] J.-J. Xiao, A. Ribeiro, Z.-Q. Luo, and G. B. Giannakis, "Distributed compression-estimation using wireless sensor networks," *IEEE Signal Processing Magazine*, vol. 23, pp. 27–41, July 2006.

[18] Z. Q. Luo, "Universal decentralized estimation in a bandwidth constrained sensor network," *IEEE Trans. Inform. Theory*, vol. 51, pp. 2210–2219, Jun. 2005.

[19] M. Gastpar and M. Vetterli, "Power, spatio-temporal bandwidth, and distortion in large sensor networks," *IEEE Journal on Selected Areas in Communications*, vol. 23, pp. 745–754, Apr. 2005.

[20] M. Gastpar, "Uncoded transmission is exactly optimal for a simple Gaussian sensor network," *IEEE Trans. Inform. Theory*, vol. 54, pp. 5247–5251, Nov. 2008.

[21] J. J. Xiao, S. Cui, Z. Q. Luo, and A. Goldsmith, "Linear coherent decentralized estimation," *IEEE Trans. Signal Process.*, vol. 56, pp. 757–770, Feb. 2008.

[22] S. Cui, J. J. Xiao, Z. Q. Luo, A. Goldsmith, and H. V. Poor, "Estimation diversity and energy efficiency in distributed sensing," *IEEE Trans. Signal Process.*, vol. 55, pp. 4683–4695, Sep. 2007.

[23] J. C. Liu and C. D. Chung, "Distributed estimation in a wireless sensor network using hybrid MAC," *IEEE Trans. Veh. Technol.*, vol. 60, pp. 3424–3435, Sept. 2011.

[24] I. F. Akyildiz, W. Su, Y. Sankarasubramaniam, and E. Cayirci, "A survey on sensor networks," *IEEE Commun. Magazine*, vol. 40, pp. 102–114, Aug. 2002.

[25] C. Chong and S. P. Kumar, "Sensor networks: evolution, opportunities, and challenges," *Proc. IEEE*, vol. 91, pp. 1247–1256, Aug. 2003.

[26] M. Tubaishat and S. Madria, "Sensor networks: an overview," *IEEE Potentials*, vol. 22, pp. 20–23, April-May 2003.

[27] D. Puccinelli and M. Haenggi, "Wireless sensor networks: applications and challenges of ubiquitous sensing," *IEEE Circuits and Systems Magazine*, vol. 5, pp. 19–31, Sept. 2005.

[28] D. Estrin, L. Girod, G. Pottie, and M. Srivastava, "Instrumenting the world with wireless sensor networks," in *Proc. IEEE Int. Conf. Acoustics, Speech and Signal Processing*, (Salt Lake City, UT, USA), pp. 2033–2036, May 2001.

[29] V. C. Gungor and G. P. Hancke, "Industrial wireless sensor networks: Challenges, design principles, and technical approaches," *IEEE Trans. Industrial Electronics*, vol. 56, pp. 4258–4265, Oct. 2009.

[30] S. M. Kay, *Fundamentals of Statistical Signal Processing: Estimation Theory*. Prentice-Hall, Inc., Englewood Cliffs, New Jersey 07632, 1993.

[31] V. A. P. Viswanath and D. N. C. Tse, "Optimal sequences, power control and user capacity of synchronous CDMA systems with linear MMSE multiuser receiver," *IEEE Trans. Inform. Theory*, vol. 45, pp. 1968–1983, Sept. 1999.

[32] H. H. Nguyen and E. Shwedyk, "Bandwidth constrained signature waveforms for maximizing the network capacity of synchronous CDMA systems," *IEEE Trans. Commun.*, vol. 49, pp. 961–965, June 2001.

[33] I. S. Gradshteyn and I. M. Ryzhik, *Table of Integrals, Series, and Products*. Academic Press, New Jersey, 2007.

[34] A. Papoulis and S. U. Pillai, *Probability, Random Variables and Stochastic Processes (Fourth Edition)*. McGraw-Hill Companies, Inc., New York 10020, 2002.

[35] J. J. Xiao, S. Cui, Z. Q. Luo, and A. Goldsmith, "Power scheduling of universal decentralized estimation in sensor networks," *IEEE Trans. Signal Process.*, vol. 54, pp. 413–422, Feb. 2006.